

Design of polymeric nanocarriers for nitric oxide (NO) delivery via raft polymerization

Author:

Agustina, Sri

Publication Date:

2014

DOI:

<https://doi.org/10.26190/unsworks/16670>

License:

<https://creativecommons.org/licenses/by-nc-nd/3.0/au/>

Link to license to see what you are allowed to do with this resource.

Downloaded from <http://hdl.handle.net/1959.4/53317> in <https://unsworks.unsw.edu.au> on 2024-04-26

**DESIGN OF POLYMERIC NANOCARRIERS
FOR NITRIC OXIDE (NO) DELIVERY
VIA RAFT POLYMERIZATION**

SRI AGUSTINA

A thesis submitted in fulfilment of the requirements for the degree of
Master of Engineering

UNSW



**School of Chemical Engineering
The University of New South Wales
March 2014**

Certificate of Originality

I hereby declare this submission is my own work and to the best of my knowledge it contains no materials previously published or written by another person, or substantial proportions of material which have been accepted for the award of any other degree or diploma at UNSW or any other educational institution, except where due acknowledgment is made in the thesis. Any contribution made to the research by others, with whom I have worked at UNSW or elsewhere, is explicitly acknowledged in the thesis.

I also declare that the intellectual content of this thesis is the product of my own work, except to the extent that assistance from others in the project's design and conception or in style, presentation and linguistic expression is acknowledged.

(Signed) 

(Date) 25 / 03 / 2014

Acknowledgments

I would like to express my sincere gratitude to my supervisor, A/Professor Cyrille Boyer, for giving me the opportunity to carry out this research project, teaching me how to conduct scientific research, and for always keeping my best interest in mind. This work would not be possible without his guidance and inspiration. I also wish to thank Professor Tom Davis, my co-supervisor, for his kindly support. Special thanks are also addressed to Dr. Hien Duong, my mentor, for her great support and assistance, so I was able to finish this work.

I wish to thank all new and former management of Center for Advanced Macromolecular Design (CAMD): Dr. Istvan Jacenyik, Dr. Michael Whittaker, Professor Martina Stenzel, Professor Per Sutherland, and Eh Pau Pan for their excellent management in CAMD.

I am also thankful to all my research group's friends, especially for Daniel Li, Johan, Ben, and Lars, for providing me with much help in my study. I am also grateful to the staff in the School of Chemical Engineering in UNSW for their various help during the course of my study.

I also would like to express my deep appreciation to General Directorate of Higher Education, Indonesia Ministry of National Education for their support in granting the scholarship during this project.

Special thanks to my parents and my family, for their love, encouragement and support, which have always been the source of inspiration in my work.

Table of Contents

Certificate of Originality	i
Acknowledgments.....	iii
Abstract.....	vi
Chapter 1. Introduction to the thesis	1
1.1 Introduction	1
1.2 The aim of this thesis.....	3
1.3 Publication.....	4
1.4 References	4
Chapter 2. Well-defined, biocompatible polymeric nanocarriers for NO delivery system via RAFT polymerization	6
2.1 Introduction	6
2.2 NO and NO delivery systems.....	8
2.3 Polymeric Nanocarriers for drug delivery.....	27
2.4 Synthesis of NO polymeric nanocarriers via RAFT polymerization process.....	40
2.5 Conclusions	46
2.6 References	47
Chapter 3. Instrumental analysis.....	56
3.1 Gel permeation chromatography (GPC) measurements.....	56
3.2 Nuclear Magnetic Resonance (NMR).....	58
3.3 UV-visible spectroscopy	59
3.4 Dynamic light scattering (DLS)	60
3.5 Fourier Transform Infrared (FT-IR) spectroscopy.....	62
3.6 Transmission Electron Microscopy (TEM).....	63
3.7 Confocal microscopy.....	64
3.8 References	65
Chapter 4. Synthesis of core crosslinked star (CCS) as macromolecular organic nitrate via RAFT polymerization	66
4.1 Introduction	66

4.2	Experimental part	67
4.3	Result and discussion	74
4.4	Conclusions	85
4.5	References	86
Chapter 5. Core crosslinked star –NO nanoparticles for antimicrobial application		88
5.1	Introduction	88
5.2	Experimental part	90
5.3	Result and discussion	98
5.4	Conclusions	114
5.5	References	114
Chapter 6. Conclusion and Future Directions		119
6.1	Conclusions	119
6.2	Further study.....	120

Abstract

Nitric Oxide (NO) has been used in many biomedical applications since 1992, and known as one of the most important mediators of intra and extracellular processes. It is also a major target of the pharmaceutical industry. NO utility is limited by its short half-life, instability during storage, and potential toxicity. Polymeric nanocarriers are currently being used for NO delivery to overcome these limitations. However, in some application its stability and half time to deliver NO still become the major issues. The improvement of the stability and capability of NO by using nanoparticles will become necessary in the future.

The objective of this thesis is to explore the reversible addition fragmentation chain transfer (RAFT) polymerization technique to synthesis of well-defined, biocompatible, and stable polymeric nanocarriers for NO delivery. Core Crosslinked Star (CCS) polymeric nanoparticles with different functionality in the core had been prepared and used as NO carriers. The potent of NO nanoparticles in biomedical application and as an antibacterial agent was observed through NO release activity and its stability analyses. The result of this study suggested that the core crosslinked star (CCS) polymer nanoparticles have significant potent as NO carriers with high concentration of NO release and good stability.

List of abbreviations

AIBN	2,2'-azobisisobutyronitrile
ATRP	Atom transfer radical polymerization
RAFT	Reversible addition-fragmentation chain transfer
LRP	Living radical polymerization
OEG-A	Oligo(ethylene glycol) methyl ether acrylate
PDI	Polydispersity index
VBC	Vinylbenzyl chloride
CCS	Core cross-linked star
EPR	Enhanced permeation retention
CRP	Controlled radical polymerization
CLRP	Controlled/living radical polymerization
MWD	Molecular weight distribution
MW	Molecular weight

Chapter 1. Introduction to the thesis

1.1 Introduction

Nitric Oxide (NO) known as free-radical gas molecule actively involved in the immune system response¹ and regulate several biological functions in the cardiovascular², respiratory³, and nervous system⁴. NO has complex chemistry of produce and release mechanism that makes this radical gas can do wide range of biological function and shown great potent in multiple therapeutic applications.^{5,6} It is produced endogenously from L-arginine catalysed by nitric oxide synthase (NOS). Thus, NO was proclaimed “Molecule of the Year” by journal Science in 1992 and in 1998, three scientists, Furchgott, Ignarro, and Murad, were awarded the Nobel Prize in physiology and medicine for their contribution to elucidating the role of nitric oxide in the functions of living organisms. The decrease in endogenous production of NO due to aging, inactivity, smoking, high cholesterol, fatty diets, and lack of healthy food has been associated with many serious medical problems such as hypertension, diabetes, liver fibrosis, cardiovascular illness, neurodegenerative diseases and several cancers.⁷

Due to its gaseous property, NO is very unstable and difficult to handle during storage or delivery. In order to stabilize the radical until such time as its release is required, it is reliant on compounds capable of releasing, usually known as NO donor. NO donors can be classified into different types based on their chemicals natures. In general, it has a low molecular weight and the ability to be able

released spontaneously, either in the presence or absence of the catalyst during the process.⁸ There are three most commonly NO donors that have been used widely in biomedical and therapeutic applications: S-nitrosothiols, diazeniumdiolates (NONOates), and nitrates NO donor.⁷

Despite of the advantages to be used in therapeutic and biomedical area, NO donors also has some limitations that make it really difficult to be delivered in many applications. There are including its short half-life, instability during storage, and also potential toxicity.⁹ In order to overcome these limitations, nanoparticles are currently being used as NO carriers (nanocarriers). Nanoparticles have the ability to load high amounts of NO, quite stable, and shown high efficacy in biological activity.^{10,11} For specific medical application, these materials also can be modified and optimized that can enhanced the half-life of NO donors.

The use of polymeric nanoparticles for drug delivery are really promising because it can be used to increase the aqueous solubility of drugs and to modulate drug activity by passive or active targeting to different tissues.¹² One of the most widely used as drug delivery carriers is star polymer, which has unique structures that consist of a three dimensional architecture where linear arms are linked by a central core. Star polymer with high-molecular-weight cross-linked cores surrounded by many polymeric arms, known as core cross-linked star (CCS) polymer and have been proposed recently to use for drug delivery application.¹³ The CCS polymer is ideally suited for use as a potential drug delivery device

because of the large loading capacity of the hydrophobic core, the size of which can be easily altered through the use of a ‘spacer monomer’ during the core formation step.¹⁴ Due to its ability to synthesize various architecture of a wide variety of polymers with water solubility under mild conditions, RAFT polymerization has become the most provable technique to synthesize polymeric nanocarriers for drug delivery, including star polymer.¹⁵⁻¹⁷

1.2 The aim of this thesis

The development of new NO delivery system with high efficacy and capability of releasing optimal amounts of NO at the right time and the right places will be harness to overcome NO limitations. The objective of this thesis is to design new biocompatible and stable polymeric nanocarriers that can be used for NO delivery with optimal NO loading. In this study, we proposed a core crosslinked star (CCS) polymer as a nanocarrier for NO delivery.

The synthesis star polymeric nanoparticles had been conducted via reversible addition fragmentation chain transfer (RAFT) polymerization. Two polymer stars with the same polyethylene glycol corona and different functionalities in the core have been synthesized using arm-first method. Some work also has been focused by preparing two types of NO donors: nitrates and diazeniumdiolates (NONOates) for different application area. We prepared star-nitrate nanoparticles for anticancer application based on its slow release mechanism. Star-NONOates nanoparticles would be used as antibiotics drugs since it can release NO spontaneously and faster through hydrolysis reaction.

The NO release testing and kinetic study had been done to justify the stability and the biocompatibility of NO nanoparticles. Biological and antimicrobial testing also has been done to probe the potent of NO nanoparticles in biomedical application and as antibacterial agent. Griess Assay method had been used to determine NO release concentration and also to observe the stability of NO nanoparticles in solution.

1.3 Publication

Two papers are in preparation.

1.4 References

- (1) Bogdan, C. *Nat Immunol* **2001**, 2, 907.
- (2) Naseem, K. M. *Molecular Aspects of Medicine* **2005**, 26, 33.
- (3) Ichinose, F.; Roberts, J. D.; Zapol, W. M. *Circulation* **2004**, 109, 3106.
- (4) Calabrese, V.; Mancuso, C.; Calvani, M.; Rizzarelli, E.; Butterfield, D. A.; Giuffrida Stella, A. M. *Nat Rev Neurosci* **2007**, 8, 766.
- (5) Vallance, P. *Fundamental & Clinical Pharmacology* **2003**, 17, 1.
- (6) Carpenter, A. W.; Schoenfisch, M. H. *Chemical Society Reviews* **2012**, 41, 3742.
- (7) Bill Cai, T.; Wang, P. G.; Holder, A. A. In *Nitric Oxide Donors*; Wiley-VCH Verlag GmbH & Co. KGaA: 2005, p 1.
- (8) Riccio, D. A.; Schoenfisch, M. H. *Chemical Society Reviews* **2012**, 41, 3731.

- (9) Webb, D. J.; Megson, I. L. *Expert Opinion on Investigational Drugs* **2002**, *11*, 587.
- (10) Body, S. C.; Hartigan, P. M.; Shernan, S. K.; Formanek, V.; Hurford, W. E. *Journal of cardiothoracic and vascular anesthesia* **1995**, *9*, 748.
- (11) Kapadia, M. R.; Chow, L. W.; Tsihlis, N. D.; Ahanchi, S. S.; Eng, J. W.; Murar, J.; Martinez, J.; Popowich, D. A.; Jiang, Q.; Hrabie, J. A.; Saavedra, J. E.; Keefer, L. K.; Hulvat, J. F.; Stupp, S. I.; Kibbe, M. R. *Journal of Vascular Surgery* **2008**, *47*, 173.
- (12) Liechty, W. B.; Kryscio, D. R.; Slaughter, B. V.; Peppas, N. A. *Annual review of chemical and biomolecular engineering* **2010**, *1*, 149.
- (13) Vassiliou, A. A.; Papadimitriou, S. A.; Bikiaris, D. N.; Mattheolabakis, G.; Avgoustakis, K. *Journal of Controlled Release* **2010**, *148*, 388.
- (14) Aryal, S.; Prabakaran, M.; Pilla, S.; Gong, S. *International Journal of Biological Macromolecules* **2009**, *44*, 346.
- (15) Boyer, C.; Stenzel, M. H.; Davis, T. P. *Journal of Polymer Science Part A: Polymer Chemistry* **2011**, *49*, 551.
- (16) Kedar, U.; Phutane, P.; Shidhaye, S.; Kadam, V. *Nanomedicine: Nanotechnology, Biology and Medicine* **2010**, *6*, 714.
- (17) Gregory, A.; Stenzel, M. H. *Expert Opinion on Drug Delivery* **2011**, *8*, 237.

Chapter 2. Well-defined, biocompatible polymeric nanocarriers for NO delivery system via RAFT polymerization

2.1 Introduction

Nitric Oxide (NO) is a free radical gas that is known as a toxic air pollutant from industrial processing and automobile exhaust. The identification of NO as an endothelium-derived relaxing factor (EDRF) by Furchgott, Ignarro, and Murrad in 1987 has changed this perspective and become the starting point to begin the investigation about the role of this radical gaseous in biological function.^{1,2} This biological functions are including the association of NO in cardiovascular³, vasodilation⁴, immune response⁵, cancer therapy⁶⁻⁸, antimicrobial⁹ and wound healing¹⁰.

The roles of NO in many biomedical applications have been limited by its short half-life, instability during storage, and potential toxicity.¹¹ To overcome these limitations, the development of small molecules that can release optimal NO loading has been proposed and known as NO donors. However, there is still some shortage of NO distribution and stability from this small molecule. For example, most NO donor can be decomposed too rapidly and only have a half-life for few minutes or seconds.¹² The use of polymeric nanoparticles as NO nanocarriers later proved can enhance the half-life and improve the biodistribution of NO donors.¹³ These materials have capability to load high amounts of NO, quite stable, and can

deliver a drug directly to a specific target site with multiple mechanism of NO release.^{1,14,15} The NO release mechanisms are including spontaneous release of NO, chemical reaction and enzymatic oxidation. In addition of these advantages, the surfaces can also be chemically modified and optimized by the attachment of targeting moiety.

Polymeric nanocarriers for NO delivery ideally would be multifunctional and has specific molecular weight that can improve the stability and therapeutic delivery of NO.^{12,13} With the ability to synthesize various architecture of wide variety of polymers with defined and pendant functionalities, controlled molecular weights, and narrow polydispersities using mild condition (such as aqueous solutions and room temperatures), the RAFT technique appears to be one of the most amenable techniques to the generation of nanoscale polymeric systems for drug delivery, including NO delivery.^{16,17}

The purpose of this chapter is to briefly outline the underlying theories of free-radical polymerization and living polymerization, particularly on the reversible addition-fragmentation chain transfer (RAFT) process, which is demonstrated as a versatile and powerful tool to prepare complex polymer nanocarriers structures with novel properties for NO delivery. The synthesized of well-defined core cross-linked star polymer with different condition and specific functionality will be highlighted. In particular, NO delivery system, including NO donor compounds, its classification and application as an anti-microbial agent, will be discussed in details.

2.2 NO and NO delivery systems

2.2.1 NO and therapeutic opportunities

Nitric Oxide (NO) known as free-radical gas molecule that in 1992 was awarded as 'Molecule of the Year'.¹⁸ These small molecules with 30 gram/moles of molecular mass have first known as the toxic air pollutant and later as a biological messenger in mammals. The identification of multiple biological roles of NO then made some studies have been proposed to investigate the potent of NO in biomedical and therapeutic applications.^{11,19,20}

NO associated with many diverse physiological processes in human body whereas its effects are largely concentration dependent by the regulation of two major biochemicals signaling pathways: physiological and immunology signal.^{2,20} It is generated biologically by enzyme NO synthase (NOS) through the stepwise oxidation of L-arginine via N-hydroxyarginine intermediate into NO, citrulline and NADP.²⁰ There are three major distinct isoform of NOS : neuronal (nNOS), inducible (iNOS) and endothelial (eNOS).²¹ These NO synthase generate NO in different level NO concentration for specific functions. Neuronal and endothelial NOS produce low nanomolar NO concentration to promote the main biological functions of NO including vasodilation and neuro transmission.^{22,23} Meanwhile, the micromolar levels of NO produced by inducible NOS.²² At this level concentration, NO has indirect effect on biomolecules. It involves in the inflammatory reaction and host defense pathogens.^{22,24}

2.2.2 NO in cardiovascular diseases

NO has significant role in the cardiovascular system, which is produced from vascular endothelial cells and influences the cellular activities of smooth muscle cells, platelets, and immune cells.²⁵ It is generated to maintain proper blood flow and pressure. Figure 2.1 below shows the activity of NO in the vascular endothelium and its effects on cellular activities. After converted from L-arginine, NO diffuses into vascular smooth muscle cells and reacts with the enzyme soluble guanylate cyclase, to stimulate the production cyclic guanosine monophosphate (cGMP).² This mechanism then will lead to relaxation of the smooth muscle cells and dilation of blood vessels.

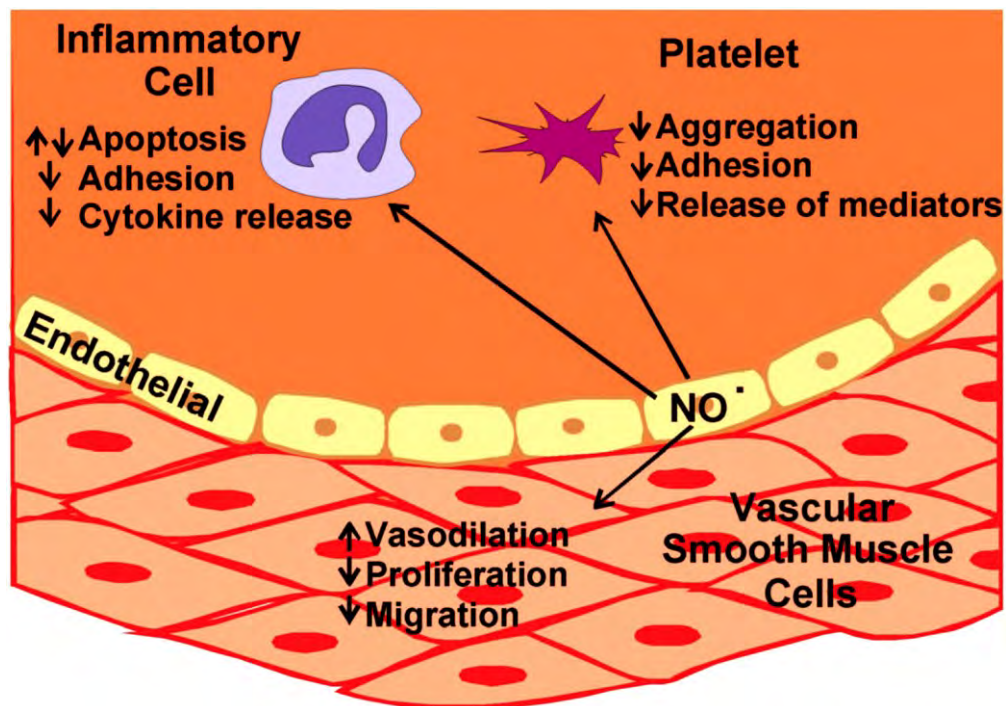


Figure 2.1 The role of NO in the vascular endothelium²

Endothelial dysfunction can cause several cardiovascular conditions, including atherosclerosis, heart failure, diabetes, hypertension, coronary heart disease, and stroke.²⁶ Delivery of exogenous NO has been proposed as an attractive therapeutic option to overcome the cardiovascular diseases. Glyceryl trinitrate (GTN) is the most widely used organic nitrate that been used in the cardiovascular therapies, although its therapeutic applicability limited by the induction of tolerance.¹⁵ The capability to deliver therapeutic NO levels to diseased cardiovascular tissue become more desirable.

2.2.3 NO for cancer therapy

The role of NO in tumor biology was first identified by the observation of nitrite and nitrate synthesis through the activation of macrophages, that can cause the toxicity of tumor cells.¹⁵ This anti-tumor activity then will become the foundation to develop the function of NO as a potential oncologic agent.

In cancer biology, NO has dual role that really depends on NO concentration and lifetime. The inducible NO synthase (iNOS) will generate NO that can acts as a tumor progressor and suppressor. Large NO concentrations at micromolar level produce reactive nitrogen species to react with reactive oxygen species, and generate oxidative and nitrosative stress as the result. At this concentration level, NO will damage the DNA and lead to cell apoptosis.²⁷ Otherwise, NO act as pro-angiogenic and pro-tumor formation at lower concentrations. In this phenomenon, NO may induce *p53* gene alterations or mutations which cause tumor cell

resistance.^{8,15} The mechanism of NO activity in cancer biology has shown in figure 2.2 below.

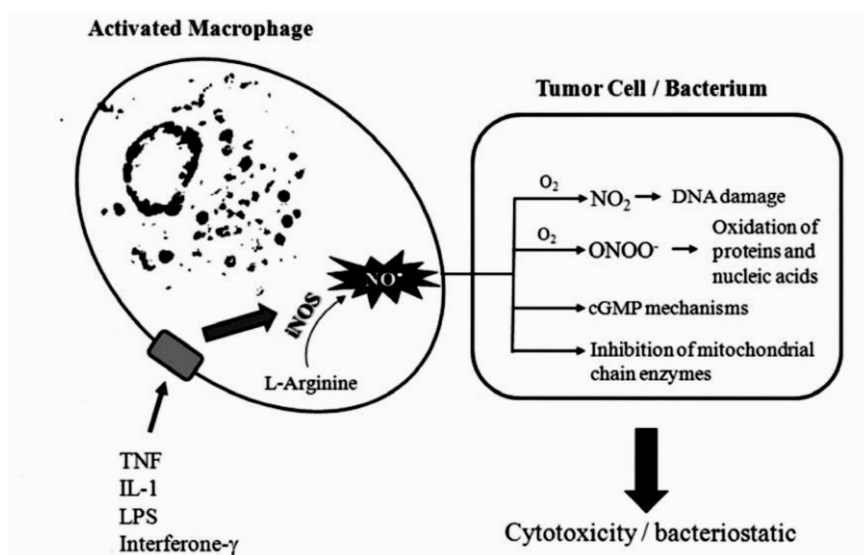


Figure 2. 2 The mechanism of an NO activity in cancer biology¹⁵

Delivery of high concentration of NO specifically to the tumor site has become the main key for NO application in cancer biology. Due to its dual role as a tumor promoter and repressor, there is still vacillation to use NO for cancer treatment. As the alternative solution, some researchers have proposed to combine NO-antitumor therapy with other therapies as the co-administration.

Some conventional drugs also may be modified to obtain better effect in antitumor therapy. For example, the advantage of combination therapy from NO-releasing non-steroidal anti-inflammatory drugs (NSAIDs). The combination of NO release with NSAID will enhance the antitumor properties, as well as the serious gastrointestinal and renal side effects.^{28,29} Our group also reported the

combination of cisplatin delivery with NO using nanocarriers. This study was using *in vitro* experiments on a neuroblastoma BE(2)-C cell line. The encapsulation of S-nitrosoglutathione into polymeric nanoparticles substantially improves NO stability in aqueous media and its combination with cisplatin delivery has shown to enhance the antitumor activity of chemotherapeutic agents.³⁰ These all alternatives solutions may lead to a better new generation of NO drug for cancer treatment application.

2.2.4 NO for antimicrobial application

The importance role of NO in immunology was first identify between 1985 and 1990, defined as product from the activation macrophages by cytokines, microbial compounds or both, derived from the amino acid L-arginine by the enzymatic activity of iNOS.⁵ It has become the evident that NO exerts its antimicrobial effects on a wide range of microorganism such as bacteria, viruses, fungi, and yeast.³¹

Recently, the emergence of bacterial resistance and the lack of new antibacterial drugs have made microbial infections increasingly more difficult to treat. The bacteria survival mechanism has been appointed caused by the formation of biofilms³²⁻³⁴. Biofilms are surface-attached bacteria communities that enclosed in a self-produced matrix which acts as a barrier and protective membrane.³⁵ It consists of different bacterial communities held together by an extra-cellular polysaccharide (EPS) matrix materials, DNA and proteins. Bacteria embedded in

biofilms are up 10 – 1000 fold more resistant to antimicrobial agents than their planktonic counterparts.³³

Figure 2.3 described the mechanism of biofilm formation, which includes 4 important steps: contamination, surface attachment, maturation of biofilm and surface detachment. Biofilm formation begins with the introduction of cell environment, where the bacteria will sense the environmental conditions and start contaminating cell surfaces. This first mechanism varies among bacteria. After the bacteria fit into the cell surface environment, they start to attract other bacteria to make colonies. The cell-cell interactions among these bacteria will lead to the next step which is the development of the mature biofilm. Protective membrane will then build as a barrier and cause biofilm to be a tenacious clinical problem. Another property also been developed, including increased resistance to UV light, the rates of genetic exchange and secondary metabolite production.³³ The last step of biofilm formation is the detachment of bacteria colonies and return to the planktonic growth mode. The cycle will start again after the free bacteria plankton finds another surface and start make new colonies.³⁶

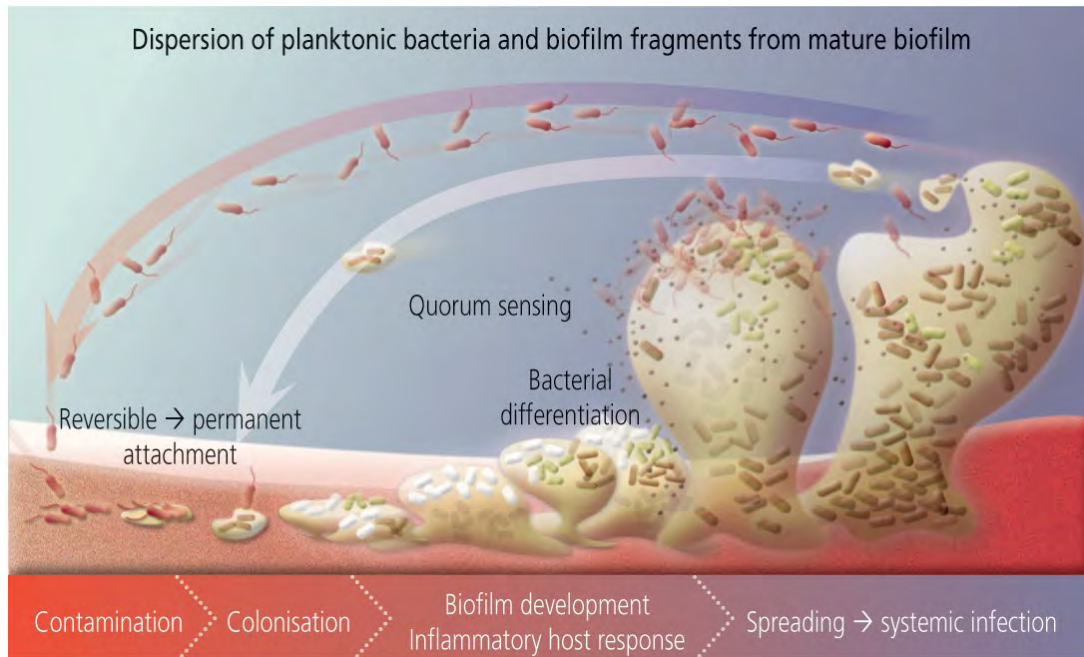


Figure 2.3 Schematic cycle of biofilm formation³⁶

High concentration of NO from induced NO synthase (iNOS) has the capability to act as biofilm inhibitor. NO will react to form reactive nitrogen and oxygen intermediates. These reactive compounds are toxic and can bind DNA, proteins and lipids thereby inhibiting or killing target pathogens.⁹

2.2.5 NO donors

Due to its properties as an unstable radical gas, NO gas is very difficult to handle and has a very short half-life in vivo, less than 1 second in the presence of oxygen and hemoglobin.³⁷ In order to stabilize the radical until such time as its release is required, it is reliant on small molecule carriers of NO, usually called as NO

donors. Previous studies has proved that NO donors can enhanced NO half-live, so it can sustainably release NO gas with a predictable estimated dose.¹⁵

NO donors can be classified into several types of NO donors based on the release mechanism and the similarity of compound parent structures. Generally, NO donors have a low molecular weight and the ability to be able released spontaneously, either in the presence or absence of the catalyst during the process.³⁸ The ability is influenced by chemical properties that owned by NO donors naturally. Including NO donors that have a low molecular weight compounds are nitrates, nitrites, N-nitroso, C-nitroso, certain heterocycles, metal-NO complexes, and diazeniumdiolates. Scatena, et.al has been summarized that the most important thing due to the development of new NO donor drugs is how to release NO at the specific tissue site with an optimal concentration, so as to achieve the maximum therapeutic effect and minimize toxic effects at the same time.³⁹

Currently, there are three most commonly used NO donor in clinical applications based on summarizing decades of NO researches:^{11,38,40}

- **Organic nitrates**

Organic nitrates are the most commonly used NO donor drugs with the general formula (RONO₂).²¹ It usually has four (pentaerythryl tetranitrate [PETN]), three (glyceryl trinitrate [GTN]), two (isosorbide dinitrate [ISDN]), or one (isosorbide-5-mononitrate [ISMN]) nitrooxy groups attached to a

simple organic carrier molecule.⁴¹ The structures from this class NO donors above have shown in the figure 2.4.

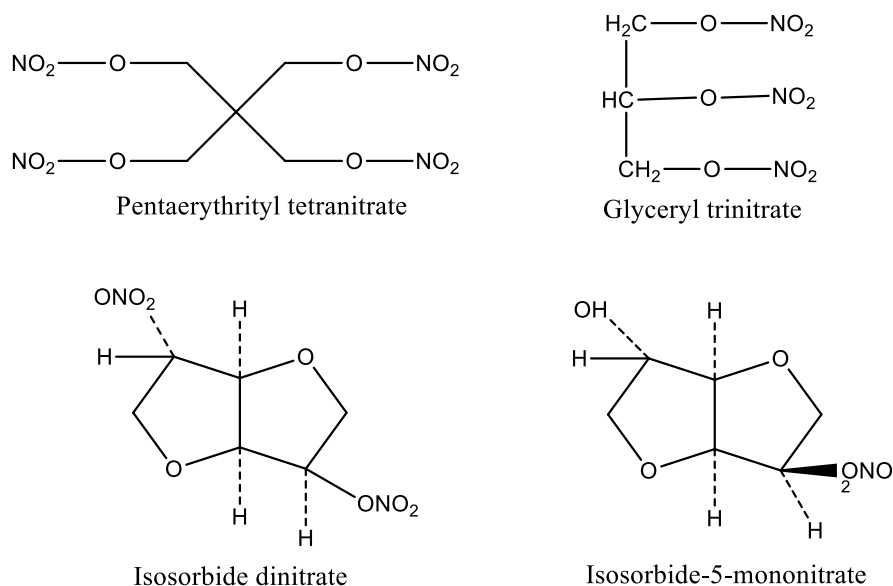


Figure 2. 4 Chemical structure of organic nitrates NO donors⁴⁰

The organic nitrates therapeutically targeted for cardiovascular disorder and many other pathologies and diseases. Glycerol trinitrate (GTN or most known as Nitroglycerin) is the best studied nitrate, used mainly in acute relief of pain associated with angina. For over decades, GTN has proven to be a safe agent in the cardiovascular system, with minimum side effect profile including hypotension and headaches.¹⁵ Meanwhile, the ISMN has been used for the treatment of chronic angina due to its slower release preparation. The only organic nitrates with poor or free nitrate tolerance, PETN, are considered as effective therapy for treatment of heart and circulation diseases.

Generally the organic nitrates release NO through chemical reaction with acid, alkali, metal, and thiols. Classic organic nitrates have been shown to

react with thiols at very slow rates and release small amounts of NO. Some authors also notified that novel organic nitrates are capable of releasing considerably larger amounts of NO in a non-enzymatic reaction with thiols in single buffer solution.⁴² The propose mechanism reactions of organic nitrates with thiols are shown in figure 2.5 below.

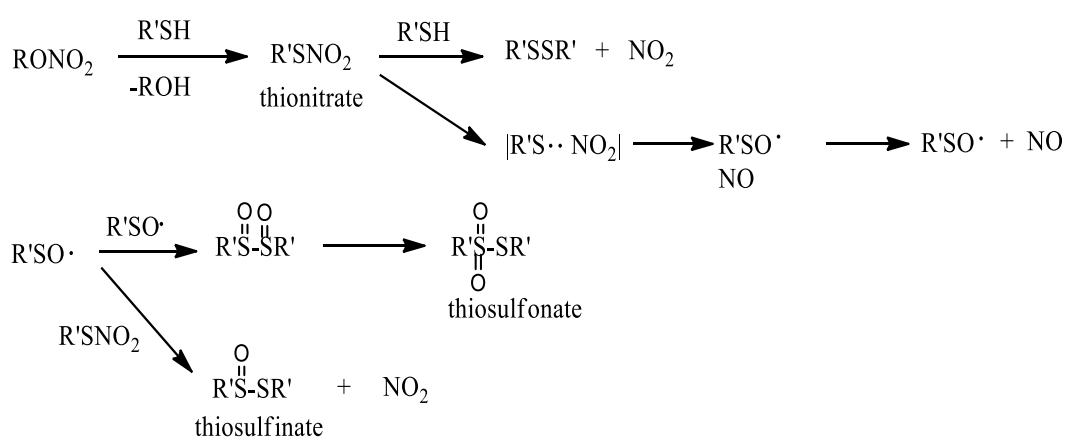


Figure 2.5 Mechanism for the reaction of organic nitrates with thiols⁴³

However, there are some organic nitrates compounds can release NO by more than one route, e.g. generate NO by enzymatic catalysis process. GTN releases one molar equivalent of NO from the terminal position after bioactivation by mitochondrial aldehyde dehydrogenase (mtALDH). Through these two mechanisms, NO releases for organic nitrates are highly independent on a number of factors including enzymes, free thiols and lights.⁴⁴

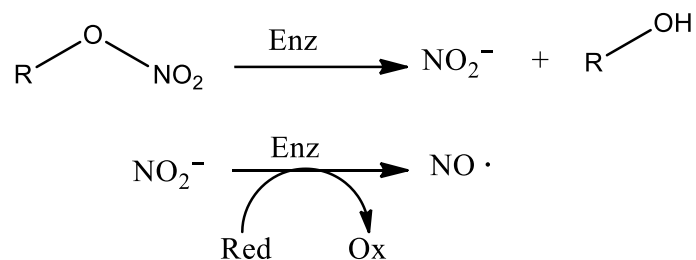


Figure 2. 6 Primary enzymatic NO-release mechanisms for organic nitrates

Recently, there are some interests in the development of new nitrate compounds using hybrids and original types of nitrates. New therapeutic targets for nitrates also have been explored to make more wide application for organic nitrates NO donors. For example, the long transdermal ISDN is suggested to be used in preeclamptic women to avoid maternal hypertension and foetal distress. The same GTN NO donors can be considered used in the treatment of children with anal fissure, inflammatory bowel disorder, and Crohn's diseases without incurring side effects such as headache or significant decrease of blood pressure.¹¹

- **Diazeniumdiolates (NONOates)**

The diazeniumdiolates are a group of compounds also known as 'NONOates' with the basic structures: $\text{X}-[\text{N}(\text{O})\text{NO}]^+$, in which 'X' is typically a secondary amine that bond to diolate group via a nitrogen atom.⁴⁵ This class of NO donors that have a wide range of half-lives from 2 seconds to 20 hours. Diazeniumdiolates compound was first synthesized by Drago, et.al in 1960

and being more explored until now particularly by Keefer's Group at the NCI.⁴⁶

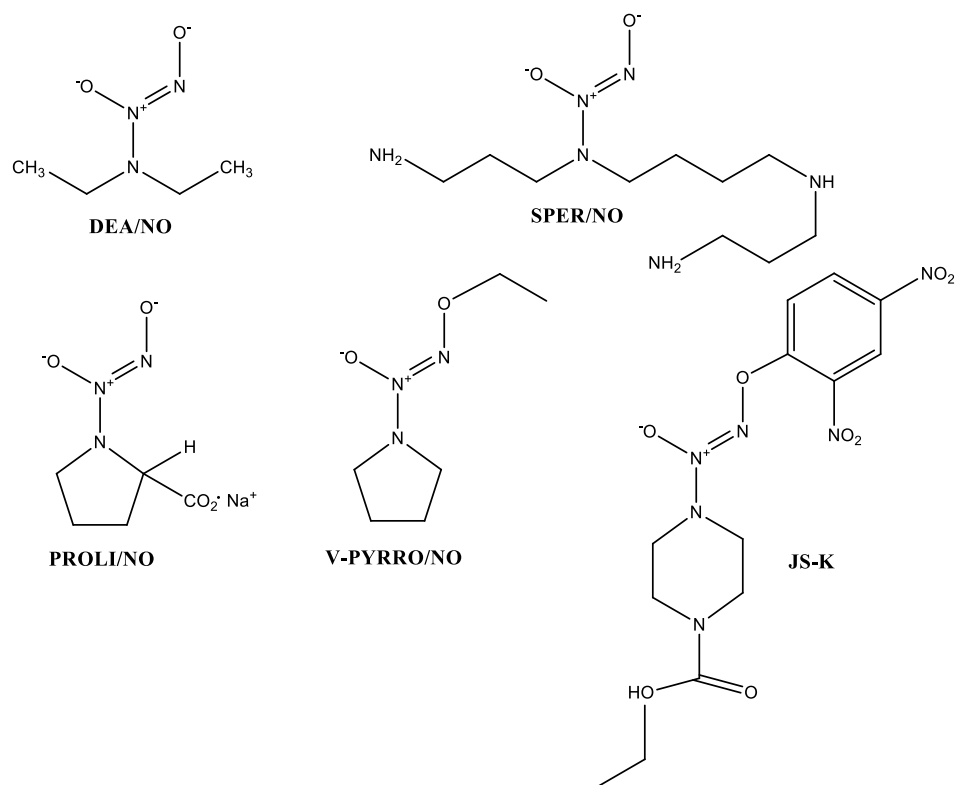


Figure 2. 7 Chemical structures of five diazeniumdiolates compounds (NONOates)³⁸

Diazeniumdiolates become more attractive because they are stable as solids, but can be triggered to release NO at controlled rates by simple chemical reactions by hydrolysis. It can be decomposed spontaneously in solution at physiological pH and temperature. The amount of NO generated can be calculated as most of them generated 2 moles of NO per NO donor. The rate of decomposition is dependent on the structure of the nucleophile.⁴⁷ Proposed NO release mechanism has shown in the figure 2.10.

An attractive feature of this class of compounds is that their decomposition is not catalyzed by thiols or biological tissue, unless specifically designed to. NO release from this type of NO donors follows simple first-order kinetics. This process reaction make the release can be predicted accurately.

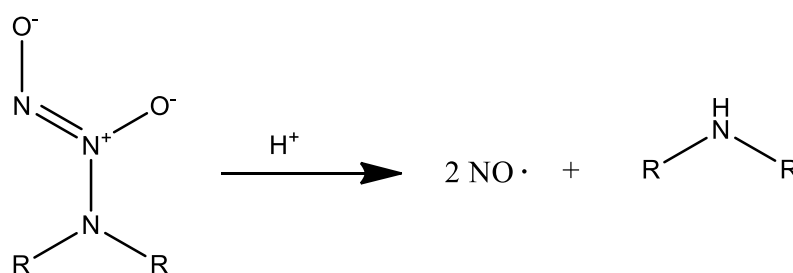


Figure 2. 8 Proposed NO release mechanism of diazeniumdiolate NO donors¹⁰

The therapeutic potential of diazeniumdiolates has been intensively studied in recent years. Application of diazeniumdiolates is claimed as a method to treat pulmonary hypertension, among many other diseases. Several numbers of NONOates are being investigated for use as vasodilators or as chemotherapeutics.⁴

At present, NONOates is not much used clinically, although they have been tested frequently in experimental models of cardiovascular diseases. This is because the parent compound may become toxic when the diazeniumdiolates group is converted to be a reactive N-nitroso group. Several different NONOates have been shown effective to lower pulmonary vascular resistance, with different effects to systemic vascular resistance^{48,49}, depending on the design of the nucleophile adduct. NONOates may also have

a use in the treatment of erectile dysfunction by enhancing blood flow to the penis.⁵⁰

Modification of the structure of the nucleophile adduct to protect the terminal oxygen of the diolate moiety can stabilize the drug in solution and potentially engender a selective NO release in different organs, vascular beds or specific cell types.⁵¹ The use of this modified NONOates has received interest from the viewpoint of targeting delivery of high concentrations of NO specifically of tumor cells.⁵²

The NONOates groups were also a highly efficient antibacterial agent⁹. Diethylenetriamine, a ubiquitous polyamine found in both eukaryotic and prokaryotic cells can be used to make the NONOate DETA-NO.⁵³ DETA-NO is effective to against gram negative and gram positive bacteria.^{54,55} Further study then confirm that NONOates, especially those based on established medication, are a promising source of NO releasing antimicrobials.

At present, conjugated NONOates holds a great deal of promise, especially for the treatment of certain cancers, although further characterization of these drugs is essential before they reach larger clinical trials. The potential for oral preparations of NONOates has yet to be fully clarified, although transdermal preparations have already been developed.⁵⁶ However, experimentally, the NONOates remains an invaluable scientific tool for researching NO physiology.

- **S-Nitrosothiols**

The S-nitrosothiols has a general formula 'RSNO', which contains a single chemical bond between a thiol (sulphydryl) group (R-SH) and the NO moiety. This class of NO donors are typically unstable and its biological activity really influenced by the molecular environment of the parent thiol. However, there are two relatively stable compounds in this class include: S-nitroso-N-acetylpenicillamine (SNAP) and S-nitrosogluthathione (GSNO). Many reactions have been served by these compounds for the storage, transfer, and delivery of NO.⁵⁷

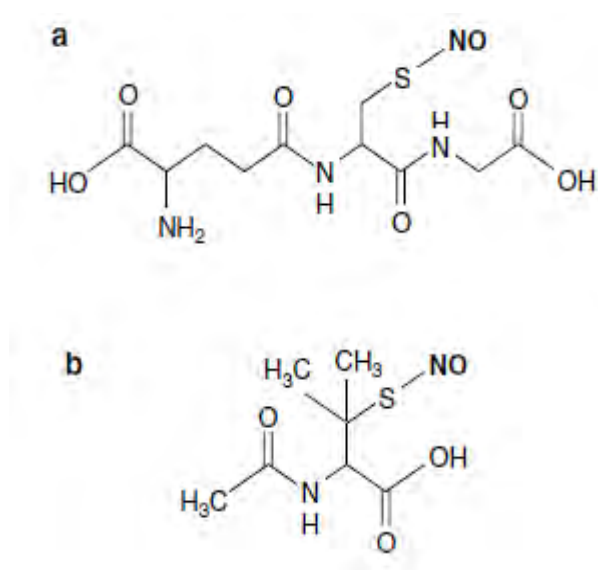


Figure 2. 9 Chemical structures of S-Nitrosothiols : (a) GSNO and (b) SNAP¹⁵

SNAP is relatively stable tertiary S-nitrosothiols, which functions as an NO donor with potent vasodilator activity. The stability of SNAP in solution varies from seconds to hours depending on temperature, buffer composition and metal content. The half-life of SNAP is approximately six hours at pH of

6.0 – 8.0 and temperature of 37 °C, in the presence of transition-metal ion chelators.⁵⁸

The second of the RSNO compounds with relative stability is GSNO. It serves as a good source of NO based on the cleavage of the S-NO bond. GSNO stability varies from seconds to hours in solution, depending on temperature, buffer composition, and metal content.

Decomposition of RSNO compounds yields NO, NO⁺ and NO⁻. The S-NO bond can be disrupted by heat, UV-light, and some metal ions, superoxide, and seleno compounds. Metal ions (Cu⁺⁺, Fe⁺⁺, Hg⁺⁺, and Ag⁺), especially copper, serve as important catalysts for the decomposition of RSNOs.^{59,60}

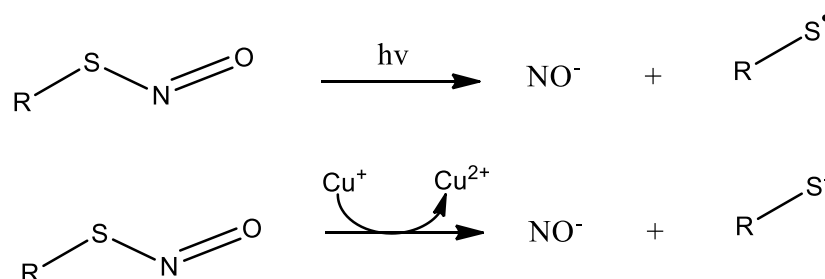


Figure 2. 10 NO release mechanism from S-Nitrosothiols NO donors¹⁰

Despite that S-nitrosothiols are not used clinically at present, but it has numbers of potential advantages over other classes of NO donor. In some application GSNO show tissue selectivity give the result better profile of action compare to classical organic nitrates. The ability of S-nitrosothiols to directly transfer NO⁺ species allows biological activity to be passed on through a chain of other thiols without the release of free NO. This

mechanism of bio-activation may make S-nitrosothiols less susceptible to conditions of oxidative stress by effectively protecting the NO moiety from attack by oxygen-centered free radicals.^{61,62}

Recently, S-nitrosothiols only used in some number of animal and clinical studies, that have demonstrated their advantageous features, especially in the cardiovascular system⁵⁷, preeclampsia treatment and cancer treatment¹⁵. S-nitrosothiols have a promising future based on reports from previous studies. The incorporation of this class NO donors for cardiovascular system has been effectively proved and provided.

2.2.6 Nanocarriers for NO delivery

NO donors have some limitations that make it really difficult to be delivered in many biomedical applications. There are including its short half-life, instability during storage, and also potential toxicity. In order to overcome these limitations, nanomaterials are being used as NO carriers. Nanomaterials have the ability to load high amounts of NO, quite stable, and shown high efficacy in biological activity.¹⁴ For specific medical application, these materials also can be modified and optimized.

The application of nanomaterials for NO delivery has many advantages in order to improve the releasing process. Nanocarriers not only improve the solubility issue but also the stability and therapeutic delivery of NO.¹³ The existence of this particle can enhance a target of NO, the interaction of NO with blood vessels,

through the use of antibody moieties to selectively target drug-delivery vehicles to blood vessels.⁶³

Some reports have been published on the delivery of NO using diverse structures of polymeric nanoparticles. Oliveira, et.al have developed and characterized PLGA nanoparticles containing the NO donor agent (*trans*-[RuCl([15]ane)(NO)]²⁺).¹³ Jain, et.al demonstrated the stabilization of NO pro-drug and anticancer lead compounds via their incorporation into polymer-protected nanoparticles composed of polystyrene-*b*-PEG (PS-*b*-PEG) and PLA-*b*-PEG may enhanced their therapeutic effects.⁶⁴ Yoo, et.al described PLGA microparticles containing NO donor that efficiently delivered NO to the vaginal mucosa, resulting in improved vaginal blood perfusion which may have implications in the treatment of female sexual dysfunction.⁶⁵

Another potential clinical application of polymeric nanocarriers is in tumor therapeutic. Kanayama, et.al reported that PEGylated polymer micelles may be capable of delivering exogenous NO to tumor cells in photocontrolled manner, resulting in an NO-mediated antitumor effect.⁶⁶ Duan, et.al designed a polymeric carrier system to deliver NO into tumorigenic tissues at micromolar concentrations. A highly water solubility and biodegradable multiarm polymer nanocarrier, sugar poly-(6-O-methacryloyl-D-galactose), was synthesized using MADIX/RAFT polymerization. Using newly synthesized diazeniumdiolate NO donors, the result shown that after the injection of NO nanoparticles there were 50% tumor inhibition and a 7 week extension of the average survival time. This

study indicated that polymeric system in NO-based tumor therapy has great promising in the future.⁶⁷

Another study that explored the possibility of polymeric nanoparticles as NO carriers has made by Stasko and Schoenfisch, by using dendrimers for NO storage or delivery system. The study demonstrated the ability of a dendritic scaffold to store NO using N-diazoniumdiolate NO donor.⁶⁸ Followed by Benini, et.al reported the use of PAMAM dendrimers with S-nitrosothiols exteriors that shown the ability of dendrimers to store high concentration of NO on a single molecular framework.⁶⁹ Hydrogel also has interesting delivery system that been widely used in biomedical applications. Friedman, et.al reported that the gradual release of NO from material arises from a combination of the features of glassy matrices and hydrogels.⁷⁰ The results showed that NO-releasing hydrogels/glass hybrid nanoparticles may be preferable to other NO releasing compounds because they do not depend on chemical decomposition or enzymatic catalysis but rather only on the rate of hydration.

Polymeric nanocarriers for NO delivery system become more interesting compare to another type of nanocarriers due to its properties and ability, including lipid-based and inorganic nanocarriers. In addition to improve the solubility and biodistribution matters, some polymers nanocarriers have been made to be able degrade into nontoxic monomer inside the body. It also generally highly stable in biological fluids and have been approved for therapeutic use and application. Based on previous studies, it has been summarized that there are some requirements of nanoparticles properties for NO delivery system. These materials

has required to be able release NO at a slow rate, sufficiently small (less than 100 nm) so it can penetrate tissues under mild pressure, and relatively stable.

2.3 Polymeric Nanocarriers for drug delivery

The biocompatible nanotechnologies for drug delivery have been grown fast over the last half of a century. Nanoparticles applied as drug delivery systems are submicron-sized particles (10-100 nm), devices, or systems that can be made using a variety of materials including polymers, lipids (liposomes), and organometallic compounds. Recently, biodegradable nanoparticles have been used as potential drug delivery devices because of their ability to circulate for a prolonged period time target a particular organ, as carriers of DNA in gene therapy, and their ability to deliver proteins, peptides, and genes.⁷¹

The use of polymeric nanocarriers for drug delivery has been really attracted due to some specific advantages over another type of drug carriers, such as liposome. These system applications in medicine are really promising because it can be used to increase the aqueous solubility of drugs and to modulate drug activity by passive or active targeting to different tissues. It also may increase the duration of drug circulation in the blood, allowing a reduction in the dose required to achieve therapeutic levels over an extended period of time. Another advantage from nanocarriers drug delivery system is the ability to deliver a drug directly to a target site, reducing its toxicity which contributes to a decrease in side effects.^{72,73}

In spite of these advantages, there are some limitations from polymeric nanocarriers as drug delivery system. Due to their small size and large surfaces, the intent to form particles aggregate will make polymeric nanocarriers difficult to handle physically in liquid and dry forms. In addition, the limitation of drug loading and burst release also become practical problems that have to be overcome before polymeric nanocarriers can be used clinically.

There are three polymeric nanomaterial classes that the most widely used as drug delivery vehicles: block copolymer micelles, dendrimers (hyperbranched), and star polymer. Each type has been displaying certain advantages and disadvantages that can improve or will diminish the stability and capability to distribute the drug.⁷⁴

2.3.1 Micelles

The potential of micelles to be used as drug delivery devices has grown since the late of 1960s, due to its easily controlled properties and good pharmacological characteristic.⁷⁵ Micelles are formed when amphiphiles compounds are placed in the water. They consist of an inner core of assembled hydrophobic segments capable of solubilizing lipophilic substances and an outer hydrophilic corona serving as stabilizer interface between the hydrophobic core and the external aqueous environment. The size, charge, and surface properties can be select simply by adding new ingredients to the mixture of amphiphilic substance. The modification can be done before micelle preparation and/ or by variation of the preparation method. It depends on the delivery purpose of the micelle application.⁷⁶

Amphiphilic diblock copolymers are mainly used for the preparation of polymeric micelles, which ease of these copolymers has unique advantages for drug delivery. An appropriate polymer can be chosen to achieve critical purposes so as to modify the drug release profile, to prolong circulation time or to introduce targeting moieties. However, the linear structures of diblock copolymers have issued the micelle stability, as the influence of molecular architecture to polymer's physical properties.⁷⁷

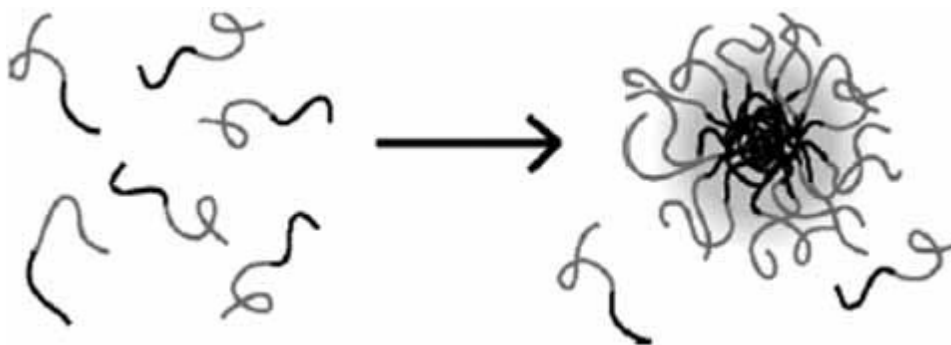


Figure 2. 11 Model of polymeric micelles compounds. The dark regions represent the hydrophobic blocks and lighter regions represent hydrophilic blocks⁷⁵

There are some advantages that can be provided by using micelles as drug delivery vehicles. The ability of micelles to deliver drug at specific target contributed by their higher intrinsic water solubility thus increase the bioavailability. Micelle's small size, unique nanoscopic architecture, good stability and the compatibility with the drug of choice are all the advantages of micelles to be used for drug delivery system.⁷⁸

One such problem that related to micelle's stability is a property which known as polymer's critical micelle concentration (CMC). The CMC represents a specific concentration above which the formation of micelles is thermodynamically favorable. Consequently, when the concentration of the copolymer solution drops below the CMC the micelles will disassemble. This is major concern for their application as drug carriers in vivo since severe dilution, which occurs upon injection into the bloodstream, can alter the micelle structure and size, and potentially result in total dissociation. This makes it difficult to control the rate of drug release and can even lead to serious toxicity issues if the micelles spontaneously dissociate and release high concentration of the drug.^{79,80}

The advantageous biocompatibility, biostability, and biodistribution of polymeric micelles have been attempted many researchers to use it for targeted drug delivery as well, in particular with regards to targeting solid tumors, cancer, and any other treatment. A poly(ethylene glycol)-b-poly(aspartic acid) (PEG-b-poly(aspartic acid)) micelles that carry physically bound doxorubicin (DOX) in their cores has progressed into phase II clinical trials at the National Cancer Institute in Japan for treatment of pancreatic cancer.⁸¹ Many other micelles formulations of anticancer drug are being tested in the same manner for preferential tumor accumulation such as cisplatin⁶⁶, methotrexate, paclitaxel, and camptothecin.⁷⁶ Overall, the use of micelles as drug delivery vehicles has been proved to be highly effective.

2.3.2 Dendrimers

Dendrimers are monodisperse macromolecules that have three-dimensional structure. These globular macromolecules are highly branched with many arms originating from central core.⁸² The first reports of dendrimers studies were about two decades ago, which only focused on the synthesis process and dendrimers chemical-physical properties. However, the potential of dendrimers in biological applications just started to explore in the past decade. This invention led to another discovery, that dendrimers are really promising in so many fields of bioscience including drug delivery, immunology and antimicrobials applications.⁸³

There are two general procedures to synthesis dendrimers that will have different branching resulting at the end of the reaction⁸², which are:

1. The divergent method, where repeat monomers are branched outward from a central core
2. The convergent method developed by Frechet et.al., where the synthesis begins at the periphery and grows inward.

The convergent approach affords better control of the ultimate dendritic architecture than the divergent approach does. But compare to the convergent method, the divergent method has been shown to be suitable for larger-scale production of dendrimers. The stepwise synthesis of dendrimers affords molecules with highly regular branching pattern, a unique molecular weight or a low polydispersity index, and a well-defined number of peripheral groups.

The application of dendrimers in biomedical application have been explored by numerous research group and becoming the most attractive research areas. Starting in 1993, the first report of the use of PAMAM (polyamidoamine) dendrimers for gene transfection had been published by Haensler and Szoka.⁸⁴ Followed by another research group, that reported the efficient transfer of genetic material by using the same type of dendrimers. Recently, dendrimers also have been used in Magnetic Resonance Imaging (MRI) as carriers of chelating groups for MRI agents.⁸³

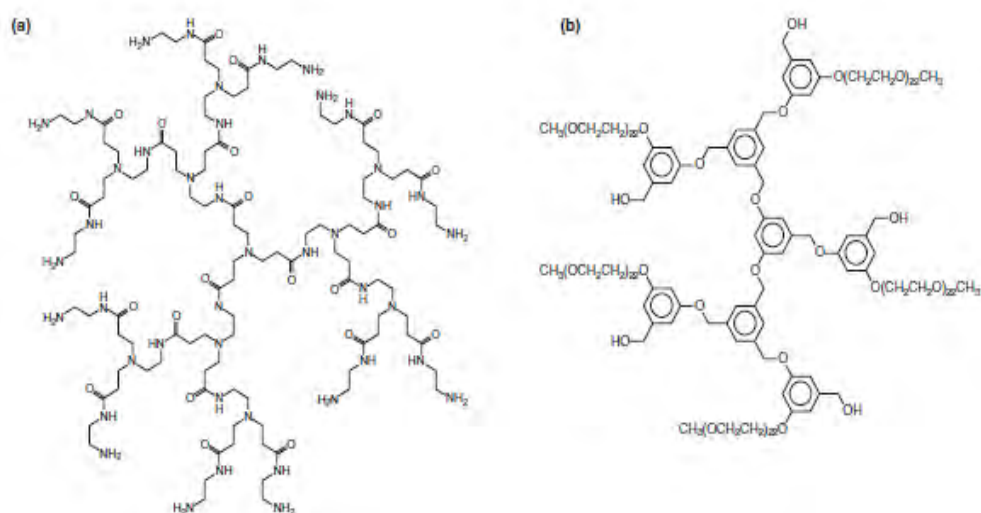


Figure 2. 12 Description of biocompatible dendrimers for drug delivery. (a) PAMAM dendrimer. (b) Polyaryl ether dendrimer⁸⁴

Due to the well-defined structure, compact globular shape, size monodispersity and controllable functionality, dendrimers are the excellent candidates for drug delivery vehicles.^{82,83} It can be used as potential drug delivery carriers in two ways:

1. Drug molecules can be physically entrapped inside the dendritic structure, by using the internal ‘cavity’ of an appropriately designed dendritic structure or based on multiple noncovalent and hydrophobic interaction.
2. Drug molecules can be covalently attached onto surface or other functionalities to afford dendrimer-drug conjugate.

Dendrimers morphology, dendritic unimolecular micelles, has offered other advantages as drug delivery vehicles compare with conventional polymeric micelles. It can form unimolecular micelles in which the hydrophilic and hydrophobic segments are connected covalently. Micelle’s structure also can be maintained at every concentration and in a variety of solvents, because it is more static rather than dynamic.

The application of dendrimers as drug delivery vehicles has been started by exploits its excellent capability to attach drug molecules into the dendrimers periphery. The conjugation of PAMAM dendrimers with cisplatin as a potent anticancer drug, the antitumor drug, and any others drugs has demonstrated the advantages of dendrimers for drug delivery.⁸⁴

In every drug-dendrimers conjugation system, it has shown that the water solubility and circulation time can be increased, as the opposite of the systemic toxicity that will be decrease. This recent research has shown that dendrimers can provide practical solutions to drug delivery issues such as solubility, bio-distribution and targeting. On the other hand, it is still a challenge to prepare

dendrimers that can be eliminated from the body at reasonable rates and to solve the tissue localization problems.

2.3.3 Star Polymer

Started in 1948, the first star polymer molecules had been synthesized by Schaeffgen and Flory.⁸⁵ Both researchers used ϵ -caprolactam in the presence of either cyclohexanonetetrapropionic or dicyclohexanoneoctacarboxylic and obtained tetra- and octachain star shaped polyamides. Followed by Morton and coworkers in 1962 that had successfully synthesized four-arm star polystyrene (PS) using anionic polymerization method.^{85,86} Furthermore, the study of star polymer synthesis has become more interesting using many different systems, such as: cationic, group transfer, or living ring-opening metathesis polymerization.⁸⁷

A star polymer has unique properties in terms of the relationship between arm number, arm molecular weight and solvent viscosity. It consists of a three-dimensional architecture where linear arms are linked by a central core. Hadjichristidis (1999) has been explained through his paper that a star polymer represent an interesting class of macromolecules because it can has a very high molecular weight but still possess the solubility and viscosity which similar with linear or branched polymer of relatively low molecular weight.⁸⁸

Based on the chemical compositions of the arm species, star polymer can be classified into two categories: homo-arm (or regular) star polymer or miktoarm (or

heteroarm) star copolymers.⁸⁶ Homoarm star polymer consists of a symmetrical structure comprising radiating arm with identical chemical composition and similar molecular weight. In contrast, a miktoarm star molecule contains two or more arm species with different chemical compositions and/or molecular weight and/or different periphery functionality.⁸⁹ The differences of homoarm and miktoarm star molecule can be seen at the figure 2.13 below.

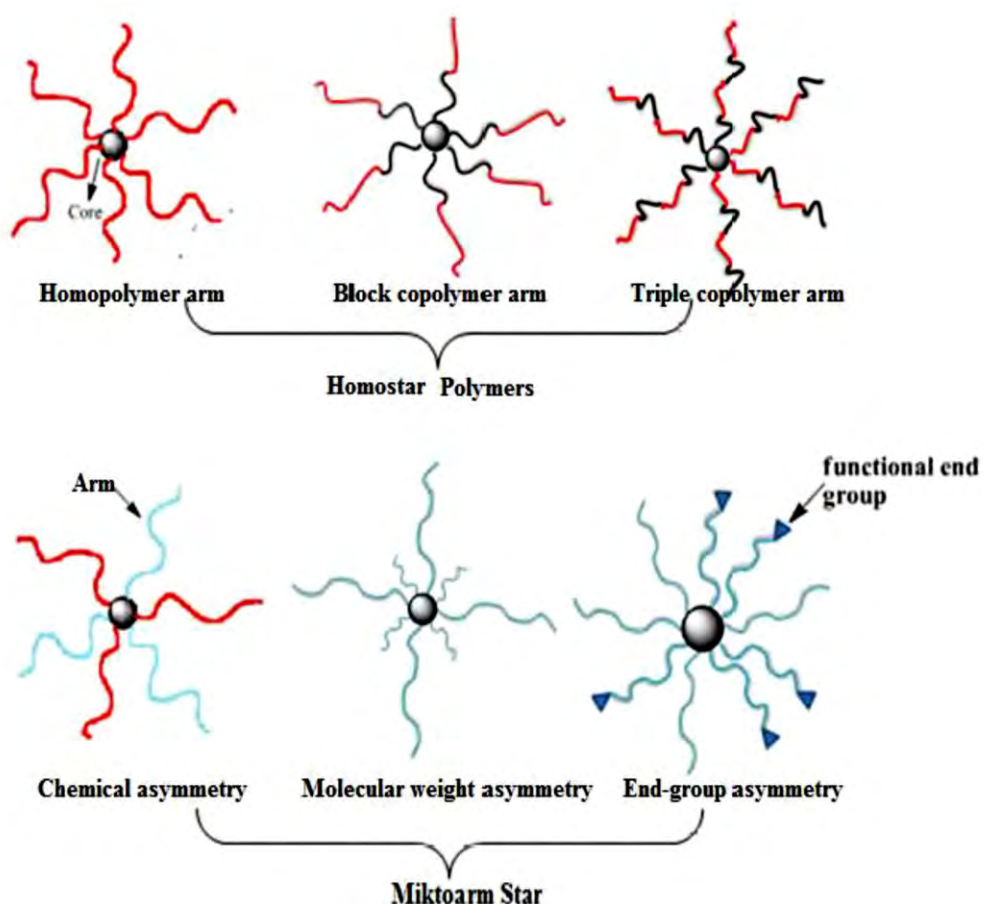


Figure 2. 13 The structures of homostar and miktoarm polymer⁸⁶

Another way to classify the star polymer is based on the molecule architecture. Star polymer can be divided into dendristar and core cross-linked star (CCS) polymer, which the preparation also using two different ways. Compared to

dendristar, the CCS polymer has become more interesting both in research and application area due to their unique three dimensional architecture and properties.⁸⁷

The CCS polymer consists of a highly cross-linked core domain surrounded by a number of radiating linear arms, typically ranging from anywhere between 10 and 100 arms per star, depending on the reaction condition. The architectural make up of this type of polymer generates some very interesting rheological properties in that CCS polymers have very high molecular weight. However, the solubility and viscosity characteristic are similar to linear or branched polymers with relatively low molecular weight. Properties such as these have led to a wide range of potential applications for CCS polymer particularly in the areas of drug delivery.⁹⁰

In general, well-defined star polymer can be prepared via controlled polymerization techniques using three approaches: arm first approach, core first approach, and coupling onto (grafting to) approach.⁸⁹ The arm-first technique attaches several linear polymer chains to each other at a single point either by using a multifunctional low molecular weight molecule or a crosslinking agent. The core-first technique employs a multifunctional initiator, and the numbers of arms is directly given by the number of initiating sites on the core. The last method can be described as the combination of controlled polymerization and coupling reaction. A well-defined polymer using as 'the arm', is prepared via controlled polymerization and coupled to a multifunctional linking agent that acts as 'the core'. The comparison of all three methods can be seen at the Figure 2.14.

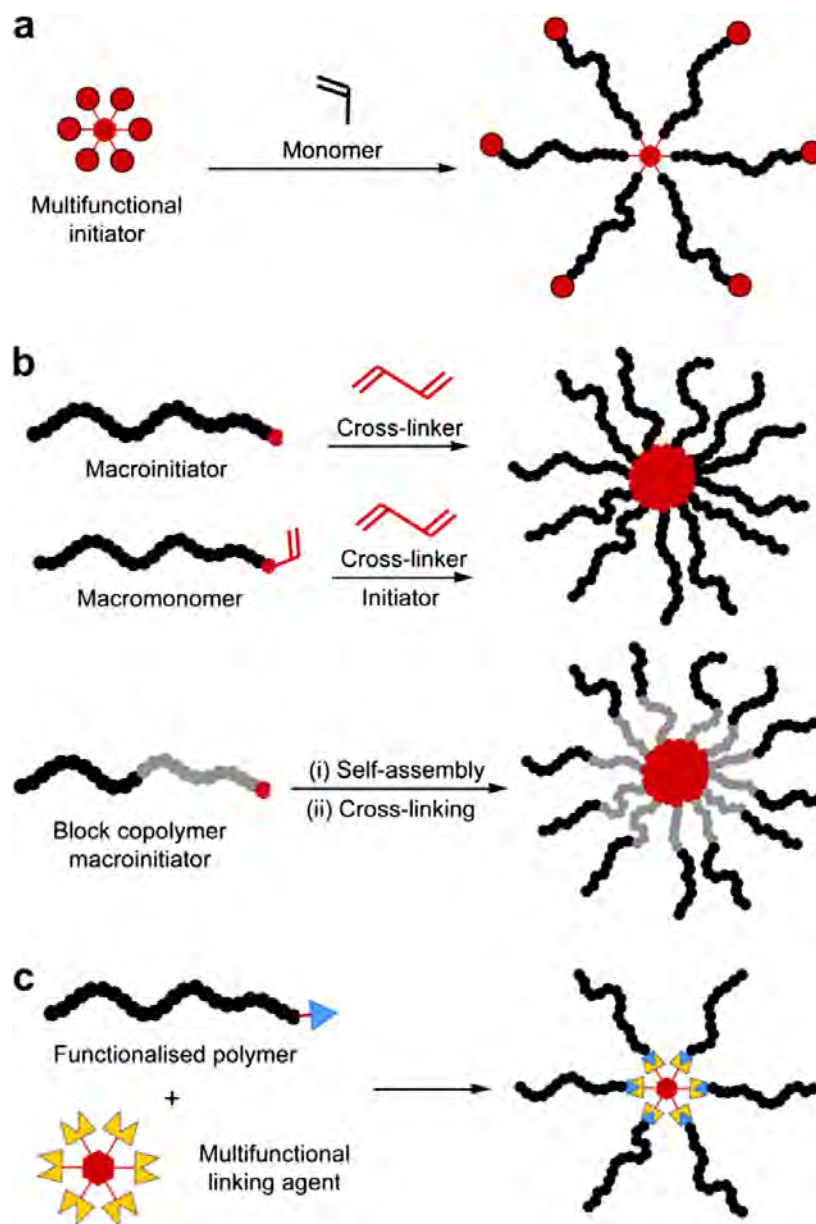


Figure 2.14 Schematic drawing of the synthesis of star polymer: comparison of the ‘arm-first’ method, ‘core-first’ method and coupling onto method⁹⁰

The limitation of arms number on the star polymer to the initial functionality of the initiator, and typically result in a relatively low-molecular weight with limited drug loading capacity, has cause the lack of using ‘core-first’ to synthesis star polymer . To overcome this problem the ‘arm-first’ approach can be used as living

linear arms capable of further chain extension are initially synthesized. These terminally reactive linear polymer chains are subsequently used to initiate the polymerization of a class-linkable monomer such that the active arms ends are coupled together. Gao, et.al has described that this technique involves the copolymerization of linear macromonomer with cross-linker using low-molar-mass initiators.⁹¹ Both these technique result in star polymer with high-molecular-weight cross-linked cores surrounded by many polymeric arms, known as core cross-linked star (CCS) polymer.

Star polymers are gaining interest because of their characteristic rheological and dilute solution properties. The combination of unique rheological properties and the ability to employ controlled polymerization techniques to obtain well-defined structures makes this class of macromolecule very attractive for use in a variety of applications including that of drug delivery. The CCS polymer is ideally suited for use as a potential drug delivery device because of the large loading capacity of the hydrophobic core, the size of which can be easily altered through the use of a 'spacer monomer' during the core formation step. The ability to independently control the length and type of arm relative to the core is also very attractive property for pharmaceutical applications.^{87,92}

Star polymers have attracted significant attention due to their potential feature in drug delivery system. Duan, et.al has successfully synthesized a multiarm poly(acrylic acid) star polymer via macromolecular design, using the interchange (MADIX)/reversible addition fragmentation chain transfer (MADIX/RAFT) for

polymerization⁶⁷. The drug release result has shown that the star polymer is suitable for the multimodal delivery of both hydrophilic (cisplatin) and hydrophobic (NO donating prodrug) chemotherapeutic, as either a single-drug chemotherapy or a combinational regimen. Some studies that highlighted the use of star polymer as drug delivery vehicles also have been done by CAMD researchers. The synthesis of very well-defined, narrow polydispersity 'arm-first' POEGMA-based star polymers composed of aldehyde functional biodegradable cores using RAFT polymerization has been reported by Liu, et.al.⁹³ Aldehyde groups in the star cores were exploited to reversibly attach doxorubicin through condensation reaction. In vitro studies (cytotoxicity and cell uptake) confirmed the viability of using star polymers as drug carriers.

Previous study from CAMD team also has exploited the potency of glutathione-sensitive star polymer for release of drug in cells for the synergetic effect of NO and cisplatin, an anticancer drug. In this study, the concentration of glutathione, a natural tripeptide buffering the thiol-disulfide balance of cells, can be as high as 10 nM. Recently, some preliminary studies have been focused on the development of degradable CCS polymers with the potential to control the rate of drug release relative to the degradation rate.

2.4 Synthesis of NO polymeric nanocarriers via RAFT polymerization process

As various nanosystem have been developed, the importance of polymer architecture-properties relationship has gradually been realized and emphasized. Polymer architecture describes the shape of a single polymer molecule, which often determines its physicochemical properties. Including in NO delivery system, the structures of nanoparticles that been use as nanocarriers have significantly impact the stability and biodistribution along the NO release mechanism. Due to its ability to synthesize various architecture of a wide variety of polymers with water solubility under mild conditions, RAFT polymerization has become the most approvable technique to new generation of NO polymeric nanocarriers.

RAFT polymerization was first reported by the Australian CSIRO group in 1998. The mechanism of RAFT polymerization as originally proposed operates as degenerative chain transfer process. The RAFT process is similar to conventional free radical polymerization but incorporates a chain transfer agent (CTA). The CTA typically contains a thiocarbonylthio moiety that is reactive towards radicals, subsequently facilitating the fragmentation of the resulting intermediate radical species. The well-defined complex macromolecules made by RAFT can be used to build nanostructures such as micelles, vesicles, and nanoparticles.^{16,94} In addition, synthetic polymers can be combines with biomolecules or inorganic nanoparticles to address problems in medicine and nanotechnology. Generic structure of the RAFT chain transfer agent is shown in the figure 2.15.

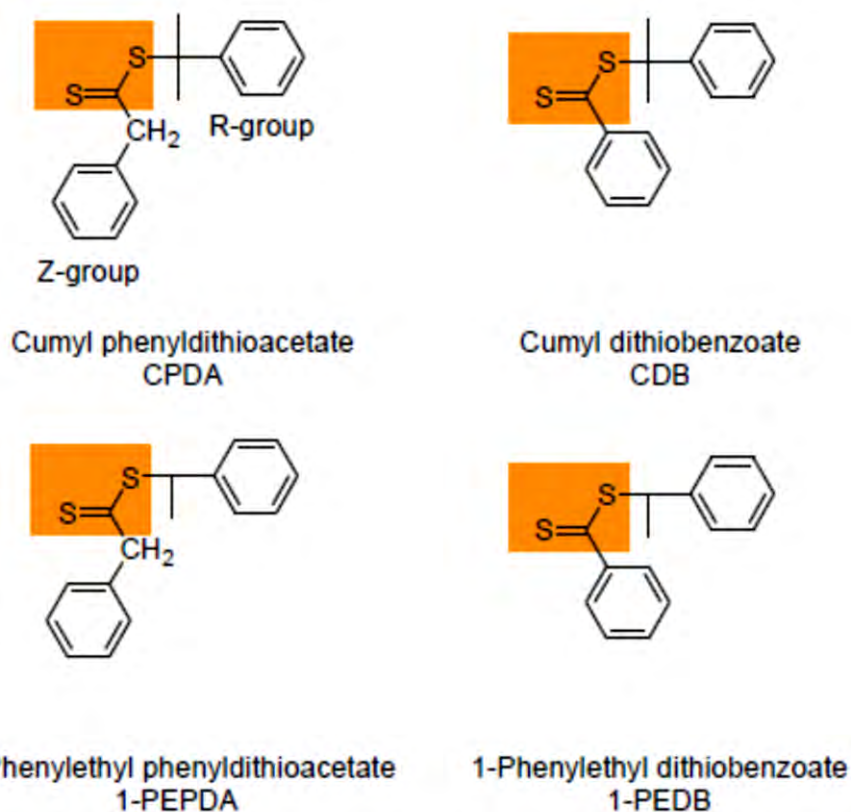


Figure 2.15 Chemical structures of RAFT chain transfer agent (CTA) or RAFT agents¹⁶

The generally mechanism for RAFT polymerization is shown in Figure 2.16. Begins with initiation step as the first step when a radical is generated (step 1), followed by the reaction of this radical with RAFT agent (step 2). The initiation process in the first step can be triggered by so many different sources, such as heat (thermal autoinitiation) and light (direct photochemical by ultraviolet light). In the second step, the radical will react with the RAFT agent to generate a new radical and the active propagative radical.

Based on previous work, it has been confirmed that this RAFT agent can be all consumed in the condition of appropriate choices due to the highly reactive C=S bond of the RAFT agent. Polymer chain will be growth in the propagation step (step 3) by adding monomer, and the termination reaction (step 4) take place at the end *via* combination or disproportionation mechanism.

RAFT polymerization has been use as an effective process to design complex polymeric architectures, such as block copolymer, graft, star, dendrimers and micelle. Variety of copolymer is easily synthesized through this process under mild condition. The AB type of block copolymer can be produced by sequential addition of monomer “B” to a macro-RAFT agent which produced by the polymerization of monomer “A” mediated by the RAFT agent.⁹⁵

Graft copolymer also can be prepared using RAFT process via the “grafting from” technique or the “grafting through” technique. The “grafting from” technique involves the functionalization of a polymer backbone or substrate with a RAFT agent or with radical initiation. In the other hand, the “grafting through” technique involves the polymerization of a polymer chain showing reactive vinyl groups at its chain ends.¹⁶

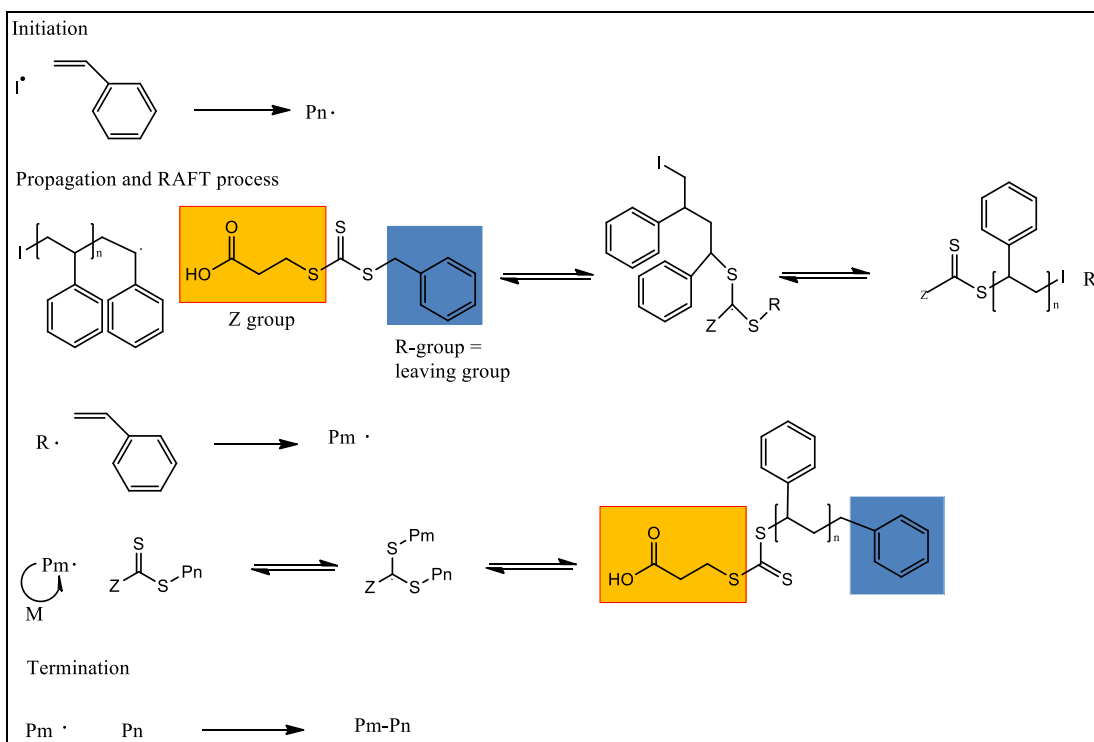


Figure 2. 16 Generally accepted mechanism of RAFT/MADIX polymerization¹⁶

Another polymer structure that can achieve via RAFT polymerization is highly branched polymers and star polymers. Highly branched polymers can be prepared using RAFT agent that bears a polymerizable vinyl group or by polymerizing a monofunctional monomer in the presence of difunctional monomer and RAFT agent. Star polymer can be synthesized via RAFT using two main mechanisms: the core first approach and the arm first approach. The core first approach requires the use of multifunctional RAFT agent, where the polymer chains (arms) are grown from the core. The arm first approach involves the synthesis of polymeric arms of predetermined molecular weight, which are joined together post polymerization.^{16,96}

Figure 2.17 has shown various types of polymers with complex structures that can be achieved by using RAFT polymerization as the method.

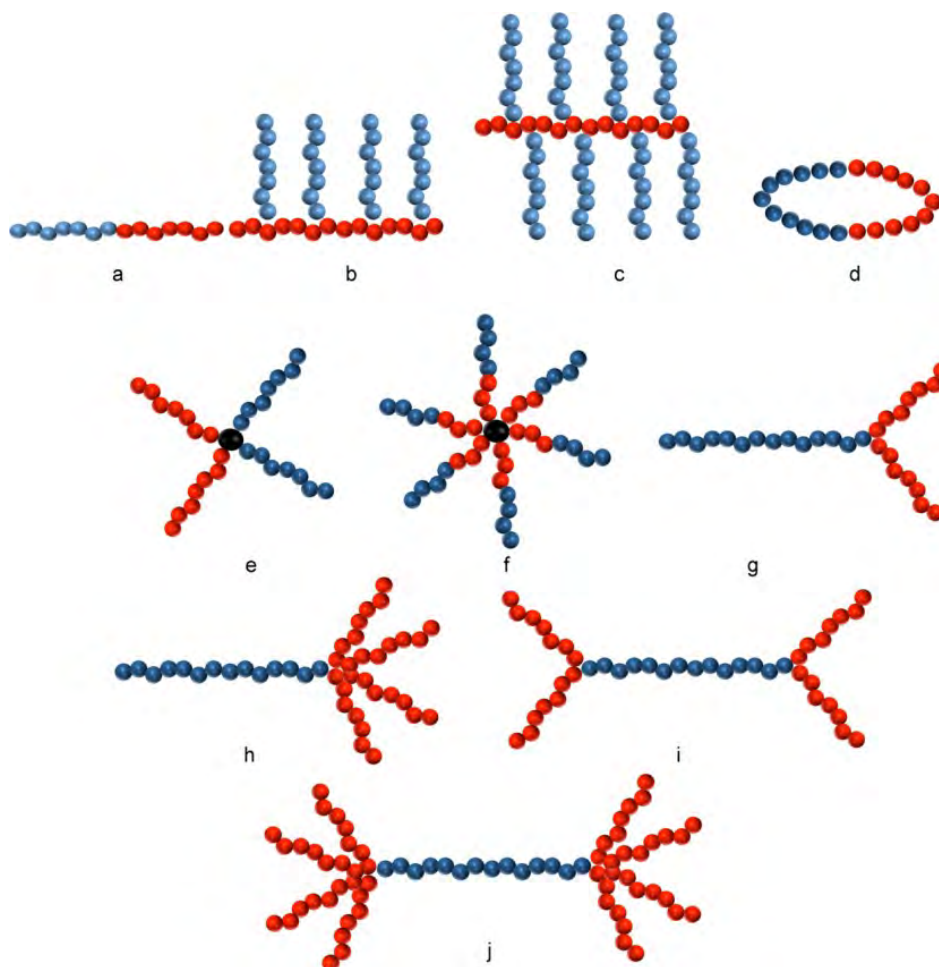


Figure 2.17 Complex architectures accessible via the RAFT process¹⁷

There are not many reports about the preparation of NO nanoparticles using RAFT polymerization. Only few studies has been done but generally all the result has showed the potent and interesting conclusion about RAFT method to be used in NO delivery system. Jo, et.al have designed block copolymer micelles using N-acryloylmorpholine and N-acryoyl-2,5-dimethylpiperazine.⁹⁷ RAFT

polymerization was employed to synthesize well-defined block copolymers and then prepared hydrophobic poly(N-diazeniumdiolate)(poly(NONOate)). Other polymeric nanoparticles include: matrix of ethylene/vinylacetate and multi arm (star) polymer.⁶⁷ All these works have showed good results in which the polymer architecture were successfully synthesized and achieved higher concentration of NO release. The formation of micelles NO-nanoparticles by Jo and coworkers is shown in figure below.

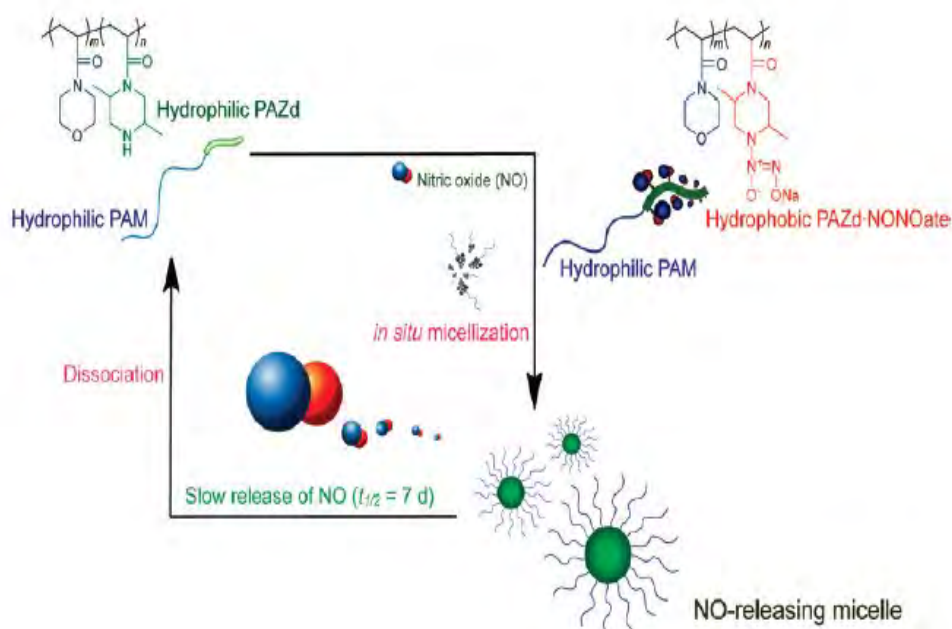


Figure 2. 18 In situ formation of PAM-PAZd•NONOate micelles⁹⁷

The synthesis of NO-functionalized polymer nanoparticles for NO delivery using RAFT polymerization also had been reported by our group. A straight forward and versatile method was used to conjugate nitrosoglutathione (GSNO) NO donor to polymeric nanoparticle.⁷¹

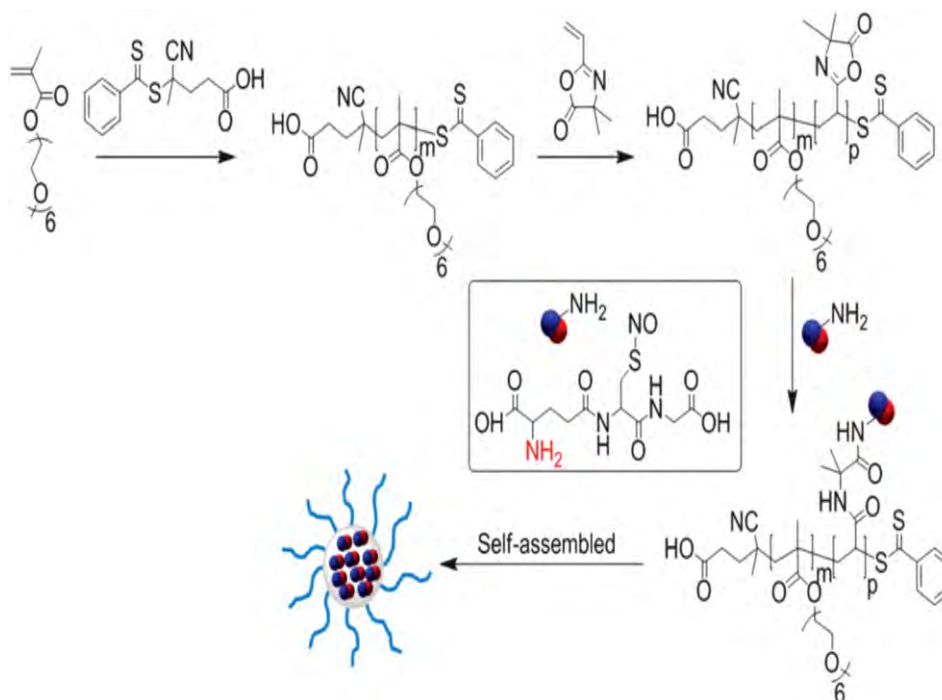


Figure 2. 19 Synthesis of NO-functionalized polymeric nanoparticles⁷¹

The result showed that NO-nanoparticles from RAFT process is quite stable and could efficiently release NO intracellular. Another preliminary study to prepare NO-nanoparticles via RAFT polymerization also confirmed this conclusion and become a platform to continue this work by preparing different polymeric NO-nanoparticles with higher stability and biodistribution.

2.5 Conclusions

Polymeric nanoparticles can be used to improve the stability and bio distribution of NO delivery. There are some properties requirements of polymeric nanoparticles for NO delivery, which includes: can release NO at slow rate, sufficiently small less than 100 nm, and high stability during the penetration or

NO release process. These properties may only be held by polymeric nanoparticles with specific and complex structure, such as block copolymer, micelles, and multi arm (star) polymer. RAFT polymerization has the ability to prepare various architectures of wide variety polymers with defined end and pendant functionalities. Previous works reported that synthesized of polymeric NO-nanoparticles using RAFT polymerization can improve the stability and bio distribution issues during NO release.³⁰ This conclusion will be used as a platform to develop other polymeric nanoparticles with different structures as NO nanocarriers.

2.6 References

- (1) Body, S. C.; Hartigan, P. M.; Shernan, S. K.; Formanek, V.; Hurford, W. E. *Journal of cardiothoracic and vascular anesthesia* **1995**, *9*, 748.
- (2) Carpenter, A. W.; Schoenfisch, M. H. *Chemical Society Reviews* **2012**, *41*, 3742.
- (3) Naseem, K. M. *Molecular Aspects of Medicine* **2005**, *26*, 33.
- (4) Ichinose, F.; Roberts, J. D.; Zapol, W. M. *Circulation* **2004**, *109*, 3106.
- (5) Bogdan, C. *Nat Immunol* **2001**, *2*, 907.
- (6) Sonveaux, P.; Jordan, B. F.; Gallez, B.; Feron, O. *European journal of cancer (Oxford, England : 1990)* **2009**, *45*, 1352.
- (7) Coulter, J. A.; McCarthy, H. O.; Xiang, J.; Roedl, W.; Wagner, E.; Robson, T.; Hirst, D. G. *Nitric Oxide* **2008**, *19*, 192.
- (8) Muntané, J.; la Mata, M. D. *World journal of hepatology* **2010**, *2*, 337.

- (9) Schairer, D. O.; Chouake, J. S.; Nosanchuk, J. D.; Friedman, A. J. *Virulence* **2012**, *3*, 271.
- (10) Nichols, S. P.; Storm, W. L.; Koh, A.; Schoenfisch, M. H. *Advanced Drug Delivery Reviews* **2012**, *64*, 1177.
- (11) Webb, D. J.; Megson, I. L. *Expert Opinion on Investigational Drugs* **2002**, *11*, 587.
- (12) Riccio, D. A.; Schoenfisch, M. H. *Chemical Society Reviews* **2012**, *41*, 3731.
- (13) Saraiva, J.; Marotta-Oliveira, S. S.; Cicillini, S. A.; Eloy, J. d. O.; Marchetti, J. M. *Journal of drug delivery* **2011**.
- (14) Kapadia, M. R.; Chow, L. W.; Tsihlis, N. D.; Ahanchi, S. S.; Eng, J. W.; Murar, J.; Martinez, J.; Popowich, D. A.; Jiang, Q.; Hrabie, J. A.; Saavedra, J. E.; Keefer, L. K.; Hulvat, J. F.; Stupp, S. I.; Kibbe, M. R. *Journal of Vascular Surgery* **2008**, *47*, 173.
- (15) Huerta, S., Chilka, S., & Bonavida, B. *international Journal of Oncology* **2008**, *33*, 909.
- (16) Boyer, C.; Stenzel, M. H.; Davis, T. P. *Journal of Polymer Science Part A: Polymer Chemistry* **2011**, *49*, 551.
- (17) Gregory, A.; Stenzel, M. H. *Expert Opinion on Drug Delivery* **2011**, *8*, 237.
- (18) Bill Cai, T.; Wang, P. G.; Holder, A. A. In *Nitric Oxide Donors*; Wiley-VCH Verlag GmbH & Co. KGaA: 2005, p 1.
- (19) Vallance, P. *Fundamental & Clinical Pharmacology* **2003**, *17*, 1.

- (20) Murad, F. *Angewandte Chemie International Edition* **1999**, *38*, 1856.
- (21) Rodeberg, D. A.; Chaet, M. S.; Bass, R. C.; Arkovitz, M. S.; Garcia, V. F. *The American Journal of Surgery* **1995**, *170*, 292.
- (22) Griffith, O. W.; Stuehr, D. J. *Annual Review of Physiology* **1995**, *57*, 707.
- (23) Calabrese, V.; Mancuso, C.; Calvani, M.; Rizzarelli, E.; Butterfield, D. A.; Giuffrida Stella, A. M. *Nat Rev Neurosci* **2007**, *8*, 766.
- (24) Scatena, R.; Bottoni, P.; Martorana, G. E.; Giardina, B. *Expert Opinion on Investigational Drugs* **2005**, *14*, 835.
- (25) Welch, G.; Loscalto, J. *Journal of Cardiac Surgery* **1994**, *9*, 361.
- (26) Pacher, P.; Beckman, J. S.; Liaudet, L. *Physiological Reviews* **2007**, *87*, 315.
- (27) Wink, D. A.; Vodovotz, Y.; Laval, J.; Laval, F.; Dewhirst, M. W.; Mitchell, J. B. *Carcinogenesis* **1998**, *19*, 711.
- (28) Wallace, J. L. *British Journal of Pharmacology* **2007**, *152*, 421.
- (29) Rigas, B. *Current opinion in gastroenterology* **2007**, *23*, 55.
- (30) Duong, H. T. T.; Kamarudin, Z. M.; Erlich, R. B.; Li, Y.; Jones, M. W.; Kavallaris, M.; Boyer, C.; Davis, T. P. *Chemical Communications* **2013**, *49*, 4190.
- (31) Ghaffari, A.; Miller, C. C.; McMullin, B.; Ghahary, A. *Nitric Oxide* **2006**, *14*, 21.
- (32) Arciola, C. R.; Campoccia, D.; Speziale, P.; Montanaro, L.; Costerton, J. W. *Biomaterials* **2012**, *33*, 5967.
- (33) O'Toole, G.; Kaplan, H. B.; Kolter, R. *Annual Review of Microbiology* **2000**, *54*, 49.

- (34) Phillips, P.; Sampson, E.; Yang, Q.; Antonelli, P.; Progulske-Fox, A.; Schultz, G. *Wound Healing Southern Africa* **2009**, *1*, 10.
- (35) Donlan, R. M. *Clinical Infectious Diseases* **2001**, *33*, 1387.
- (36) Phillips, P.; Wolcott, R.; Fletcher, J.; Schultz, G. *Wounds International* **2010**, *1*, 1.
- (37) Ignarro, L. J. *Nitric oxide: biology and pathobiology*; Academic press, 2000.
- (38) Miller, M. R.; Megson, I. L. *British Journal of Pharmacology* **2007**, *151*, 305.
- (39) Scatena, R.; Bottoni, P.; Pontoglio, A.; Giardina, B. *Current medicinal chemistry* **2010**, *17*, 61.
- (40) Yamamoto, T.; Bing, R. J. *Proceedings of the Society for Experimental Biology and Medicine* **2000**, *225*, 200.
- (41) Lehmann, J. *Expert Opinion on Therapeutic Patents* **2000**, *10*, 559.
- (42) Fung, H.-L.; Chung, S.-J.; Bauer, J. A.; Chong, S.; Kowaluk, E. A. *The American Journal of Cardiology* **1992**, *70*, B4.
- (43) Nicolescu, A. C., Queen's University, 2004.
- (44) Coneski, P. N.; Schoenfisch, M. H. *Chemical Society Reviews* **2012**, *41*, 3753.
- (45) Maragos, C. M.; Morley, D.; Wink, D. A.; Dunams, T. M.; Saavedra, J. E.; Hoffman, A.; Bove, A. A.; Isaac, L.; Hrabie, J. A.; Keefer, L. K. *Journal of medicinal chemistry* **1991**, *34*, 3242.

- (46) Drago, R. S.; Paulik, F. E. *Journal of the American Chemical Society* **1960**, *82*, 96.
- (47) Hrabie, J. A.; Klose, J. R.; Wink, D. A.; Keefer, L. K. *The Journal of Organic Chemistry* **1993**, *58*, 1472.
- (48) Vanderford, P. A.; Wong, J.; Chang, R.; Keefer, L. K.; Soifer, S. J.; Fineman, J. R. *Journal of cardiovascular pharmacology* **1994**, *23*, 113.
- (49) Brilli, R. J.; Krafte-Jacobs, B.; Smith, D. J.; Roselle, D.; Passerini, D.; Vromen, A.; Moore, L.; Szabó, C.; Salzman, A. L. *Journal of Applied Physiology* **1997**, *83*, 1968.
- (50) Talukdar, A.; Wang, P. G. In *Nitric Oxide Donors*; Wiley-VCH Verlag GmbH & Co. KGaA: 2005, p 55.
- (51) Saavedra, J. E.; Billiar, T. R.; Williams, D. L.; Kim, Y.-M.; Watkins, S. C.; Keefer, L. K. *Journal of Medicinal Chemistry* **1997**, *40*, 1947.
- (52) Cai, T. B.; Wang, P. G. *Expert Opinion on Therapeutic Patents* **2004**, *14*, 849.
- (53) Tabor, H.; Tabor, C. W. In *Advances in Enzymology and Related Areas of Molecular Biology*; John Wiley & Sons, Inc.: 2006, p 203.
- (54) Rauli, R.; McElhaney-Feser, G.; Hrabie, J.; Cihlar, R. *Rec Res Devel Microbiol* **2002**, *6*, 177.
- (55) Dukelow, A. M.; Weicker, S.; Karachi, T. A.; Razavi, H. M.; McCormack, D. G.; Joseph, M. G.; Mehta, S. *CHEST Journal* **2002**, *122*, 2127.
- (56) Shabani, M.; Pulfer, S. K.; Bulgrin, J. P.; Smith, D. J. *Wound Repair and Regeneration* **1996**, *4*, 353.

- (57) Al-Sa'doni, H.; Ferro, A. *Clin. Sci.* **2000**, *98*, 507.
- (58) Singh, R. J.; Hogg, N.; Joseph, J.; Kalyanaraman, B. *Journal of Biological Chemistry* **1996**, *271*, 18596.
- (59) Veleparampil, M. M.; Aravind, U. K.; Aravindakumar, C. T. *Advances in Physical Chemistry* **2009**, *2009*.
- (60) Williams, D. L. H. *Accounts of chemical research* **1999**, *32*, 869.
- (61) Williams, D. L. H. In *The Chemistry of Amino, Nitroso, Nitro and Related Groups*; John Wiley & Sons, Ltd: 2003, p 665.
- (62) Al-Sa'doni, H. H.; Khan, I. Y.; Poston, L.; Fisher, I.; Ferro, A. *Nitric Oxide* **2000**, *4*, 550.
- (63) Han, G.; Martinez, L. R.; Mihu, M. R.; Friedman, A. J.; Friedman, J. M.; Nosanchuk, J. D. *PLoS ONE* **2009**, *4*, e7804.
- (64) Jain, A.; Jain, S. K. *Critical Reviews™ in Therapeutic Drug Carrier Systems* **2008**, *25*.
- (65) Yoo, J.-W.; Lee, J.-S.; Lee, C. H. *Journal of Biomedical Materials Research Part A* **2010**, *92A*, 1233.
- (66) Nishiyama, N.; Kataoka, K. *Pharmacology & Therapeutics* **2006**, *112*, 630.
- (67) Duan, S.; Cai, S.; Yang, Q.; Forrest, M. L. *Biomaterials* **2012**, *33*, 3243.
- (68) Stasko, N. A.; Schoenfisch, M. H. *Journal of the American Chemical Society* **2006**, *128*, 8265.
- (69) Svenson, S.; Tomalia, D. A. *Advanced Drug Delivery Reviews* **2012**, *64*, *Supplement*, 102.

- (70) Friedman, A. J.; Han, G.; Navati, M. S.; Chacko, M.; Gunther, L.; Alfieri, A.; Friedman, J. M. *Nitric Oxide* **2008**, *19*, 12.
- (71) Duong, H. T. T.; Marquis, C. P.; Whittaker, M.; Davis, T. P.; Boyer, C. *Macromolecules* **2011**, *44*, 8008.
- (72) Liechty, W. B.; Kryscio, D. R.; Slaughter, B. V.; Peppas, N. A. *Annual review of chemical and biomolecular engineering* **2010**, *1*, 149.
- (73) Jagur-Grodzinski, J. *Polymers for Advanced Technologies* **2009**, *20*, 595.
- (74) Qiu, L.; Bae, Y. *Pharm Res* **2006**, *23*, 1.
- (75) Kedar, U.; Phutane, P.; Shidhaye, S.; Kadam, V. *Nanomedicine: Nanotechnology, Biology and Medicine* **2010**, *6*, 714.
- (76) Ebrahim Attia, A. B.; Ong, Z. Y.; Hedrick, J. L.; Lee, P. P.; Ee, P. L. R.; Hammond, P. T.; Yang, Y.-Y. *Current Opinion in Colloid & Interface Science* **2011**, *16*, 182.
- (77) Riess, G. *Progress in Polymer Science* **2003**, *28*, 1107.
- (78) Tyrrell, Z. L.; Shen, Y.; Radosz, M. *Progress in Polymer Science* **2010**, *35*, 1128.
- (79) Venkataraman, S.; Hedrick, J. L.; Ong, Z. Y.; Yang, C.; Ee, P. L. R.; Hammond, P. T.; Yang, Y. Y. *Advanced Drug Delivery Reviews* **2011**, *63*, 1228.
- (80) Gaucher, G.; Dufresne, M.-H.; Sant, V. P.; Kang, N.; Maysinger, D.; Leroux, J.-C. *Journal of Controlled Release* **2005**, *109*, 169.
- (81) Sawdon, A.; Peng, C. A. *Nanomedicine for Drug Delivery and Therapeutics* **2013**, 438.

- (82) Cheng, Y.; Xu, Z.; Ma, M.; Xu, T. *Journal of Pharmaceutical Sciences* **2008**, *97*, 123.
- (83) Patri, A. K.; Majoros, I. J.; Baker Jr, J. R. *Current Opinion in Chemical Biology* **2002**, *6*, 466.
- (84) Esfand, R.; Tomalia, D. A. *Drug Discovery Today* **2001**, *6*, 427.
- (85) Hadjichristidis, N. *Journal of Polymer Science Part A: Polymer Chemistry* **1999**, *37*, 857.
- (86) Hadjichristidis, N.; Iatrou, H.; Pitsikalis, M.; Mays, J. *Progress in Polymer Science* **2006**, *31*, 1068.
- (87) Wiltshire, J. T.; Qiao, G. G. *Australian Journal of Chemistry* **2007**, *60*, 699.
- (88) Hadjichristidis, N.; Pispas, S.; Pitsikalis, M.; Iatrou, H.; Vlahos, C. In *Branched Polymers I*; Roovers, J., Ed.; Springer Berlin Heidelberg: 1999; Vol. 142, p 71.
- (89) Hadjichristidis, N.; Pitsikalis, M.; Pispas, S.; Iatrou, H. *Chemical Reviews* **2001**, *101*, 3747.
- (90) Blencowe, A.; Tan, J. F.; Goh, T. K.; Qiao, G. G. *Polymer* **2009**, *50*, 5.
- (91) Gao, H.; Matyjaszewski, K. *Macromolecules* **2006**, *39*, 4960.
- (92) Khanna, K.; Varshney, S.; Kakkar, A. *Polymer Chemistry* **2010**, *1*, 1171.
- (93) Liu, J.; Duong, H.; Whittaker, M. R.; Davis, T. P.; Boyer, C. *Macromolecular Rapid Communications* **2012**, *33*, 760.
- (94) Barner, L.; Davis, T. P.; Stenzel, M. H.; Barner-Kowollik, C. *Macromolecular Rapid Communications* **2007**, *28*, 539.

- (95) Gregory, A.; Stenzel, M. H. *Progress in Polymer Science* **2012**, *37*, 38.
- (96) Barner-Kowollik, C.; Davis, T. P.; Stenzel, M. H. *Australian Journal of Chemistry* **2006**, *59*, 719.
- (97) Jo, Y. S.; van der Vlies, A. J.; Gantz, J.; Thacher, T. N.; Antonijevic, S.; Cavadini, S.; Demurtas, D.; Stergiopoulos, N.; Hubbell, J. A. *Journal of the American Chemical Society* **2009**, *131*, 14413.

Chapter 3. Instrumental analysis

This chapter will describe all the instruments used in the preparation of polymers and star polymers. All these instruments have been used to characterize and identified the polymers at the end of reaction, before and after purification process.

3.1 Gel permeation chromatography (GPC) measurements.

Gel permeation chromatography (GPC) also known as Size Exclusion Chromatography, is one of the most widely used analytical techniques for determination of molecular weight and molecular weight distribution of natural and synthetic polymers. Compare to other techniques, such as ultra-centrifugation, fractional precipitation and alternative fractional methods, it becomes more attractive because easier to obtain a qualitative chromatogram.

The principle of GPC operation is the separation of molecules based on their hydrodynamic radius (R_h) or volume (V_h), not molecular weight. The separation process takes place in GPC column which are packed with porous material such as polystyrene gel, glass beads, silica gel, etc. During the separation process, the larger molecules will elute faster through the porous packing materials than the smaller molecules. After the sample elutes from the column, it passes through a detector or series of detectors. At the end of the process, the output will be analyzed by data processing system (computer).

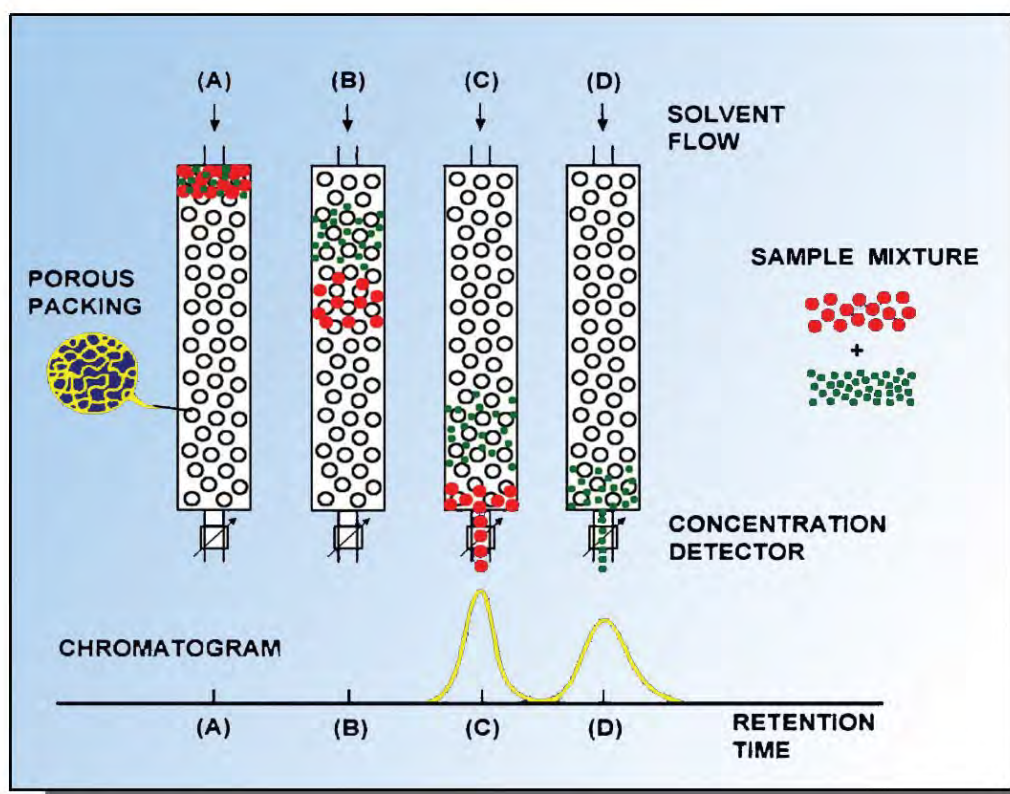


Figure 3. 1 Illustration of GPC separation mechanism¹

The GPC that been used in this study is a DMAc GPC. Polymers analyzed were performed in *N,N*-dimethylacetamide [DMAc; 0.03% w/v LiBr, 0.05% 2, 6-di-butyl-4-methylphenol (BHT)] at 50 °C (flow rate = 1 mL.min⁻¹) using a Shimadzu modular system comprised of an SIL-10AD auto-injector, a PL 5.0-mm bead-size guard column (50 × 7.8 mm) followed by four linear PL (Styragel) columns (105, 104, 103, and 500Å) and an RID-10A differential refractive-index detector. Calibration was achieved with commercial polystyrene standards ranging from 500 to 106 g/mol.

3.2 Nuclear Magnetic Resonance (NMR)

Nuclear Magnetic Resonance (NMR) is a technique for determination of organic compounds through measurement of the interaction between an oscillating radio-frequency electromagnetic field with a collection of nuclei immersed in a strong external magnetic field. These nuclei of many elemental isotopes have a characteristic spin (**I**) and it parts of atoms that are assembled into molecules. Some nuclei have integral spins (e.g. $I = 1, 2, 3 \dots$), some have fractional spins (e.g. $I = 1/2, 3/2, 5/2 \dots$), and a few have no spin, $I = 0$ (e.g. ^{12}C , ^{16}O , ^{32}S). Isotopes of particular interest and use to organic chemists are ^1H , ^{13}C , ^{19}F and ^{31}P with $I = 1/2$. A spinning charge produces a magnetic field, and in an external magnetic field (B_0) obtains two states: $+ 1/2$ aligned with the external and $-1/2$ opposed to the external field. In an energy field, the external magnetic field strength is the demarcation between the two spin states, but the difference is always very small. In this case, the small energy difference (ΔE) as a frequency is usually given ranging from 20 to 900 (106 Hz) determined by the magnetic field strength and the specific nucleus.

If a sample is placed in a magnetic field, and is subjected to radio frequency (RF) energy at the appropriate frequency, the energy will be absorbed through nuclei in the sample. The frequency of the radiation necessary for absorption of energy depends on the characteristic of the type of nucleus (e.g. ^1H , or ^{13}C), the chemical environment of the nucleus and spatial location in the magnetic field.

Structures of the synthesized compounds were analyzed by ^1H NMR spectroscopy. It used a Bruker DPX 300 spectrometer at 300 MHz for hydrogen nuclei and 75 MHz for carbon nuclei. In this study, most of the NMR spectra were recorded using a Bruker 300 MHz spectrometer at 25 °C. Different deuterated solvents including deuterated chloroform (CDCl_3), deuterated dimethyl sulfoxide (d-DMSO), and deuterated acetonitrile (CD_3CN) were used to dissolve samples. The use of these solvents and the monomer conversion determined by NMR will also be discussed in later chapters.

3.3 UV-visible spectroscopy

Ultraviolet-visible spectrophotometry is routinely used in analytical chemistry for the quantitative determination of different analyzes. According to the absorbance of different solutions and Beer's Law, concentration determination of an unknown solution or simultaneous determination of two different unknown solutions can be measured by this technology. The Beer-Lambert Law is useful for characterizing many compounds but does not hold as a universal relationship for the concentration and absorption of all substances. The method is most often used in a quantitative way to determine concentrations of an absorbing species in solution, using the Beer-Lambert law:

$$A = \log_{10} \frac{I_0}{I} = \epsilon l c$$

Where A is the measured absorbance, I_0 is the intensity of the incident light at a given wavelength, I is the transmitted intensity, L is the path length through the

sample, and c the concentration of the absorbing species. For each species and wavelength, ϵ is a constant.

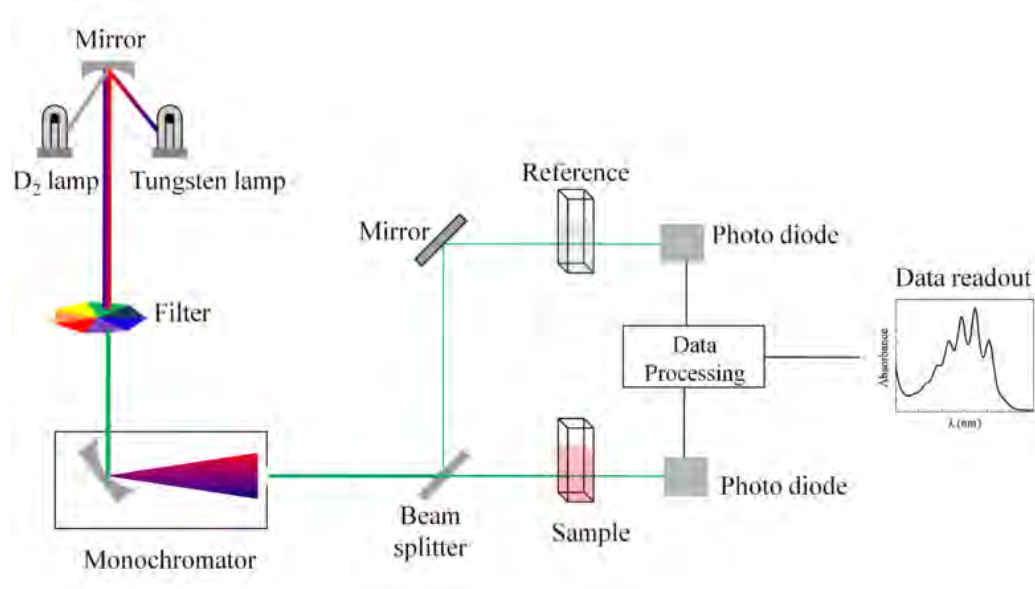


Figure 3. 2 Schematic of UV- visible spectrophotometer²

In this study, UV-visible spectra were recorded using a CARY 300 spectrophotometer (Bruker) equipped with a temperature controller.

3.4 Dynamic light scattering (DLS)

Dynamic light scattering (DLS), sometimes referred to as Photon Correlation Spectroscopy (PCS) or Quasi-Elastic Light Scattering (QELS), is a non-invasive, well-established technique for measuring the size and size distribution of particles including proteins, polymers, micelles, carbohydrates and nanoparticles dispersed or dissolved in a liquid. DLS is one of the most popularly utilized in measuring the size of particles. When shining a monochromatic light beam (such as laser) onto a solution with spherical

particles, all the particles in the solution will undergo a Brownian motion resulting in a Doppler Shift which depends on the size of particle. Therefore, the sample should be prepared by filtration or centrifugation to remove dust and artifacts from the solution. If the particles are smaller than the wavelength of light ($< 250 \text{ nm}$), the intensity of the light will be scatter in all directions (Rayleigh scattering).

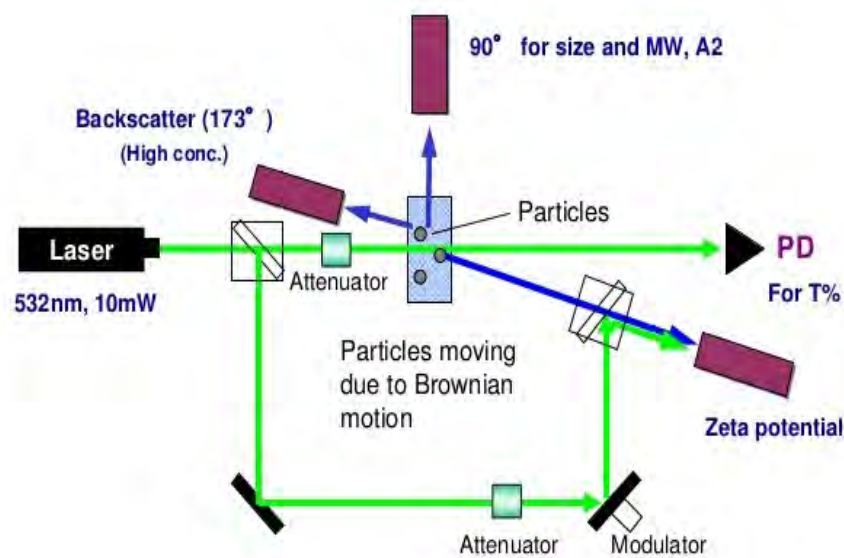


Figure 3.3 DLS measurement technique mechanism³

DLS measurements in this study were performed using a Malvern Zetasizer Nano Series running DTS software and using a 4 mW He-Ne laser operating at a wavelength of 633 nm and an avalanche photodiode (APD) detector. The scattered light was detected at an angle of 1730. The temperature was stabilized to $\pm 0.1^\circ\text{C}$ of the set temperature. To reduce the influence of larger aggregates the number-average hydrodynamic particle size is reported.

3.5 Fourier Transform Infrared (FT-IR) spectroscopy

Fourier Transform Infrared (FT-IR) spectroscopy is an analytical method that can be used to detect a range of functional groups and molecular structure. It is the preferred method of infrared spectroscopy because can provide information on the basis of chemical composition and physical state of the whole sample (Cocchi, et.al, 2004). FT-IR can be used to identify unknown materials, determine the quality or consistency of a sample, and determine the amount of components in a mixture.

FT-IR spectrometer obtains infrared spectra by first collecting an interferogram of a sample signal with an interferometer, which measures all of infrared frequencies simultaneously. At first, infrared radiation is passed through a sample, then some of the infrared radiation will be absorbed by the sample and some of it is passed through (transmitted). The resulting spectrum represents the molecular absorption and transmission, creating a characteristic frequency of the IR vibration modes such as stretch, contraction, and bend. Infrared spectroscopy detects the vibration characteristics of chemical functional groups in a sample. Just like a fingerprint, each molecular structure will produce different infrared spectrum from the others. The characteristic frequencies of IR vibration are influenced strongly on by the slight change in the molecular structure resulting in the difficulty in the interpretation of molecular structure from the IR data by itself.

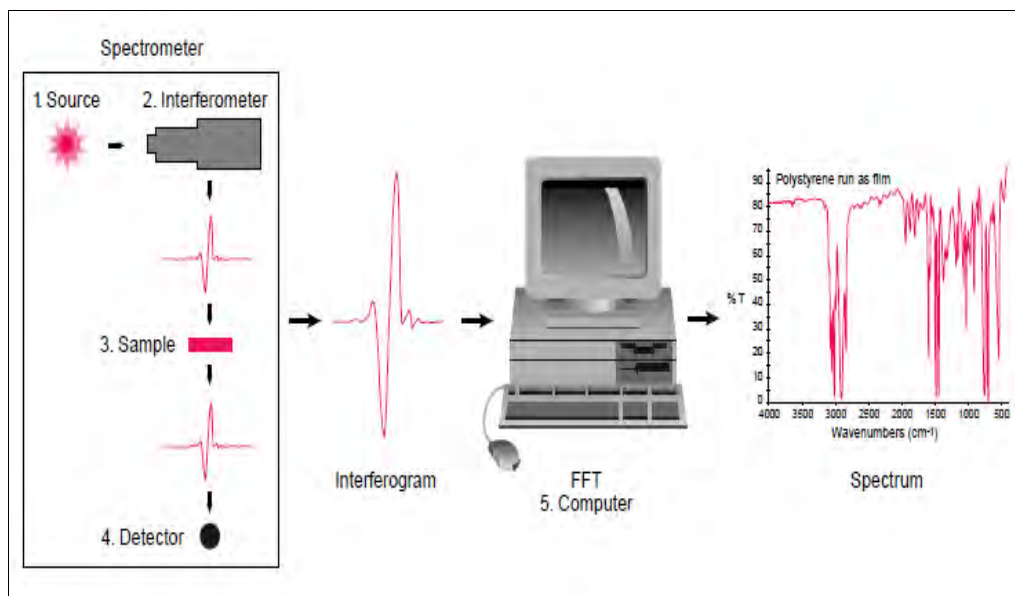


Figure 3. 4 Sample analysis process using FT-IR⁴

In this study, the FTIR measurements were performed using a Bruker IFS66\S Fourier transform spectrometer by averaging 64 scans with a resolution of 4 cm⁻¹.

3.6 Transmission Electron Microscopy (TEM)

Transmission Electron Microscopy (TEM) is one of the most powerful and versatile microscopy techniques for the characterization of materials at the atomic scale. It possesses a higher resolution than most other microscopes owing to a small de Broglie wavelength of electrons. The image is formed by the interaction with electrons and samples when the electron beam passes through the sample. It is widely exploited in physical sciences, material science, chemistry, virology and biological research to identify the structure of materials and assist in the design and manufacture of them.

The maximum resolution of a light microscope has been limited by the large wavelength of visible light (around 400–700 nm). Instead of using visible light as the probe of measurement, TEM uses an electron which has a wavelength given via the equation below.

$$k = \frac{2\pi}{\lambda} = \frac{1}{\hbar} \left(2m_0 E + \frac{E^2}{c^2} \right)^{1/2}$$

Here, h is Planck's constant ($6.63 \times 10^{-34} \text{J}\cdot\text{s}$), m_0 is the rest mass of an electron and E is the energy of the accelerated electron.

A typical TEM system consists of an illumination system, sample stage and objective lens part and projection system. The illumination system provides the electron source. The sample stage and objective lens part is the place for the interaction of the electron beam and sample. The projection system magnifies the formed image from the stage for capturing and viewing.

In this thesis, the TEM micrographs were observed using a transmission electron microscopy JEOL1400 TEM at an accelerating voltage of 100 kV. The samples were dispersed in water (5 mg/mL) and deposited onto 200 meshes, holey film, copper grid (ProSciTech). The sample was treated using positive staining agent by application of osmium tetroxide vapor.

3.7 Confocal microscopy

Confocal microscopy is an optical imaging technique used to increase optical resolution and contrast of a micrograph. It was discovered by Marvin Minsky at 1957, and has attracted the scientific and industrial community to use in

many applications such as clinical application, material sciences and lifetime imaging. In this study, the samples were observed with a Leitz Diaplan Scientific and Clinical microscope and an Olympus FV1000 Confocal Inverted Microscope, and imaged with Leica DFC 480 camera. For bacterial adhesion, images from 15 representative areas on each of triplicate samples for each surface were taken. Cells that were stained green were considered to be viable, those that stained red were considered to be dead as were those that stained both green and red.

3.8 References

1. Yau, W.W., J.J. Kirkland, and D.D. Bly, *Modern size-exclusion liquid chromatography: practice of gel permeation and gel filtration chromatography*. 1979: Wiley New York.
2. Macomber, R.S., *A complete introduction to modern NMR spectroscopy*. 1998: Wiley New York.
3. Colthup, N.B., L.H. Daly, and S.E. Wiberley, *Introduction to infrared and Raman spectroscopy*. 1990: Academic press.
4. Perkampus, H.-H., H.C. Grinter, and T. Threlfall, *UV-VIS Spectroscopy and its Applications*. 1992: Springer-Verlag New York.

Chapter 4. Synthesis of core crosslinked star (CCS) as macromolecular organic nitrate via RAFT polymerization

4.1 Introduction

Organic nitrates are the most commonly used NO donor drugs with the general formula (RONO₂). Glycerol trinitrate (GTN or most known as Nitroglycerin) is the best studied nitrate, used mainly in acute relief of pain associated with angina and has proven to be a safe agent in the cardiovascular system.¹ The organic nitrates therapeutically targeted for cardiovascular disorder and many other pathologies and diseases.²⁻⁴

Generally the organic nitrates release NO through chemical reaction with acid, alkali, metal, and thiols.⁵ Classic organic nitrates have been shown to react with thiols at very slow rates and release small amounts of NO. Some authors also notified that novel organic nitrates are capable of releasing considerably larger amounts of NO in a non-enzymatic reaction with thiols in single buffer solution and generate an S-nitrosothiols.⁶

Star polymers have attracted significant attention due to their potential feature in drug delivery system. Star polymers are gaining interest because of their characteristic rheological and dilute solution properties. The combination of unique rheological properties and the ability to employ controlled polymerization techniques to obtain well-defined structures makes this class of macromolecule very attractive for use in a variety of applications including that

of drug delivery.⁷ Star polymer with high-molecular-weight cross-linked cores surrounded by many polymeric arms, known as core cross-linked star (CCS) polymer, have been proposed recently to use for drug delivery application.⁸ The CCS polymer is ideally suited for use as a potential drug delivery device because of the large loading capacity of the hydrophobic core, the size of which can be easily altered through the use of a 'spacer monomer' during the core formation step.⁹ The ability to independently control the length and type of arm relative to the core is also very attractive property for pharmaceutical applications.¹⁰

In this study, we proposed a core crosslinked star (CCS) polymer as a nanocarrier for NO delivery. The type of NO donor that been used as the sources of NO is organic nitrate. The CCS polymeric nanocarriers had been synthesized via RAFT polymerization using arm-first method. The star with PEG coronas and vinyl benzyl chloride (VBC) functionality in the cores will then be modified using silver nitrate (AgNO_3) to form nitrate ($-\text{ONO}_2$) star polymers. The attachment of nitrate from silver nitrate into polymer scaffold was form via substituting chloro- functional group in the star polymer cores. The Griess assay method was used to observe the NO release mechanism and NO concentration determination.¹¹

4.2 Experimental part

4.2.1 Materials

Oligo(ethylene glycol) methyl ether acrylate (OEG-A), $M_w = 480 \text{ g mol}^{-1}$, 99%, Sigma-Aldrich) and vinylbenzyl chloride (VBC) were deinhibited via a

column of activated basic alumina. Deinhibited OEG-A and VBC were both stored at -18 °C. The initiator, 2,2'-azobis(isobutyronitrile) (AIBN), was crystallized twice from methanol. High-purity N₂ (Linde gases) was used for reaction solution purging. All the others chemical reactants were purchased from Sigma-Aldrich, supplied at the highest purity.

4.2.2 Characterization methods

NMR Spectroscopy. ¹H NMR spectra were recorded using a Bruker Avance 300 (300 MHz) spectrometer. *d*₃-Acetonitrile and *d*-Chloroform were used as solvents. All chemical shifts are reported in parts per million (ppm) relative to tetramethylsilane (TMS), referenced to residual the residual solvent frequencies ¹H NMR: *d*₃-Acetonitrile = 1.94, and *d*-Chloroform = 7.24 ppm. The monomer (i.e. OEGA) conversion was calculated by the following equation to give ~90% conversion, where *I*^{5.9 ppm} and *I*^{4.2 ppm} correspond to the integral of the vinyl signal from the monomer at 5.9 ppm and the ester signal from the monomer/polymer at 4.1 ppm, respectively.

$$\alpha (\text{OEGA Conversion, \%}) = \left[1 - \frac{I^{5.9 \text{ ppm}}}{\frac{I^{4.2 \text{ ppm}}}{2}} \right] \times 100\%$$

The theoretical molecular weight was calculated by the following equation below:

$$M_n (\text{Theoretical}) = \left(\left(\frac{[M]_0}{[CTA]_0} \right) \times \alpha \times MW_M \right) + MW_{CTA}$$

[M]₀: Initial monomer concentration

$[CTA]_0$: Initial RAFT agent concentration

α : Conversion of monomer

MW_M : Molecular weight of monomer

MW_{CTA} : Molecular weight of the RAFT agent

Size Exclusion Chromatography (SEC). Size exclusion chromatography or Gel Permeation Chromatography (GPC) was performed using a Shimadzu modular system comprised of a DGU-12A degasser, a LC-10AT pump, a SIL-10AD automatic injector, a CTO-10A column oven, a RID-10A refractive index detector, and a SPD-10A Shimadzu UV/vis detector. A 50 x 7.8 mm guard column and four 300 x 7.8 mm linear columns (500, 10^3 , 10^4 , and 10^5 Å pore size, 5 µm particle size) were used for the analyses. *N,N'*-dimethylacetamide (DMAc, HPLC grade, 0.05% w/v 2,6-dibutyl-4-methylphenol (BHT), 0.03% w/v LiBr) with a flow rate of 1 mL min^{-1} and a constant temperature of 50 °C was used as the eluent with an injection volume of 50 µL. Prior to injection, the samples were filtered through 0.45 µm filters. The unit was calibrated using commercially available linear poly(methyl methacrylates) standard. Chromatograms were processed using Cirrus 2.0 software (Polymer Laboratories). The arm incorporation was calculated by the following equation below with A^{arm} and A^{star} represent the area of the chromatogram of P(OEGA) arm and P(OEGA)-*b*-P(VBC)star, respectively.

$$\text{Arm Incorporation (\%)} = \frac{A^{star}}{(A^{arm} + A^{star})} \times 100\%$$

Infrared Spectroscopy. ATR-FTIR spectra of the star polymer samples were obtained using a Bruker Spectrum BX FTIR system using diffuse reflectance sampling accessories. The spectrophotometer was equipped with a tungsten halogen lamp and Si/Ca beam splitter. Spectra were obtained at regular time intervals in the MIR region of 4000 – 500 cm^{-1} at a resolution of 4 cm^{-1} (128 scans) and analysed using OPUS software.

UV-Vis Spectroscopy. UV-vis measurements were performed on a CARY 300 spectrophotometer (Bruker) using a quartz cuvette.

Dynamic Light Scattering (DLS). DLS measurements were carried out on a Malvern Zetasizer Nano Series running DTS software (laser, 4mW, $\lambda = 633$ nm; angle 173°). Polymer samples were dissolved in MilliQ grade water (1mg/mL) and filtered using 0.45 μm syringe filter prior to analysis. The samples were transferred to their respective disposable cuvettes for analysis.

Transmission Electron Microscopy (TEM). The sizes of the star polymers were observed using a JEOL 1400 transmission electron microscope. It was operated at an acceleration voltage of 80 kV. The samples were prepared by casting the polymer solution (1 mg mL^{-1}) onto a Formvar-coated copper grid. No staining was applied.

4.2.3 Synthesis

4.2.3.1 Synthesis RAFT agent : 2-propanoic acid butyltrithiocarbonate (PABTC)

Triethylamine was added drop wise to a stirring solution of Butane thiol and carbon disulfide in dichloromethane (DCM). The solution was left to stir at room temperature for 2 hours and then 2-bromopropionic acid dissolved in DCM was added drop wise. The resulting solution was stirred overnight at room temperature. All the solution was extracted by 0.1 M hydrochloric acid 5 times. Subsequently, the solvent was removed by rotary evaporation, and the product was purified by column chromatography with mixtures of ethyl acetate/petroleum sprite (1/5 v/v). The product was isolated by evaporation of the solvents and further dried in a vacuum oven at room temperature overnight to form yellow powder.

^1H NMR (300 MHz, CDCl_3) δ 4.90 (q, $J = 7.4$ Hz, 1H), 3.41 (td, $J = 7.4$, 1.2 Hz, 2H), 2.44 – 1.91 (m, 18H), 1.78 – 1.57 (m, 4H), 1.51 – 1.31 (m, 2H), 1.07 – 0.75 (m, 3H).

4.2.3.2 Synthesis of Arm Homopolymer : Oligoethylene Glycol-acrylate (OEG-A)

Synthesis of P(OEGA). OEG-A₄₈₀ (15g, 0.0312 mol), CTA (0.3562g, 0.0015 mol) and AIBN (0.0244g, 1.4×10^{-4} mol) were placed into a round bottom flask equipped with a magnetic stirrer. The reactants were dissolved in Acetonitrile (54mL) and the reaction mixture was degassed with N_2 under ice (0°C) for 30 minutes. The reaction mixture was then placed into an oil bath preheated to 70°C and the polymerisation was run for 6 h. Upon completion,

the reaction was quenched in an ice bath for 15 mins. The polymer was purified via 3 repetitions of precipitating with petroleum ether and centrifuging (5mins, 8000rpm). The purified polymer was then placed into a vacuum oven overnight to remove remaining solvent. In this study, we prepared two polymers with different molecular weight: 10,000 and 15,000 g/mol.

4.2.3.3 Synthesis of VBC star polymer via arm-first methodology

POEGA homopolymers, and AIBN were introduced into a vial with a magnetic stirrer with toluene under the condition of [Polymer] : [Crosslinker] : [AIBN]= 1.0 : 8.0 : 0.2. Crosslinker (*N,N'*- Methylene bisacrylamide) and vinyl benzyl chloride were added, and the vials were sealed and purged with nitrogen for 20 minutes in an ice bath. After that, the degassed solution was placed in an oil bath at 70°C for 24 hours. Following polymerization, the star polymers were sampled for ¹H NMR, FTIR and GPC analysis. Star polymer was purified by precipitation three times using diethyl ether, and analyzed by ¹H NMR. The purification process allows the removal of traces of unreacted cross-linker and VBC monomer. In addition, the unreacted arm was removed, and this process does not alter the PDI of the star polymer.

4.2.3.4 Modification of VBC-star into VBC star-nitrate nanoparticles

VBC star polymer was dissolved in acetonitrile. AgNO₃ was then added to the solution at a composition of 1:10 (w/w) to VBC star polymer. The reaction mixture was covered and stirred in a preheated oil bath at 70 °C for 24 hours. Solvent was removed under reduced pressure. The polymer was purified by precipitation in chloroform (CHCl₃) followed by centrifugation (6500 rpm for

5 minutes) to remove unreacted silver nitrate. The resulting polymer was characterized using ^1H NMR, TEM, DLS, and FT-IR.

4.2.3.5 NO release testing

VBC star-nitrate was dissolved in DMSO, and then a solution of glutathione (GSH) in DMSO (1 mL) was added dropwise into the polymer solution. The NO release reactions were carried out in a preheated oil bath at 37 and 60 °C. The vials were removed from the oil bath at certain time over a period of 1 and 24 hours. The reaction mixtures were then dialyzed against distilled water to remove DMSO and unreacted glutathione. The polymer was freeze-dried and analysed by ^1H NMR and FTIR.

4.2.3.6 Determination of NO release using Griess reagent kit

NO released from the nanoparticles at predetermined time intervals was quantified by the standard Griess reagent kit (G7921), which is widely used for nitrite determination. VBC star-nitrate was dissolved into 240 μL water and then incubated with nitrate reductase compounds for 3 hours, in order to reduce nitrate into nitrite. Followed by preparing the Griess reagent, then mixed it with 300 μL of the nitrite-containing sample and 2.6 mL of deionized water and incubated for 30 minutes at room temperature. Nitrite concentrations in the samples should fall within the linear range of the assay (approximately 1–100 μM). UV-vis absorbance of the resulting solution was determined at 548 nm, and the total nitrite concentration in the sample solution was calculated from a standard curve and converted to cumulative NO release. The reaction proposed for Griess reaction described as follow:

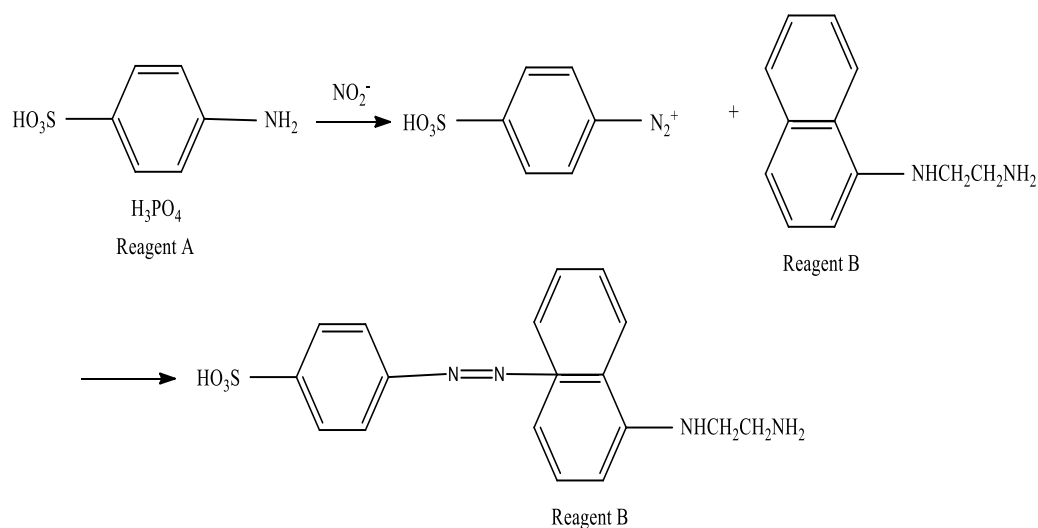


Figure 4. 1 Schematic of Griess Reaction for NO determination

4.3 Result and discussion

4.3.1 Polymer characterization

Well-defined core crosslinked star polymer was synthesized using ‘arm-first’ method. As the first step, arm polymers were prepared via RAFT polymerization. Two different molecular weight of poly(oligoethylene glycol acrylate) arms were prepared in the presence of 2-propanoic acid butyltrithiocarbonate (PABTC) as the RAFT agent and AIBN as the initiator. The arm polymers solutions were heated at 70 °C in acetonitrile for about 7 hours to achieve 60 - 70% conversion. This low conversion was intended to maintain high end group functionality, and it was determined via ^1H NMR analysis. ^1H NMR analysis reveals the characteristic signals of OEG-A at 4.2, 3.6, 3.3, and 1.5-2.0 ppm attributed to CH_2O ester, CH_2O ether, CH_3O , and $\text{CH}=\text{CH}_2$ backbone, respectively (**Figure 4.2**).

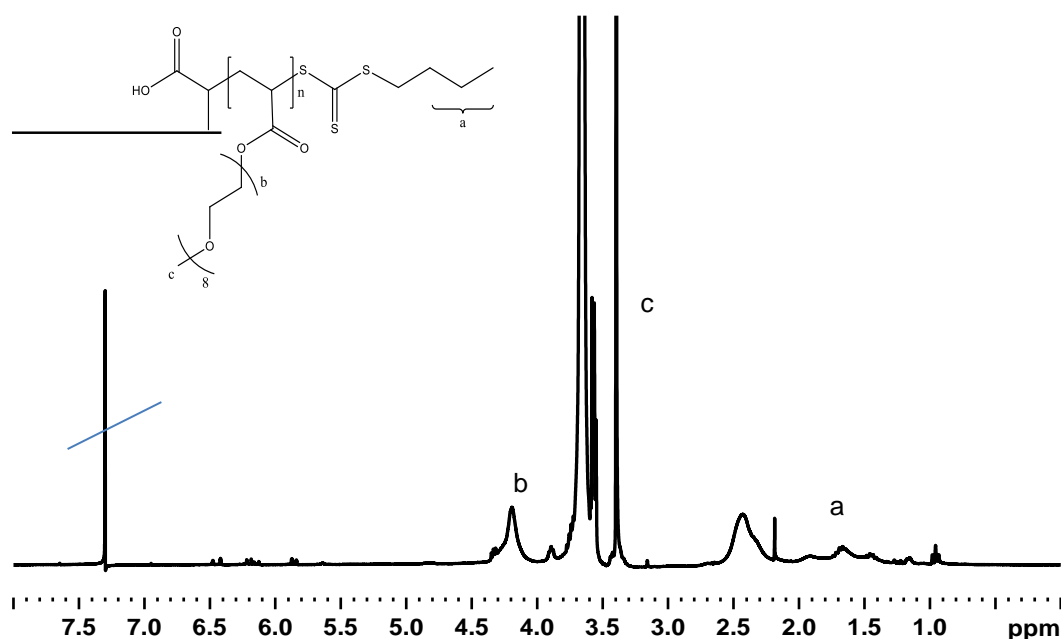


Figure 4. 2 ^1H NMR spectrum of P(OEG-A) homopolymer obtained via RAFT polymerization recorded in CdCl_3 at $20\text{ }^\circ\text{C}$, M_n (NMR) = $10000\text{ g}\cdot\text{mol}^{-1}$

The presence of the RAFT end-group was confirmed by UV_vis spectroscopy (absorbance peak at 305 nm, data not shown) and by ^1H NMR analysis, with CH adjacent to the trithiocarbonate at 4.4 ppm and at 2.8 ppm (S- CH_2 signal). Experimental molecular weights assessed by both GPC and NMR analyses which are in good agreements with the theoretical values. The molecular weight obtained from two different arm polymers after 7 hours reaction are 10000 and 15000 gram/mol with narrow polydispersity index (PDI) below 1.2 and high RAFT functionality. Based on previous study, the use of different molecular weight will form different arms number and arms incorporation, since it will affect the ratio of VBC as the star functionalities¹². The optimum of star structures and VBC composition can be observed by using different molecular weight of arm polymer.

Table 1. Summary of poly(OEG-A) star synthesized via RAFT polymerization

Polymers	M_n theoretical ^a	M_n NMR ^b	M_n GPC ^c	PDI (GPC) ^c	RAFT functionality ^d
Poly(OEG-A) - P1	10000	10000	10100	1.13	> 95
Poly(OEG-A) - P2	15000	15000	15300	1.19	> 95

^aTheoretical molecular weights calculated by the following equation : $M_n = ([M]_0/[RAFT]_0) \times \alpha_M \times MW_M + MW_{RAFT}$. Where, $[M]_0$, $[RAFT]_0$, α_M , MW_M , and MW_{RAFT} correspond to initial monomer concentration, initial RAFT agent concentration, monomer conversion, molar mass of monomer, and RAFT agent, respectively

^bMolecular weights determined by ¹H NMR using the aromatic group of RAFT agent as reference

^cLinear homopolymers molecular weight and PDI obtained by DMAc GPC (using polystyrene calibration)

^dRAFT-functionality was calculated by the following equation : RAFT end functionality = $(Abs^{305} \times l/\epsilon^{305})/[Polymer]_0$, where Abs^{305} , ϵ^{305} , l , and $[Polymer]_0$ correspond to absorbance, extinction coefficient at 305 nm ($\epsilon^{305} = 15700$ mol/cm), cuvette path length and polymer concentration.

The star polymers were prepared using the optimum ratio of core crosslinked star formation based on previous study in our group.¹² The linear polymers were chain extended in the presence of a cross-linker *N,N'*-Methylene bisacrylamide, AIBN initiator and different concentrations of VBC. The objective of this star formation is to obtain at least 10 % composition of VBC, so it can achieve optimum nitrate attachment after the modification process. Due to initial hypothesis that more composition VBC obtained in the star core, there will be higher NO concentration in the VBC star-nitrate nanoparticles that can be released. The synthetic scheme of VBC star-nitrate synthesized has described in the **Figure 4.3**.

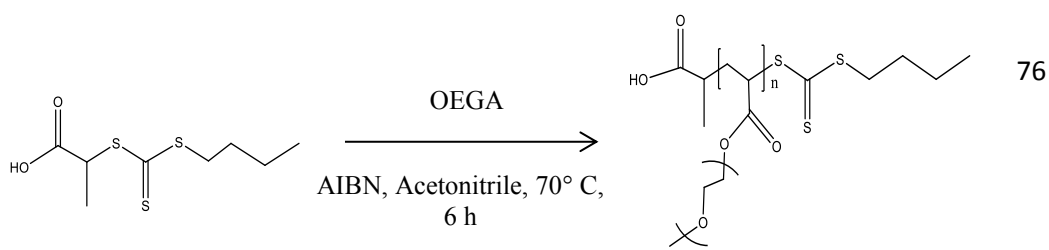


Figure 4.3 Schematic reaction for synthesise VBC star-nitrate

After star formation, the star polymers were analyzed by GPC and ^1H NMR spectroscopy to determine the arm incorporation efficiency and monomer conversions. From ^1H NMR spectroscopy using the signal at 4.6 ppm from $-\text{CH}_2\text{Cl}$ group has confirmed the presence of VBC units in the polymer (**Figure 4.4 A**). The conversion of VBC was calculated by comparing the intensity of $\text{CH}=\text{CH}_2$ peak at 5.5 – 6.5 ppm and CH_2Cl peak at 4.6 ppm. Whereas the composition can be calculated using the intensity of CH_2Cl peak at 4.6 ppm from VBC units and the intensity of CH_2O peak at 4.2 ppm correspond with OEG-A (methyl ester). The highest VBC composition in the star polymer was about 16 % (mol).

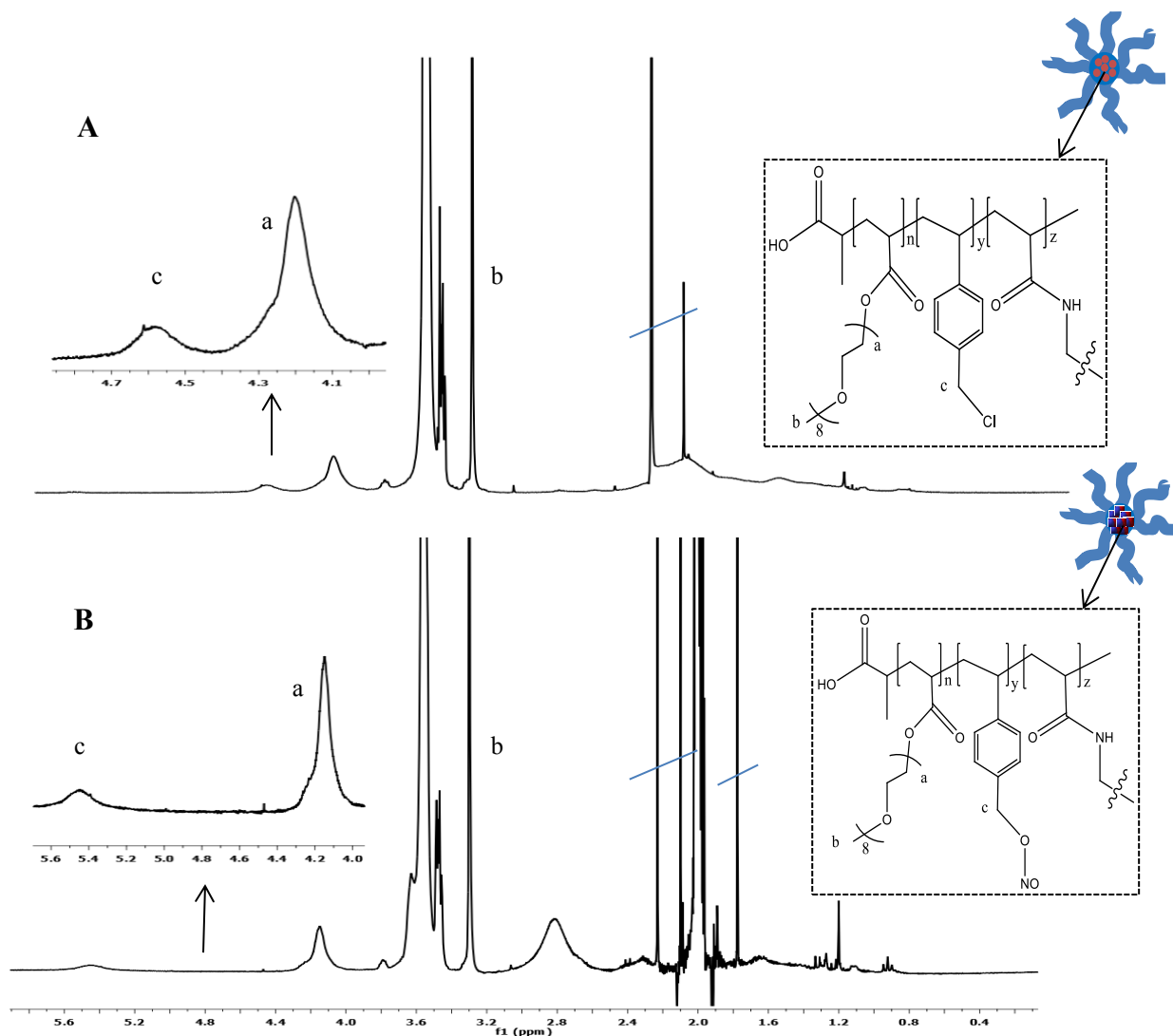


Figure 4.4 ^1H NMR spectra of VBC star polymer before (A) and after modification (B) with silver nitrate

The molecular weights of star polymers and PDI were determined using GPC analysis. The result from SEC showed a shift in the molecular weight giving M_n , SEC of 67,000 g/mol with polydispersity index of 1.18 (**Figure 4.5 A**). The ratio between the area of the chromatogram of star polymer and its precursor, P(OEGA) arm was calculated to provide an arm incorporation of ~60%. DLS analysis used to confirm the formation of nanoparticles with sizes ranging from 20 – 30 nm in water which was corroborated by the TEM results (**Figure 4.5 B & C**).

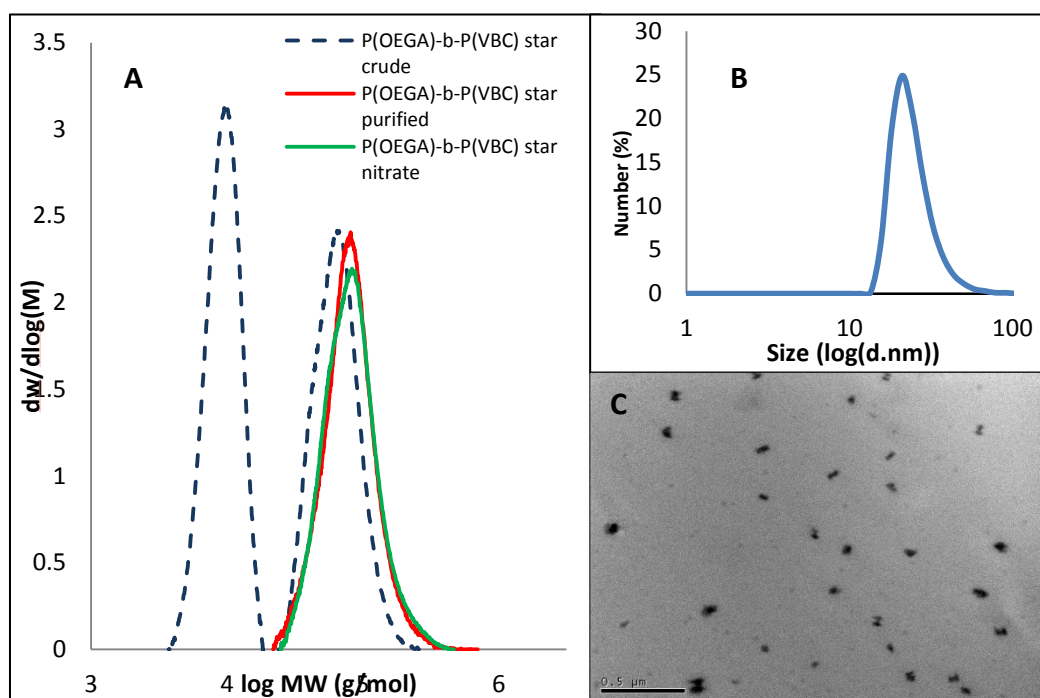


Figure 4. 5 SEC of P(OEGA)-b-P(VBC) star before and after modification with silver nitrate (A), VBC star number-weight particle size distribution by DLS (B) and TEM image (C)

The nitrate nanoparticle was prepared by modified the -chloro functional group on VBC star polymer. The VBC star was reacted with silver nitrate in Acetonitrile at 70 °C for 24 hours. The successfully substitution of nitrate to -chloro group was confirmed using 1H NMR and FTIR analysis. After nitrate modification, the chloro-proton peaks at 4.6 ppm disappear and a proton peak appears at 5.5 ppm. The peak shift indicates that the nitrate group has successfully attached to the polymer scaffold via replacing chloro-side group into nitrate (**Figure 4.4 B**). The molecular weight distribution of star nitrate based on SEC showed a M_n , SEC of 69,000 g/mol with a polydispersity index of 1.18 (**Figure 4.5 A**).

FTIR also been applied to confirm the successfully nitrate substitution into VBC star polymer. The FTIR result has shown that the reaction successful substituted the –chloro side group with nitrate by the disappearance of C-Cl peak at 511 cm^{-1} . FTIR also used to observe the appearance of NO spectra at 1250 and 1650 cm^{-1} in VBC star samples after reaction with silver nitrate (**Figure 4.6 B**). This result confirmed the successful attachment of nitrate from silver nitrate into star polymer.

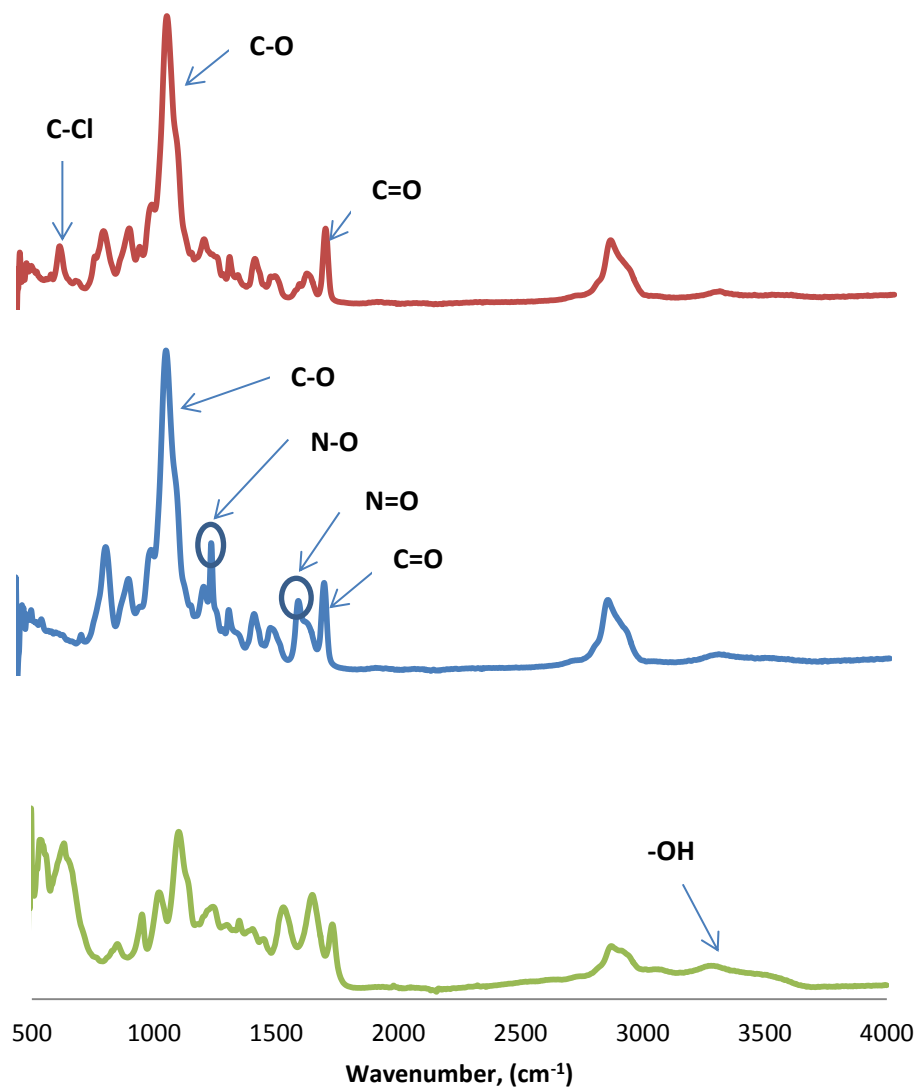


Figure 4. 6 FTIR spectra of VBC star before (A), after modification (B), and after treatment with glutathione (GSH) (C)

4.3.2 NO release mechanism and Griess assay to determine NO concentration

The most important things from the development of new NO donor drug are the capability to release NO with optimum amount at the right time. For organic nitrate NO donors, the NO release mechanism can be stimulated by two different ways: the enzymatic and non-enzymatic. The enzymatic

mechanism triggered the NO release through the activation of nitrate by enzymatic compounds, such as glutathione *S*-transferase, cytochrome P450, and/or xanthine oxidoreductase, or alternatively through catalytic activity mediated by mitochondrial aldehyde dehydrogenase (ALDH-2).¹³ On the other hand, the non-enzymatic mechanism proceed by reacted the nitrate with thiols (SH) groups. In this study, the NO release mechanism was observed by reacted VBC star-nitrate with glutathione (GSH) as reducing agent at 60 °C for 1 hour and 24 hours. The release mechanism proposed can be shown at the scheme below:



Based on the release mechanism, after the reaction with glutathione, it was expected that an –OH functional group will be formed and nitrate functional groups then will be eliminated. This result will confirm that NO can be released when the modified polymer is treated with reducing agent.

Using ¹H NMR, the confirmation of NO release has been done by the observed disappearance of the –CH₂ONO₂ signal at 5.5 ppm and the appearance of CH₂OH signal at 4.6 ppm. After 1 hour reaction with glutathione in acetonitrile, the nitrate peak slowly reduced about 50 %, and the -CH₂ functional peak at 4.6 has formed with the same broad of nitrate spectrum. It showed by the same peak intensity of –CH₂ONO₂ signal at 5.5 ppm and –CH₂ signal at 4.6 ppm. The nitrate peak at 5.5 ppm has completely disappeared after 24 hours reaction with glutathione, and the –CH₂ peak at 4.6 has appeared (**Figure 4.7**).

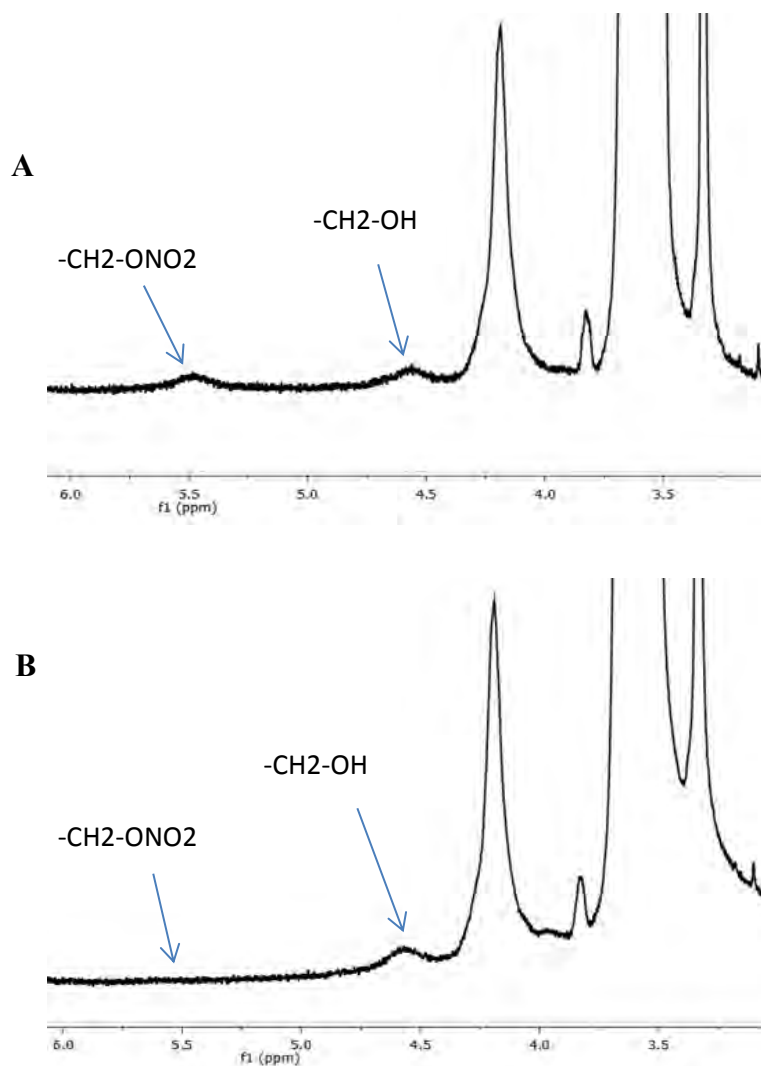


Figure 4. 7 ^1H NMR spectra of VBC star-nitrate after treatment with glutathione for 1 hour (A) and 24 hours (B)

Based on the NO release mechanism scheme of organic nitrate, we can calculate the NO concentration that is released via non-enzymatic reaction using glutathione. The NO (nitrite) concentration star nitrate is about 2.316 mM or 2,316 μM . This NO concentration is really promising because high millimolar levels of NO can promote cell apoptosis and act as tumor regression for cancer therapy.^{14,15} Figure 4.8 has described the biological effect of NO based on its concentration and duration.

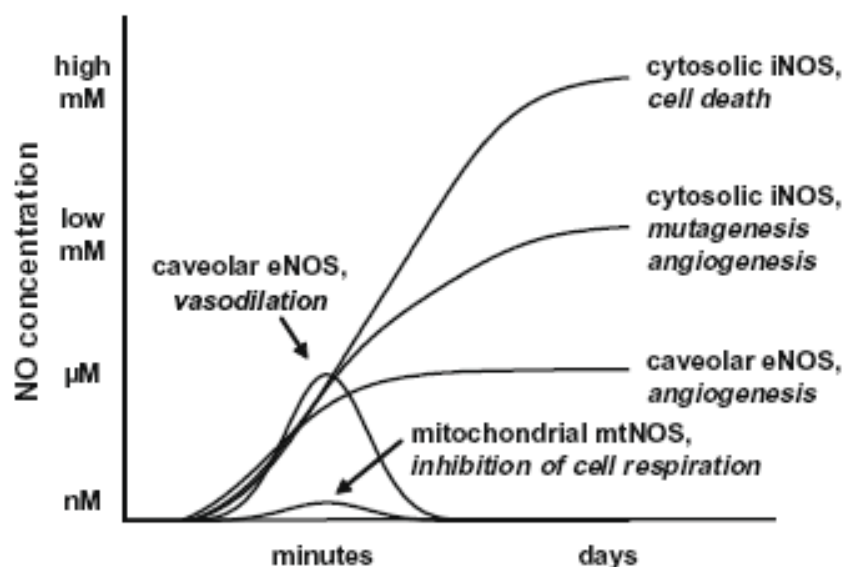


Figure 4. 8 Duration of NO production¹⁴

The NO release testing also observed using FTIR analysis, comparing the NO spectra before and after treatment with glutathione. The FTIR spectrum in Figure 4.6 C has shown the release of NO using reducing agent at 60 °C. Compare with FTIR spectra in the previous figure, it shown the disappearance of NO spectra at 1250 and 1650 cm^{-1} , and the formation of –OH spectra at 3400 cm^{-1} after the sample treated with glutathione.

The release of NO from nitrate star polymer was also determined using Griess Assay. The Griess Assay is the most commonly method to determine NO concentration.¹¹ This method not only can used to determine NO concentration, but also can be used to confirm the NO release from nanoparticles by observed the decrease in the absorption at 340 nm using UV-vis spectroscopy. The Griess reaction performed in this study according to the manufacturer's

protocols. Using Griess Assay method, the times release of NO from VBC star nitrate were observed within 2 or 3 different incubation time.

Briefly, NO star polymer was dissolved in deionized water, followed by the incubation with nitrate reductase and its cofactor to reduce the nitric oxide and nitrate into nitrite. Following the reaction protocol, the sample was incubated for 3 hours to allow a maximum release of nitric oxide and its conversion to nitrite in the aqueous medium. Subsequent addition of a Griess reagent to the nitrite sample formed a diazenium salt that was converted instantaneously to an azo dye, and will presence as UV-Vis absorption at 548 nm. The absorbance of this spectra then can be used to calculate NO concentration using calibration curve.

In this study, we observed the NO release using Griess Assay method at 3 different incubation times: 1, 3, and 12 hours. The results shown that the highest NO concentration released achieves 260 μM after 12h incubation time, very lower if it compares to NO concentration obtain that released by using thiols as the reduction agent. These results have shown that the NO release from organic nitrate is highly dependent on number of factors, including free thiols, enzymes, and light.¹⁶

The non-enzymatic release of NO from an organic nitrate in this study is very slow, shown by the ^1H NMR result that only about 50 % of NO was being release at 60 °C after 1 hr reaction with glutathione. It took 24h to be able release 100% of NO from star nitrate. Therefore, an enzymatic process must play a key role for the therapeutic effect for organic nitrate NO donors.^{3,13}

Further studies to optimize the release mechanism of this organic nitrate NO donor may overcome this limitation. The application of hyperthermia induced by superparamagnetic iron oxide nanoparticles containing nitrate to improve the non-enzymatic NO delivery is ongoing research in our group.

4.4 Conclusions

The POEGA-based core crosslinked star (CCS) star polymer with VBC functional cores, were successfully synthesized using RAFT polymerization. This star polymer then modified into VBC star-nitrate to form a new NO nanoparticles. The modification process was using silver nitrate to replace the -chloro side group into nitrate. The result confirm that VBC star nitrate has great potent to be used as NO carriers since it can release NO with high concentration and long times of release.

4.5 References

- (1) Huerta, S., Chilka, S., & Bonavida, B. *international Journal of Oncology* **2008**, *33*, 909.
- (2) Miller, M. R.; Megson, I. L. *British Journal of Pharmacology* **2007**, *151*, 305.
- (3) Bill Cai, T.; Wang, P. G.; Holder, A. A. In *Nitric Oxide Donors*; Wiley-VCH Verlag GmbH & Co. KGaA: 2005, p 1.
- (4) Webb, D. J.; Megson, I. L. *Expert Opinion on Investigational Drugs* **2002**, *11*, 587.
- (5) Body, S. C.; Hartigan, P. M.; Shernan, S. K.; Formanek, V.; Hurford, W. E. *Journal of cardiothoracic and vascular anesthesia* **1995**, *9*, 748.

- (6) Koren, E.; Torchilin, V. P. *IUBMB Life* **2011**, *63*, 586.
- (7) Wiltshire, J. T.; Qiao, G. G. *Australian Journal of Chemistry* **2007**, *60*, 699.
- (8) Vassiliou, A. A.; Papadimitriou, S. A.; Bikiaris, D. N.; Mattheolabakis, G.; Avgoustakis, K. *Journal of Controlled Release* **2010**, *148*, 388.
- (9) Aryal, S.; Prabakaran, M.; Pilla, S.; Gong, S. *International Journal of Biological Macromolecules* **2009**, *44*, 346.
- (10) Venkataraman, S.; Hedrick, J. L.; Ong, Z. Y.; Yang, C.; Ee, P. L. R.; Hammond, P. T.; Yang, Y. Y. *Advanced Drug Delivery Reviews* **2011**, *63*, 1228.
- (11) Moorcroft, M. J.; Davis, J.; Compton, R. G. *Talanta* **2001**, *54*, 785.
- (12) Liu, J.; Duong, H.; Whittaker, M. R.; Davis, T. P.; Boyer, C. *Macromolecular Rapid Communications* **2012**, *33*, 760.
- (13) Fung, H.-L.; Chung, S.-J.; Bauer, J. A.; Chong, S.; Kowaluk, E. A. *The American Journal of Cardiology* **1992**, *70*, B4.
- (14) Sonveaux, P.; Jordan, B. F.; Gallez, B.; Feron, O. *European journal of cancer (Oxford, England : 1990)* **2009**, *45*, 1352.
- (15) Carpenter, A. W.; Schoenfisch, M. H. *Chemical Society Reviews* **2012**, *41*, 3742.
- (16) Nichols, S. P.; Storm, W. L.; Koh, A.; Schoenfisch, M. H. *Advanced Drug Delivery Reviews* **2012**, *64*, 1177.

Chapter 5. Core crosslinked star –NO nanoparticles for antimicrobial application

5.1 Introduction

Despite many advances in the development of antimicrobial agents as well as many efforts in elucidating the disease mechanism, infectious disease still has a detrimental impact on human health and the global economy. At present, infectious diseases are the second leading cause of death, accounting for about 15 million deaths worldwide each year.¹ One of the major issues with antimicrobial agents is the development of drug resistance and the adverse side effects. To date, most strains of bacteria have acquired resistance to at least one common antimicrobial.² One major resistance mechanism adopted by bacteria is the formation of biofilms. Biofilms are highly-structured and surface-attached communities of cells enclosed in a self-produced matrix which acts as a barrier and protective membrane which makes the most of the biofilm associated infectious disease very challenging to treat.

Biofilms display increased resistance towards conventional antimicrobials and cause a range of problems in industrial and clinical settings.^{3,4} Bacteria embedded in biofilms exhibit upwards of 10-1000-fold higher resistance to biocides and traditional antimicrobials than their planktonic counterparts, and they are less susceptible to host immune defense.⁵ Novel strategies directly aiming at inhibition or dispersion of biofilms seems to be a key strategy in combating with microbial infectious diseases. One such strategy is to develop

novel agents that can induce biofilm dispersal, and subsequently inhibit the biofilm formation or promote biofilm cell detachment.⁶

Recently, the signalling molecule nitric oxide (NO), a diatomic free radical, was identified as a key regulator of biofilm dispersal. NO was found to be produced endogenously in late developmental stages of mature biofilms to induce dispersal events which complete the biofilm life cycle.^{6,7} Molecular analyses revealed that NO triggers a signaling pathway involving the conserved intracellular second messenger cyclic di-GMP, which in turn activates a range of effectors leading to dispersal.⁸⁻¹⁰ Further, add back of NO to established biofilms, by using NO donors could induce dispersal in a broad range of microbial species and restore sensitivity to a range of antimicrobials and antibiotics.¹¹⁻¹⁴ Thus the use of low, non-toxic levels of NO represents a promising strategy for the control of biofilms in medical and industrial contexts. However attempts at using existing NO donors to prevent biofilm formation by inducing this signaling pathway in bacteria before they turn on biofilm gene expression, have so far proven difficult as NO needs be released in a continuous fashion over longer period of times to maintain the signal at an appropriate low non-toxic level. The delivery of NO gas is very challenging as NO is an extremely reactive molecule that can react with oxygen (and other gases) resulting in a short half-life time in the body (less than 5 minutes). To improve the administration of NO, a range of small-molecules capable of decomposition under specific conditions to release NO have been developed, including nitrate, nitroprusside, S-nitrosothiols (RSNOs) and *N*-diazeniumdiolates (NONOates).¹⁵ Unfortunately, these small molecules lack

both stability and specificity. For example, NONOate compounds have a half-life of just a few minutes at 25°C. One of the strategies to overcome this challenge lies in the development of nanomaterials for the delivery of NO. Antimicrobial nanoparticles offer many advantages over the small molecule antibiotics in improving the pharmacokinetics and accumulation, reducing side-effect, and more importantly overcoming drug resistance.^{16,17} In recent work, NONOate has been successfully conjugated to different polymeric systems, including matrix of ethylene/vinylacetate,¹⁸ star polymers,¹⁹ and micelles.¹⁹⁻²² Herein, we report a novel star polymer that is able to prevent the formation of the model organism *Pseudomonas aeruginosa*, and confine growth of the bacterial population to the suspended liquid, while keeping the surface free of biofilm.

5.2 Experimental part

5.2.1 Materials

The monomer 2-vinyl-4,4-dimethyl-5-oxazolone was synthesized using a previously reported method²³.

2-(((Butylsulfanyl)carbonothioyl)sulfanyl)propanoic acid was synthesized according to Ferguson et al.²⁴ Oligo(ethylene glycol) methyl ether acrylate ($M_n = 480 \text{ gmol}^{-1}$) was used as received. Dialysis membranes with a molecular weight cut-off (MWCO) of 3500 Da were sourced from Fisher Biotec (Cellu Sep-T4, regenerated cellulose-Tubular membrane). Deuterated solvents, CDCl_3-d_3 and $\text{DMSO}-d_6$ were obtained from Cambridge Isotope Laboratories, Inc. High purity N_2 (Linde gases) was used for degassing. Ultrapure deionized water (17.8 $\text{m}\Omega \text{ cm}$) was obtained using a MilliQ purification system. All other

chemicals were purchased from Sigma-Aldrich. 2,2-azobisisobutyronitrile (162 g mol⁻¹, AIBN) which was purchased from Sigma-Aldrich was recrystallised from methanol before use. For the measurement of nitric oxide release, a Nitrate/Nitrite Colorimetric Assay Kit was purchased from Cayman Chemicals. A LIVE/DEAD *BacLight* Bacterial Viability Kit for was purchased from Life Technologies for fluorescence microscopy of treated biofilms.

5.2.2 Characterization methods

NMR Spectroscopy. ¹H NMR spectra were recorded using a Bruker Avance 300 (300 MHz) spectrometer. *d*₃-Acetonitrile and *d*₆-DMSO were used as solvents. All chemical shifts are reported in parts per million (ppm) relative to tetramethylsilane (TMS), referenced to residual the residual solvent frequencies ¹H NMR: *d*₃-Acetonitrile = 1.94, *d*₆-DMSO = 2.50 and D₂O = 4.79 ppm. The monomer (i.e. OEGA) conversion was calculated by the following equation to give ~90% conversion, where *I*^{5.9 ppm} and *I*^{4.2 ppm} correspond to the integral of the vinyl signal from the monomer at 5.9 ppm and the ester signal from the monomer/polymer at 4.1 ppm, respectively.

$$\alpha (\text{OEGA Conversion, \%}) = \left[1 - \frac{I^{5.9 \text{ ppm}}}{\frac{I^{4.1 \text{ ppm}}}{2}} \right] \times 100\%$$

The theoretical molecular weight was calculated by the following equation below, which resulted in 11,400 g/mol:

$$M_n (\text{Theoretical}) = \left(\left(\frac{[M]_0}{[CTA]_0} \right) \times \alpha \times MW_M \right) + MW_{CTA}$$

[M]₀: Initial monomer concentration

$[CTA]_0$: Initial RAFT agent concentration

α : Conversion of monomer

MW_M : Molecular weight of monomer

MW_{CTA} : Molecular weight of the RAFT agent

Size Exclusion Chromatography (SEC). Size exclusion chromatography or Gel Permeation Chromatography (GPC) was performed using a Shimadzu modular system comprised of a DGU-12A degasser, a LC-10AT pump, a SIL-10AD automatic injector, a CTO-10A column oven, a RID-10A refractive index detector, and a SPD-10A Shimadzu UV/vis detector. A 50 x 7.8 mm guard column and four 300 x 7.8 mm linear columns (500, 10^3 , 10^4 , and 10^5 Å pore size, 5 µm particle size) were used for the analyses. *N,N'*-dimethylacetamide (DMAc, HPLC grade, 0.05% w/v 2,6-dibutyl-4-methylphenol (BHT), 0.03% w/v LiBr) with a flow rate of 1 mL min^{-1} and a constant temperature of 50 °C was used as the eluent with an injection volume of 50 µL. Prior to injection, the samples were filtered through 0.45 µm filters. The unit was calibrated using commercially available linear poly(methyl methacrylates) standard. Chromatograms were processed using Cirrus 2.0 software (Polymer Laboratories). The arm incorporation was calculated by the following equation below with A^{arm} and A^{star} represent the area of the chromatogram of P(OEGA) arm and P(OEGA)-*b*-P(VDM)star, respectively.

$$\text{Arm Incorporation (\%)} = \frac{A^{star}}{(A^{arm} + A^{star})} \times 100\%$$

Confocal Microscopy. The glass samples with adhered bacterial cells prepared as described above were stained with Live/Dead *BacLight* Bacterial Viability Kits L-7007 (Molecular Probes, Inc., Eugene, OR) according to the manufacturer's procedure. Two ml of the two components were mixed thoroughly in 1 ml of PBS. Ten ml of this solution were then trapped between the sample and the glass microscopy slide and allowed to incubate at room temperature in the dark for 15 min. The samples were observed with a Leitz Diaplan Scientific and Clinical microscope and an Olympus FV1000 Confocal Inverted Microscope, and imaged with Leica DFC 480 camera. For bacterial adhesion, images from 15 representative areas on each of triplicate samples for each surface were taken. Cells that were stained green were considered to be viable, those that stained red were considered to be dead as were those that stained both green and red.

Transmission Electron Microscopy (TEM). The sizes of the star polymers were observed using a JEOL 1400 transmission electron microscope. It was operated at an acceleration voltage of 80 kV. The samples were prepared by casting the polymer solution (1 mg mL^{-1}) onto a Formvar-coated copper grid. No staining was applied.

5.2.3 Synthesis

5.2.3.1 Synthesis RAFT agent : 2-propanoic acid butyltrithiocarbonate (PABTC)

The synthesis of RAFT agent as described in chapter 4 at the experimental part.

5.2.3.2 Synthesis of core crosslinked star polymers

Synthesis of P(OEGA). OEG-A₄₈₀ (10.033g, 0.021 mol), CTA (0.1909g, 0.0008 mol) and AIBN (0.0258g, 1.57×10^{-4} mol) were placed into a round bottom flask equipped with a magnetic stirrer. The reactants were dissolved in Toluene (25mL) and the reaction mixture was degassed with N₂ under ice (0°C) for 30 minutes. The reaction mixture was then placed into an oil bath preheated to 70°C and the polymerisation was run for 4h. Upon completion, the reaction was quenched in an ice bath for 15mins. The polymer was purified via 3 repetitions of precipitating with petroleum ether and centrifuging (5mins, 8000rpm). The purified polymer was then placed into a vacuum oven overnight to remove remaining solvent.

Synthesis of star polymer: P(OEG-A) $M_{n=12,000g/mol}$ (1.212g, 1×10^{-4} mol), 2-vinyl-4,4-dimethylazlactone (223mg, 1.6×10^{-3} mol), *N,N*-methylenebisacrylamide (125mg, 8×10^{-4} mol) and AIBN (5mg, 3×10^{-5} mol) was dissolved in Toluene (6mL) and was transferred into a Cospak bottle equipped with a magnetic stirrer. The reaction mixture was degassed for 30mins at 0°C with N₂. The above composition resulted in a [macroCTA]:[M]:[X-linker]:[I] of 1:16:8:0.3. The reaction was also repeated at a composition of 1:16:8:0.3. The degassed and sealed reaction vessels were placed into an oil bath preheated to 70°C and the polymerisation was run for 24h. The reaction was then quenched in an ice bath for 15mins. The purification involved precipitation in diethyl ether to remove unreacted macroCTA arms and VDM monomer. The precipitation was repeated 3 times then the reaction mixture was dissolved and dialysed against methanol for 48h

to removed unreacted cross-linker. The purified star polymers were then placed in a vacuum oven overnight to remove remaining solvent.

Synthesis of VDM star-Spermine: 100mg VDM Star polymer was dissolved in acetonitrile (5mL). Separate from the star polymer (100 mg, 1.25×10^{-6} mol), Spermine (5mg, 2.47×10^{-5} mol) was dissolved in 500 μ L methanol and then the 2 solutions were transferred into a Cospak bottle. The reaction mixture was then placed into an incubator (25°C, 80rpm) for 24h. After 24h, a 100 μ L aliquot was dried and checked via FTIR to determine conversion of the VDM functional groups. The reaction mixture was then returned to the incubator to achieve full conversion of the VDM functional groups. The fully reacted star polymers were purified by dialysis against water for 48h, with the water being changed twice per day. The dialysed polymer was then freeze dried overnight.

Synthesis of NO star polymers: A solution of the desired polymer sample in acetonitrile and methanol (1:1) mixture was placed in a Parr apparatus and clamped. The apparatus was purged and evacuated with nitrogen three times, followed by charging with excess nitric oxide gas (25 °C, 5 atm) for 48 h. After 48 h, the excess NO was vented by purging with nitrogen and the solvent removed via evaporation under nitrogen to yield the desired polymer-diazeniumdiolate sample.

5.2.3.3 Nitric oxide release and biofilm inhibition study

Determination of released nitric oxide (NO): Griess Assay. Nitric oxide release was determined using the two-step. Diazeniumdiolates readily release nitric oxide upon contact with water at physiological pH. Typically, 20mg nitric

oxide containing polymer was dissolved in 240 μ L of sterile MilliQ water. To this, 50 μ L each of Nitrate reductase and cofactor were added and the solution was left to incubate on the bench top for 3 h. Following the incubation period wherein the nitrates were converted into the assayable nitrite, 150 μ L of each Griess reagent (A & B) were added and the solution left to incubate for a further 30 min. Nitrite concentrations were then measured using an UV-vis spectrometer; the absorbance at 548 nm was used to calculate the nitric oxide content from the assay's calibration curve.

Biofilm inhibition study. *Pseudomonas aeruginosa* (PAO1) was used for biofilm inhibition assays. Biofilms were grown from a 1:200 dilution of *P. aeruginosa* overnight culture in LB in 1mL M9 minimal medium in tissue-culture treated 24-well plates (BD) incubated at 37C with agitation at 80 rpm. Prior to incubation, the bacterial medium was inoculated with NO-releasing compounds at final concentrations of 100 to 400 ppm, as indicated, whilst control wells were left untreated. After 6 h of growth, the planktonic biomass was quantified by siphoning off the supernatant and measuring its OD600. The remaining biofilm was washed twice with PBS (1.0 mL), before adding crystal violet stain (1.0 mL; 0.2% crystal violet, 1.9% ethanol and 0.08% ammonium oxalate in PBS). The plates were then incubated on the bench for 20 min before washing the wells twice with PBS (1mL). The amount of remaining crystal violet stained biofilm was quantified by adding 100% ethanol (1.0 mL) and measuring OD550 of the homogenized suspension. OD measurements of control wells where no compound was added were subtracted from all value.

5.2.3.4 NO Reporter Bioassays

Overnight cultures of *P. aeruginosa nirS::gfp* reporter strain (NSGFP)^{7,10} were diluted to an OD₆₀₀ of 0.2 in fresh LB medium and grown with shaking at 37 °C to an OD₆₀₀ of 0.4. Treatments were added to 3 mL aliquots of the cultures in 50 mL Falcon tubes (BD), in duplicate, and the bacteria were incubated further for up to 3 h. After compound exposure cells were washed once in phosphate-buffered saline (PBS) and resuspended in 0.5 mL PBS. 200 µL aliquots were transferred to a microtiter plate for fluorescence measurements (excitation, 485 nm; emission, 535 nm; Wallac Victor², Perkin-Elmer).

5.2.3.5 Biofilm Prevention Assays

The laboratory strain *P. aeruginosa* PAO1 was mainly used to characterise the effects of NO star polymers on biofilm formation. PAO1 mutant strains containing a transposon Tn5-derived insertion element in key genes in mediating dispersal in response to NO, *dipA* (PA5017) and *rbdA* (PA0861), were obtained from the University of Washington *P. aeruginosa* mutant two-allele library: strains PW9424 *dipA*-A01::IS*phoA*/hah and PW2569 *rbdA*-F02::IS*lacZ*/hah, respectively²⁵. Biofilms were grown as previously described¹¹ with some modifications. Briefly in all assays, overnight cultures in Luria Bertani medium were diluted to an OD₆₀₀ of 0.005 in 1 mL M9 minimal medium (containing 48 mM Na₂HPO₄, 22 mM KH₂PO₄, 9 mM NaCl, 19 mM NH₄Cl, 2 mM MgSO₄, 20 mM glucose, 100 µM CaCl₂, pH 7.0) or Mueller

Hinton broth (Oxoid; containing 30% beef extracts, 1.75% casein hydrolysate and 0.15% starch) in tissue-culture treated 24-well plates (BD). Various treatments were added to the wells, each from a 10 μ l aliquot of a stock solution at the appropriate concentration previously sterilized by passing through a 0.22 μ m pore size filter: sodium nitroprusside (Sigma) made fresh in deionized water, spermine NONOate (Cayman chemicals) in 10 mM NaOH, or compounds VsNO, Vs and V in 10 mM NaOH. The plates were incubated at 37 °C with shaking at 180 rpm and the biofilms were allowed to grow for up to 7.5 h. After incubation, the planktonic biomass was quantified by removing the supernatant and measuring its OD600. The remaining biofilm was washed once with PBS (1 mL), before adding 0.03% crystal violet stain made from a 1:10 dilution of Gram Crystal Violet (BD) in PBS. The plates were incubated on the bench for 20 min before washing the wells twice with PBS. Photographs of the stained biofilms were obtained using a digital camera. The amount of remaining crystal violet stained biofilm was quantified by adding 1 mL 100% ethanol and measuring OD550 of the homogenized suspension. OD measurements of control wells where no bacteria were added at the beginning of the experiment were subtracted from all values (i.e. OD600 = 0.03, and OD550 = 0.10).

5.3 Result and discussion

Core cross-linked star polymers were synthesized using an ‘arm-first’ approach,²⁶ which was previously developed in our group for magnetic resonance imaging²⁷ and drug delivery²⁸ applications. Reversible addition

fragmentation transfer (RAFT) polymerization was employed to synthesize P(OEGA) arm using chain transfer agent **1** (RAFT 1, *n*-butyltrithiocarbonate) and AIBN (2,2'-azobisisobutyronitrile) as radical initiator with the ratio of OEGA:RAFT 1:AIBN = 25:1:0.1 in toluene at 70°C (**Figure 5.1**).

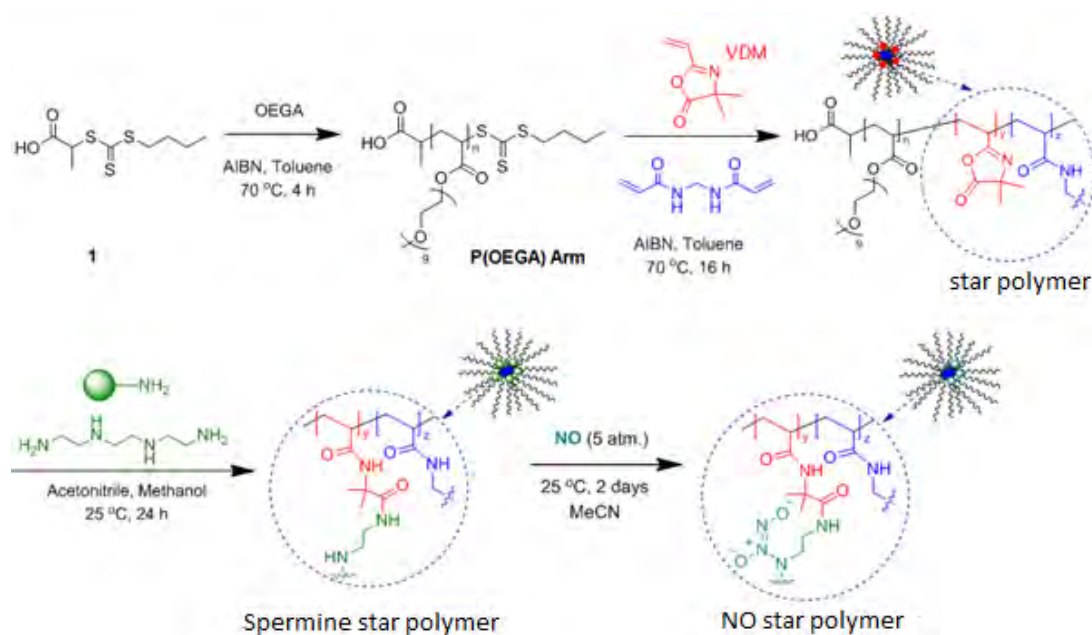


Figure 5. 1 Synthesis of P(OEGA)-b-P(VDM) star followed by spermine and NO donor conjugation

After 4 hours of reaction, ~90% OEGA conversion was achieved and the resultant polymer arm was purified through dialysis. After purification, P(OEGA) was then characterized using SEC and ¹H-NMR. The molecular weight distribution based on SEC showed a $M_{n, SEC}$ of 14,500 g/mol with a polydispersity index of 1.11, which was slightly higher than the theoretical molecular weight by ¹H-NMR ($M_{n, NMR}$ of 11,500 g/mol). This slight difference is due to the difference of hydrodynamic volume in the SEC between the P(MMA) calibration and P(OEGA) polymer (**Figure 5.2**).

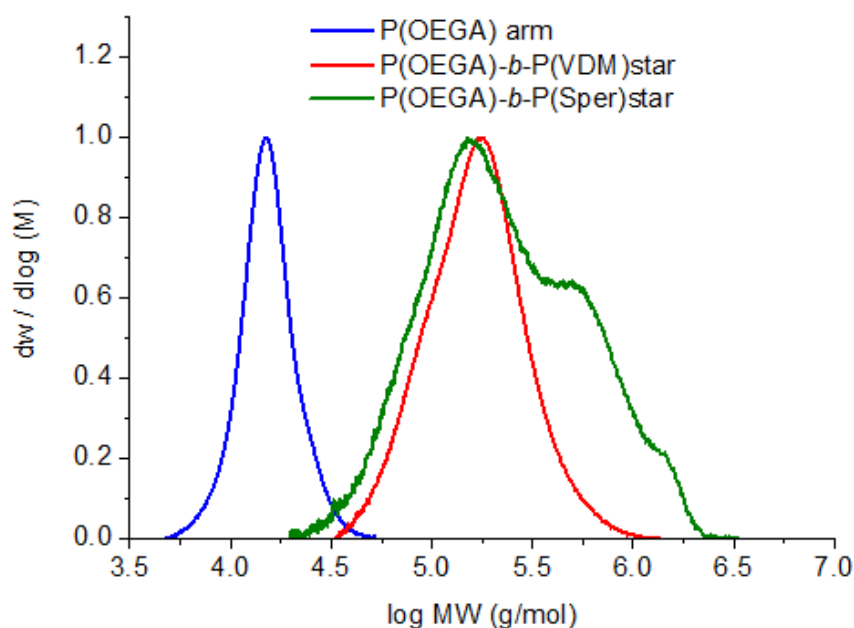


Figure 5. 2 SEC of P(OEGA) arm and P(OEGA)-b-P(VDM)star before and after spermine conjugation.

Chain extension from P(OEGA) arm was carried out in the presence of 2-vinyl-4,4-dimethyl-5-oxazolone monomer (VDM) and a cross-linker, methylenebisacrylamide.²⁹ The molar ratio between the P(OEGA) arm, VDM and the cross-linker was set to 1:16:8 followed by the addition of AIBN to this mixture in toluene. After the reaction at 70°C, the reaction mixture was purified by precipitation in diethyl ether to remove the unreacted P(OEGA) arm. The result from SEC showed a shift in the molecular weight giving $M_{n, SEC}$ of 177,000 g/mol with a polydispersity index of 1.39. The ratio between the area of the chromatogram of star polymer and its precursor, P(OEGA) arm was calculated to provide an arm incorporation of ~71%.³⁰ The incorporation of VDM monomer to the P(OEGA) arm was confirmed by ¹H-NMR via a signal

at 1.3 ppm from the VDM and the ester group from OEGA at 4.1 ppm (**Figure 5.3**).³¹

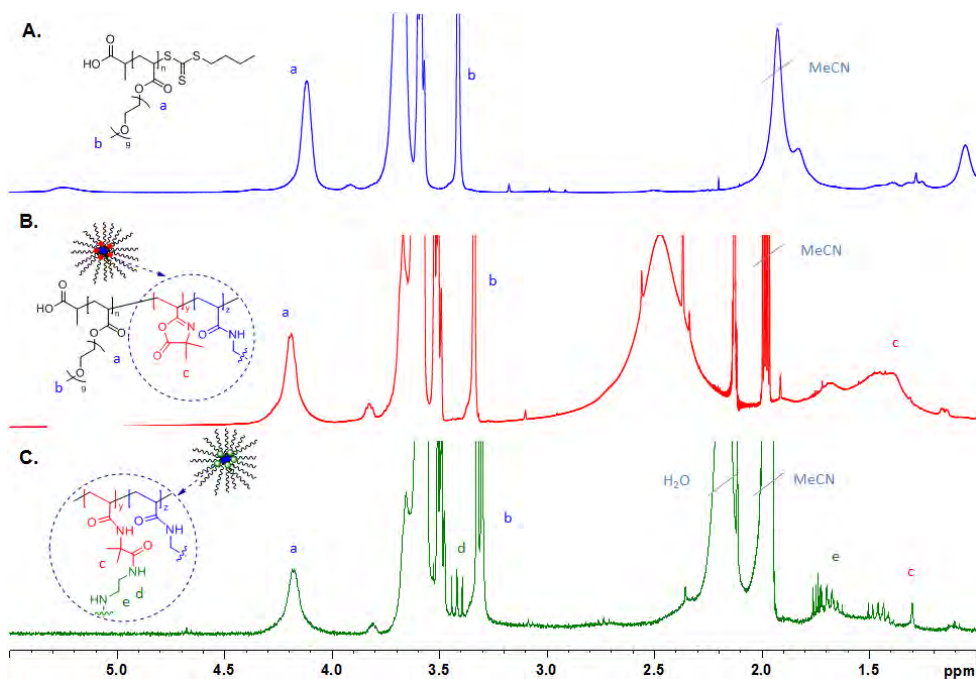


Figure 5.3 ¹H-NMR of P(OEGA) arm (A), P(OEGA)-b-P(VDM)star (B) and P(OEGA)-b-P(Sper)star (C)

In addition, ATR-FTIR has been employed to confirm the presence of oxazolone group at 1820 cm⁻¹ (**Figure 5.6 A**).³² The peak at 1630 cm⁻¹, 1720 cm⁻¹ and 1100 cm⁻¹ represents the cross-linking amide, OEGA ester and ether groups, respectively, confirming the incorporation of arm to the star polymer.³³

When spermine was reacted with VDM star polymer followed by purification by dialysis, the formation of star conjugated with spermine was confirmed by the disappearance of the characteristic azlactone peak at 1820 cm⁻¹ in the FTIR spectra, indicating the oxazolone ring opening *via* amidation.³⁴ A broad peak at around 3500 cm⁻¹ was observed characteristic to the secondary amines from the

conjugated spermine. The formation of the core cross-linked star polymer was confirmed by the DLS showing the number-weighted particle size of ~25 nm (Figure 5.4), which was corroborated by the TEM results.

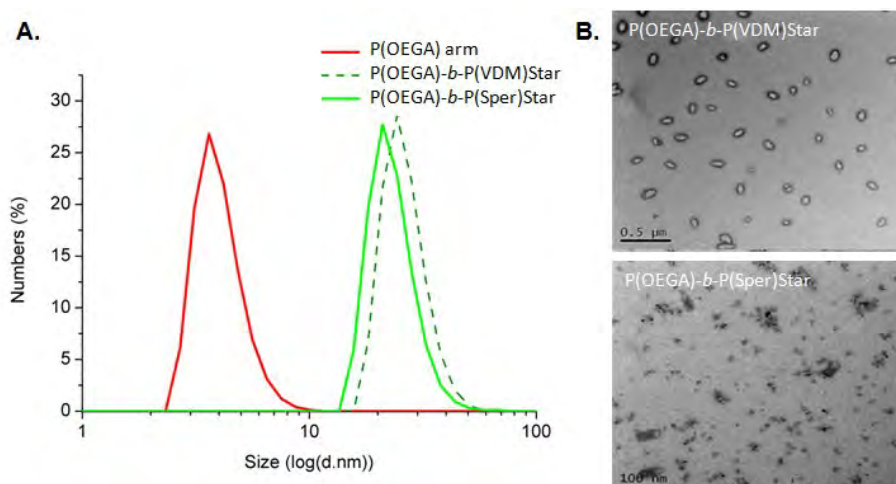


Figure 5. 4 Number-weighted particle size distribution by DLS (A) and TEM images (B) of P(OEGA)-b-P(VDM)star before and after spermine conjugation

Zeta potential measurement of initial star polymer in water revealed a neutral surface charge due to the P(OEGA) hydrophilic layers (Figure 5.5).³⁵ After conjugation of spermine, the zeta potential of star polymer shifted to +24 mV indicative of the presence of quaternary amine (NH_3^+ or NH_2^+). The effect of spermine conjugation was observed in the UV-Vis spectra through the disappearance of a peak at around 310 nm (Figure 5.6B), which is attributed to aminolysis of the trithiocarbonate RAFT group.³⁶

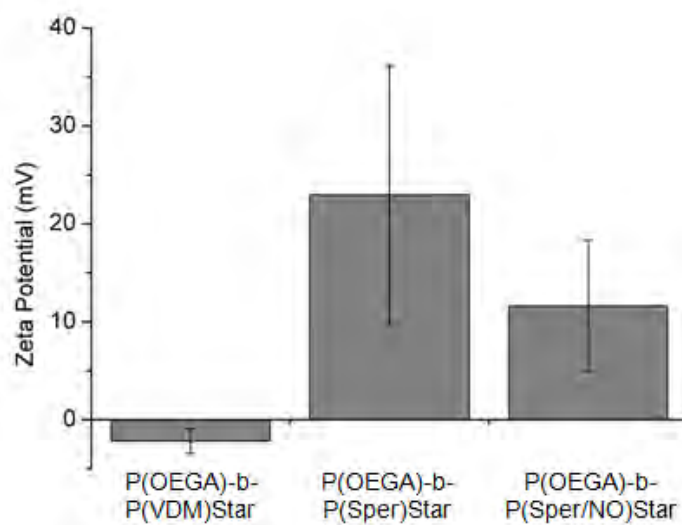


Figure 5. 5 Zeta potential measurement of P(OEGA)-b-P(VDM)star before and after spermine conjugation followed by NO (nitric oxide) conjugation

In order to conjugate nitric oxide to the nanoparticles, spermine conjugated star polymers was dissolved in acetonitrile and the solution was transferred to a Parr hydrogenation apparatus, purged with nitrogen and then stirred with NO gas for 48 h at 80 psi (5 bar) (**Figure 5.1**). Nitric oxide was reacted to the secondary amine of spermine to yield *N*-diazoniumdiolate (or NONOate) moieties, which was stabilized inside the core of the polymeric nanoparticles.³⁷ This was also confirmed by the decreasing zeta-potential of the resultant NO star polymer (+10 mV) due to the formation of the *N*-diazoniumdiolate. When the NO star polymer was dispersed in water, NO gas was released, in particularly the release will be accelerated at the pH lower than 7.0.³⁸ This was characterized by the presence of characteristic signal at around 240 nm observed by UV-Vis spectroscopy attributed to NO in water (**Figure 5.6B**).³⁹

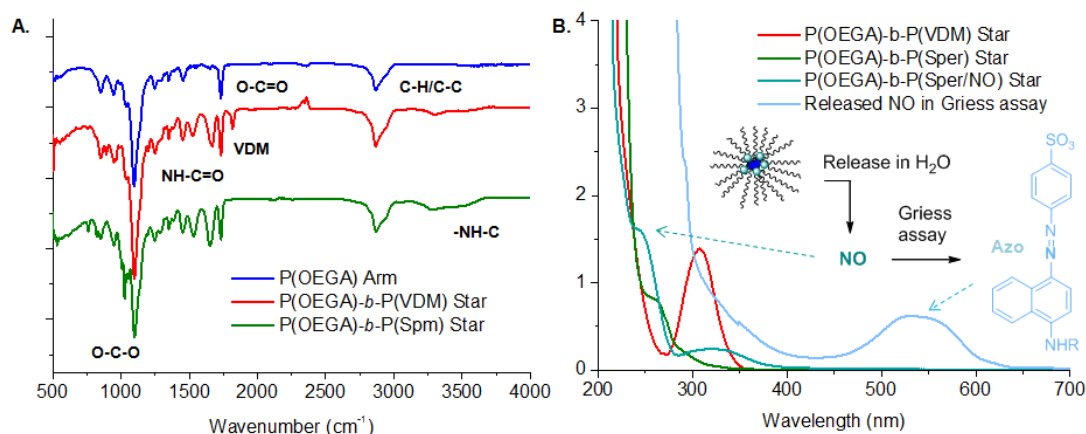


Figure 5. 6 A- ATR-FTIR of star polymer before and after spermine conjugation. B- UV-Vis absorption of nitric oxide (NO) release from the star polymer in water characterized by the absorption of NO at 250 nm and its azo dye at 548 nm (after the treatment with Griess agent)

Qualitative and quantitative analysis of the released NO from star polymer was performed using Griess assay.⁴⁰ Briefly, NO star polymer dissolved in deionized water was incubated with nitrate reductase and its cofactor to reduce the nitric oxide and nitrate to nitrite. Following the reaction protocol, the sample was incubated for 3 hours that allowed a maximum release of nitric oxide and its conversion to nitrite in the aqueous medium.⁴¹ Subsequent addition of a Griess reagent to the nitrite sample formed a diazenium salt that was converted instantaneously to an azo dye (**Figure 5.6B**). This was characterized by the presence of pink colour and UV-Vis absorption at 548 nm. Based on a calibration curve (**Figure 5.7**), the concentration of NO released from NO star polymer was quantified as 192 μM . Using the concentration of NO in the nanoparticle or star polymer the biological activity of this sample was tested on its inhibition of biofilm formation.⁴²

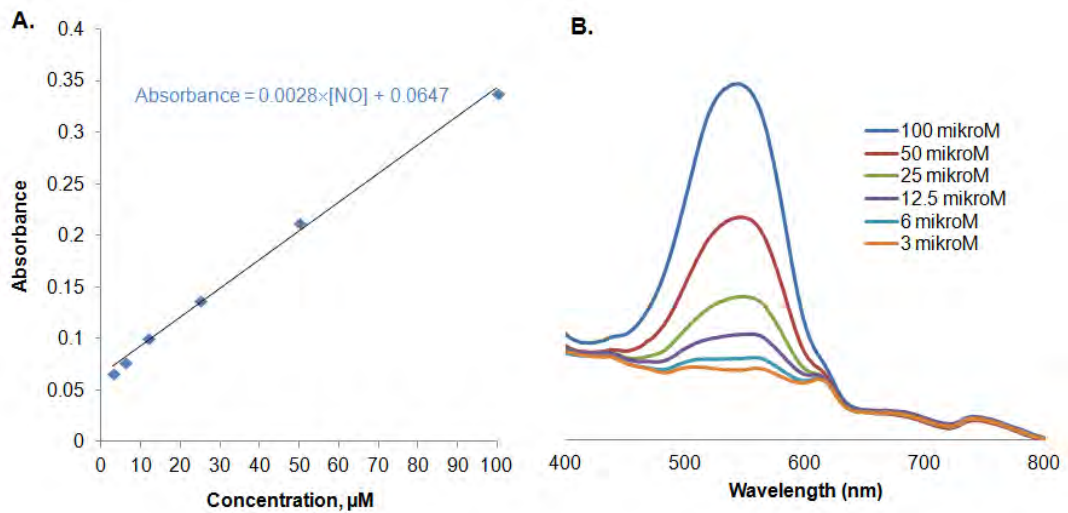


Figure 5. 7 Calibration curve (A) and UV-Vis absorption (B) of the azo dye generated in the Griess assay at different concentration of nitric oxide

Spermine conjugated star polymer sample was used as a negative control. First the ability of NO release from the polymers to induce a response in bacteria was assessed by using an engineered bacterial reporter strain that fluoresces in the presence of low doses of NO. A transcriptional fusion reporter strain, NSGFP, which co-expresses downstream green fluorescent protein (GFP) when the NO-responsive anaerobic gene *nirS* is expressed⁷ was exposed to NO star polymer at 100-400 ppm (based on NO concentration) and the spontaneous NO donor sodium nitroprusside (SNP) at 200 μM . Exposure to NO star polymer was able to induce a GFP-response and the response gradually increased over a 3 h time period (**Figure 5.8**). In contrast, the spontaneous SNP induced a rapid increase in GFP, which did not increase further after 2 h exposure. These results suggest that NO star polymer is able to induce a sustained release of NO in the presence of bacteria. When using a NO specific electrode (Apollo, World Precision Instrument), no release of NO from

400 ppm star polymer in a buffered aqueous solution could be observed, suggesting that the release is too slow to accumulate detectable NO (limit ~10 nM) (data not shown).

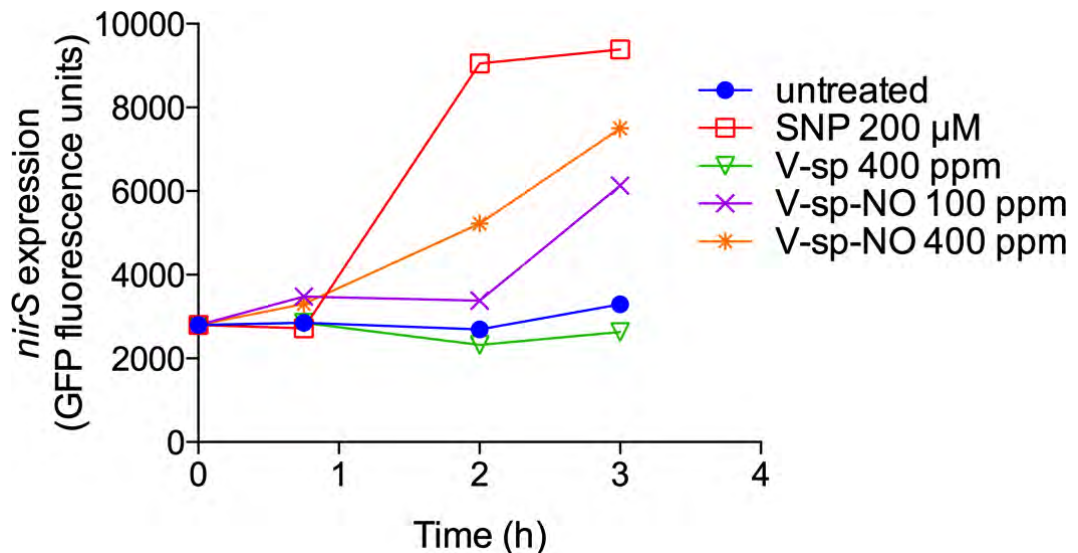


Figure 5.8 NO star polymer (V-Sp-NO) induces a slow release of NO available to bacteria. Cultures of the NO reporter mutant train, NSGFP, which express GFP under control of the NO responsive nirS promoter, were exposed to NO star polymer, spontaneous NO donor SNP or negative control spermine star polymers for up to 3 h before fluorescence measurement. Error bars represent standard error (n = 2)

The effect of NO star polymer on biofilm formation was assessed. *P. aeruginosa* biofilms grown in minimal M9 medium in the presence of 100 ppm and 400 ppm NO star polymer were strongly inhibited over the incubation period, with respectively a 90% and 95% reduction in biofilm biomass after 7.5 h compared to untreated biofilms. Concomitantly, the number of planktonic cells increased in culture wells treated with 100 ppm NO star polymer, resulting in 32% more suspended biomass after 7.5 h compared to untreated

wells (**Figure 5.9**), a result that is consistent with a non-toxic effect of NO star polymer inducing a switch from the biofilm to the planktonic mode of growth over sustained periods of time.

At 400 ppm, NO star polymer induced a slight decrease in planktonic growth by 20% compared to untreated wells, suggesting that at this concentration of NO star polymer and under these growth conditions, NO may have been released at levels showing some toxicity. The spontaneous NO donor SNP was also able to reduce biofilm formation in this system, although to a lesser extent compared to NO star polymer, by only 35-50% vs. untreated controls, while at the same time increasing planktonic growth (**Figure 5.9**).

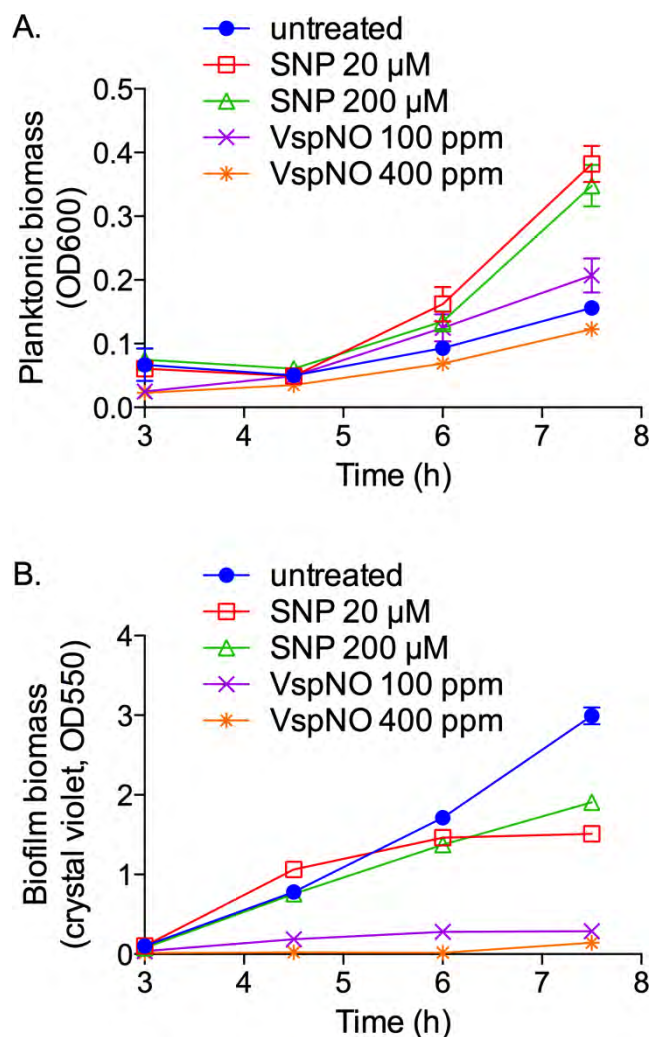


Figure 5.9 Prevention of biofilm formation in the presence of NO star polymer (V-Sp-NO). *P. aeruginosa* biofilms were grown in multiwell plates for up to 7.5 h in the presence or absence of NO star polymers or SNP from the beginning of growth. (A) Planktonic biomass was determined by measurement of the OD600 of the supernatant, and (B) biofilm biomass by crystal violet staining (OD550). Error bars represent standard error (n = 2)

When testing a range of NO star polymer concentrations, the star polymer was found to be active even at low concentrations, with 57 ppm inducing a 73% decrease in biofilm formation compared to untreated controls after 6 h, concomitant with a 55% increase in planktonic growth (**Figure 5.10**). In

contrast, spermine conjugated stars (used as a control) were unable to prevent formation of *P. aeruginosa* biofilms.

A fast NO-releasing NONOate donor, (Z)-1-[N-[3-aminopropyl]-N-[4-(3-aminopropylammonio) butyl]-amino]diazene-1,2-diolate (spermine NONOate; $t_{1/2} = 40$ min at pH 7.4, 37 °C) used at 10 μ M a concentration that store similar amounts of NO compared to NJO star polymer 100 ppm as detected by Griess assay, was also unable to inhibit biofilm formation.

Other NONOate donors with more stable NO release in buffered system compared to spermine NONOate, such as (Z)-1-[N-(2-aminoethyl)-N-(2-ammonioethyl)amino]diazene-1,2-diolate (DETA NONOate; $t_{1/2} = 20$ h at pH 7.4, 37 °C) or (Z)-1-[N-(3-aminopropyl)-N-(3-ammoniopropyl)amino]diazene-1,2-diolate (DPTA NONOate; $t_{1/2} = 3$ h at pH 7.4, 37 °C) were also tested. At concentrations that were non-toxic to bacterial growth none of these compounds showed any sustained biofilm prevention effect (data not shown).

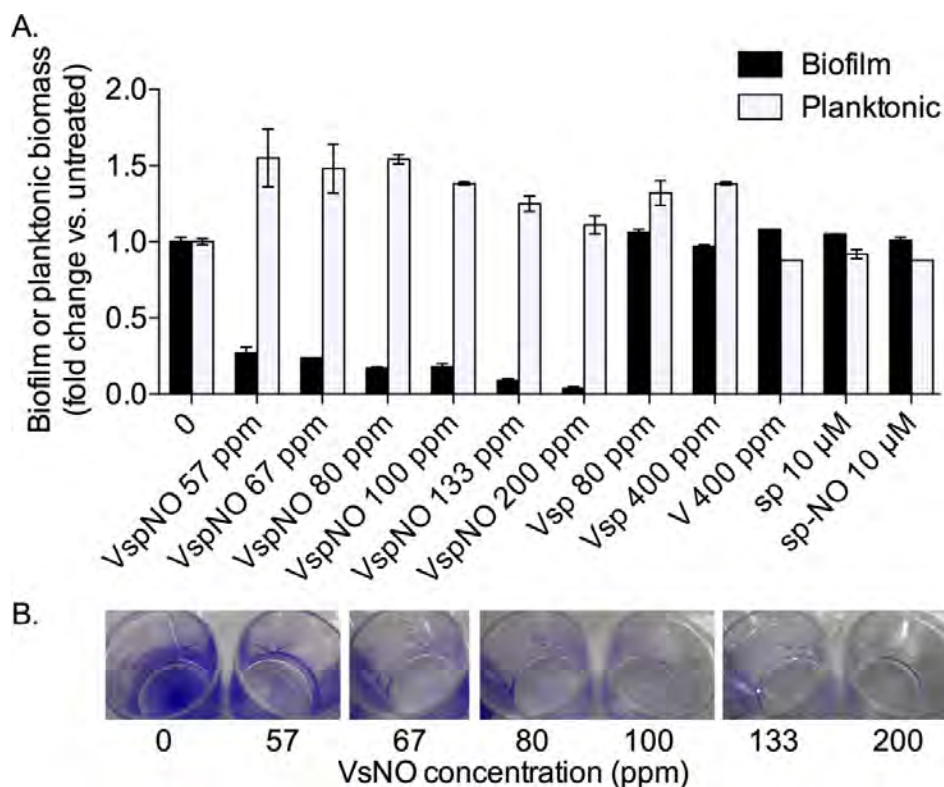


Figure 5.10 Dose dependent prevention of biofilm formation. (A) *P. aeruginosa* biofilms were grown in multiwell plates in M9 for 6 h in the presence or absence of 57-200 ppm (based on NO concentration) NO star polymer, or negative controls spermine star polymers, star polymers, or spermine before analysing biofilms by crystal violet staining. Treatment with fast NO releasing NONOate donor Sp-NO did not prevent biofilm formation over this incubation time. Error bars represent standard error ($n = 2$). (B) Stained biofilms treated with the indicated concentrations of NO star polymers

NO star polymer was also tested on biofilms grown in complex medium Mueller Hinton broth, which showed a strong inhibition effect reducing biofilm by 80% at 400 ppm with no reduction in planktonic growth (**Figure 5.11**). Under these growth conditions NO donor SNP was unable to prevent biofilm formation over a 6 h incubation period.

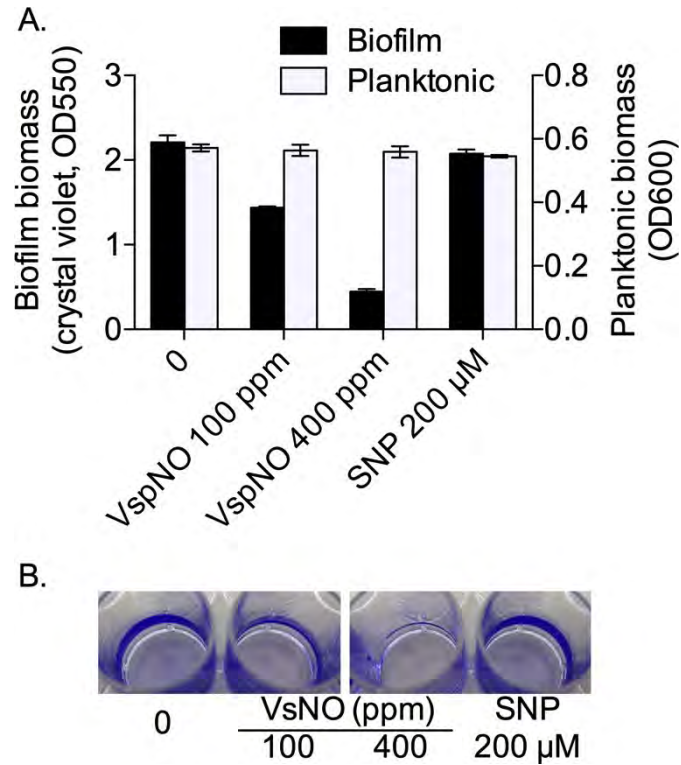


Figure 5.11 VsNO inhibits *P. aeruginosa* biofilm grown in complex medium Mueller Hinton broth. (A) Biofilms were grown for 6 h in multiwell plates in MH broth before measuring biofilm biomass by crystal violet staining. Error bars represent standard error (n = 2). (B) Stained biofilms treated or not with VsNO and SNP

To better understand the effects of NO star polymer on biofilms, NO star polymers was tested against biofilms of mutant strains impaired in key components of the NO dispersal pathway, namely the phosphodiesterases *dipA* and *rbdA* that mediate decrease in intracellular levels of 2nd messenger c-di-GMP in response to NO^{8,10}. *dipA* mutant biofilms were not affected by NO star polymer, while *rbdA* mutant biofilms showed only 50% reduction with 400 ppm NO star polymer compared to 99% reduction obtained with the wild type (**Figure 5.12**).

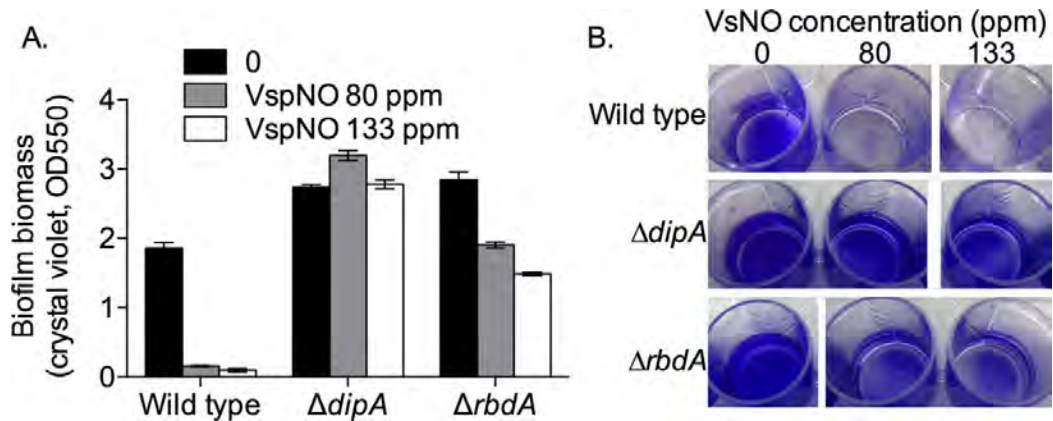


Figure 5.12 *P. aeruginosa* mutants affected in the NO-mediated dispersal signaling pathway were not affected or only partially inhibited by VsNO. (A) Biofilms were grown in multiwell plates for 6 h with or without VsNO, before measuring biofilm biomass by crystal violet staining. Error bars represent standard error (n = 2). (B) Stained mutant biofilms treated or not with VsNO

These results strongly suggest that NO star polymer inhibits the biofilm switch in planktonic cells in contact with a surface by inducing a cellular response that continuously stimulates phosphodiesterase activity and maintains low intracellular levels of c-di-GMP in the growing bacterial population, thus confining growth to an unattached free-swimming mode.

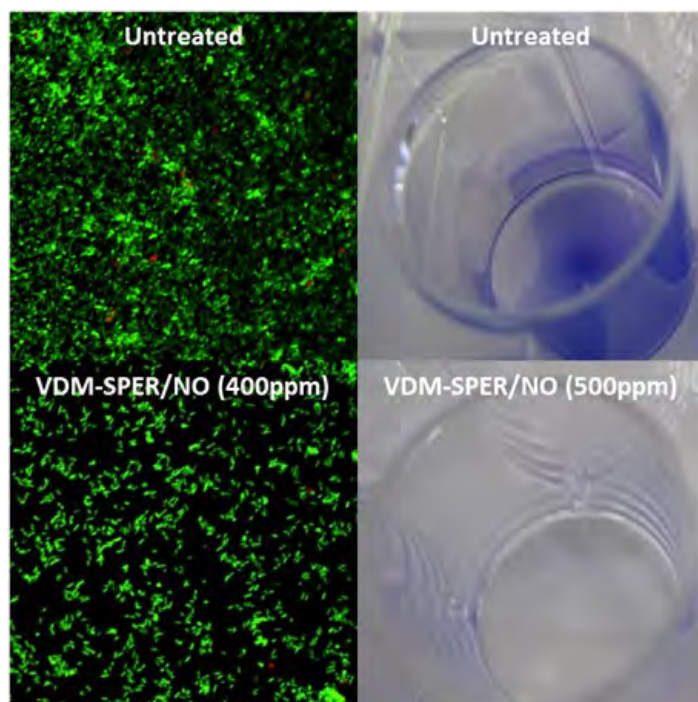


Figure 5.13 Representative confocal images showing live bacterial cells stained with SYTO 9 Scale bars = 100 μm . Treated versus untreated using NO star polymers at 2 h intervals for a 6 h period. Stained biofilms treated with the indicated concentrations of NO star polymers

Confocal microscopy was used to evaluate the ability of the NO star polymers to prevent colonisation and biofilm dispersal of *P. aeruginosa*. The areas of the surfaces covered by bacteria and the relative proportions of live and dead bacteria (stained green and red, respectively) for each surface were evaluated by image analysis and the results are shown in **Figure 5.13**. After treatment with NO star polymers, there is a significant reduction in biofilm biovolume and increased biofilm dispersal compared to the untreated control.

5.4 Conclusions

In summary, we have developed a novel star polymer with can release nitric oxide and demonstrated the great efficacy in decrease in biofilm growth of *P. aeruginosa* while minimizing the NO-mediated toxicity in planktonic growth. On-going research approach is to incorporate antibiotics to this NO star polymer system, which is expected to achieve the synergistic effects for the better efficacy for antimicrobial treatment.

5.5 References

- (1) *The world health report 2000—health systems: improving performance*. Geneva: World Health Organization, 2000.
- (2) Clatworthy, A. E.; Pierson, E.; Hung, D. T. *Nat. Chem. Biol.* **2007**, *3*, 541.
- (3) Hoiby, N.; Bjarnsholt, T.; Givskov, M.; Molin, S.; Ciofu, O. *Int. J. Antimicrob. Agents* **2010**, *35*, 322.
- (4) Flemming, H.-C. In *Biofilm Highlights*; Flemming, H.-C., Wingender, J., Szewzyk, U., Eds.; Springer Berlin Heidelberg: 2011; Vol. 5, p 81.
- (5) Davies, D. *Nature reviews. Drug discovery* **2003**, *2*, 114.
- (6) McDougald, D.; Rice, S. A.; Barraud, N.; Steinberg, P. D.; Kjelleberg, S. *Nat. Rev. Microbiol.* **2012**, *10*, 39.
- (7) Barraud, N.; Hassett, D. J.; Hwang, S. H.; Rice, S. A.; Kjelleberg, S.; Webb, J. S. *J. Bacteriol.* **2006**, *188*, 7344.
- (8) Roy, A. B.; Petrova, O. E.; Sauer, K. *J. Bacteriol.* **2012**, *194*, 2904.

- (9) Liu, N.; Xu, Y.; Hossain, S.; Huang, N.; Coursolle, D.; Gralnick, J. A.; Boon, E. M. *Biochemistry* **2012**, *51*, 2087.
- (10) Barraud, N.; Schleheck, D.; Klebensberger, J.; Webb, J. S.; Hassett, D. J.; Rice, S. A.; Kjelleberg, S. *J. Bacteriol.* **2009**, *191*, 7333.
- (11) Yepuri, N. R.; Barraud, N.; Shah Mohammadi, N.; Kardak, B. G.; Kjelleberg, S.; Rice, S. A.; Kelso, M. J. *Chemical communications (Cambridge, England)* **2013**, *49*, 4791.
- (12) Barraud, N.; Storey, M. V.; Moore, Z. P.; Webb, J. S.; Rice, S. A.; Kjelleberg, S. *Microb. Biotechnol.* **2009**, *2*, 370.
- (13) Barraud, N.; Kardak, B. G.; Yepuri, N. R.; Howlin, R. P.; Webb, J. S.; Faust, S. N.; Kjelleberg, S.; Rice, S. A.; Kelso, M. J. *Angewandte Chemie (International ed. in English)* **2012**, *51*, 9057.
- (14) Barnes, R. J.; Bandi, R. R.; Wong, W. S.; Barraud, N.; McDougald, D.; Fane, A.; Kjelleberg, S.; Rice, S. A. *Biofouling* **2013**, *29*, 203.
- (15) Yamamoto, T.; Bing, R. J. *Proc. Soc. Exp. Biol. Med.* **2000**, *225*, 200.
- (16) Pal, S.; Tak, Y. K.; Song, J. M. *Applied and Environmental Microbiology* **2007**, *73*, 1712.
- (17) Weir, E.; Lawlor, A.; Whelan, A.; Regan, F. *Analyst* **2008**, *133*, 835.
- (18) Momin, E. N.; Schwab, K. E.; Chaichana, K. L.; Miller-Lotan, R.; Levy, A. P.; Tamargo, R. J. *Neurosurgery* **2009**, *65*, 937.
- (19) Duan, S.; Cai, S.; Yang, Q.; Forrest, M. L. *Biomaterials* **2012**, *33*, 3243.

- (20) Jo, Y. S.; van der Vlies, A. J.; Gantz, J.; Thacher, T. N.; Antonijevic, S.; Cavadini, S.; Demurtas, D.; Stergiopoulos, N.; Hubbell, J. A. *J. Am. Chem. Soc.* **2009**, *131*, 14413.
- (21) Kim, J.; Lee, Y.; Singha, K.; Kim, H. W.; Shin, J. H.; Jo, S.; Han, D.-K.; Kim, W. J. *Bioconjugate Chem.* **2011**, *22*, 1031.
- (22) Mohr, P. C.; Mohr, A.; Vila, T. P.; Korth, H.-G. *Langmuir* **2010**, *26*, 12785.
- (23) Levere, M. E.; Ho, H. T.; Pascual, S.; Fontaine, L. *Polymer Chemistry* **2011**, *2*, 2878.
- (24) Ferguson, C. J.; Hughes, R. J.; Nguyen, D.; Pham, B. T. T.; Gilbert, R. G.; Serelis, A. K.; Such, C. H.; Hawkett, B. S. *Macromolecules* **2005**, *38*, 2191.
- (25) Jacobs, M. A.; Alwood, A.; Thaipisuttikul, I.; Spencer, D.; Haugen, E.; Ernst, S.; Will, O.; Kaul, R.; Raymond, C.; Levy, R.; Chun-Rong, L.; Guenther, D.; Bovee, D.; Olson, M. V.; Manoil, C. *Proc. Natl. Acad. Sci. U. S. A.* **2003**, *100*, 14339.
- (26) Syrett, J. A.; Haddleton, D. M.; Whittaker, M. R.; Davis, T. P.; Boyer, C. *Chemical Communications* **2011**, *47*, 1449.
- (27) Li, Y.; Beija, M.; Laurent, S.; Elst, L. v.; Muller, R. N.; Duong, H. T. T.; Lowe, A. B.; Davis, T. P.; Boyer, C. *Macromolecules* **2012**, *45*, 4196.
- (28) Liu, J.; Duong, H.; Whittaker, M. R.; Davis, T. P.; Boyer, C. *Macromolecular Rapid Communications* **2012**, *33*.
- (29) Ferreira, J.; Syrett, J.; Whittaker, M.; Haddleton, D.; Davis, T. P.; Boyer, C. *Polymer Chemistry* **2011**, *2*, 1671.

- (30) Boyer, C.; Whittaker, M.; Davis, T. P. *Journal of Polymer Science Part A: Polymer Chemistry* **2011**, *49*, 5254.
- (31) Duong, H. T. T.; Kamarudin, Z. M.; Erlich, R. B.; Li, Y.; Jones, M. W.; Kavallaris, M.; Boyer, C.; Davis, T. P. *Chemical Communications* **2013**, *49*, 4190.
- (32) Li, Y.; Duong, H. T. T.; Jones, M. W.; Basuki, J. S.; Hu, J.; Boyer, C.; Davis, T. P. *ACS Macro Letters* **2013**, *2*, 912.
- (33) Levere, M. E.; Ho, H. T.; Pascual, S.; Fontaine, L. *Polymer Chemistry* **2011**, *2*, 2878.
- (34) Ho, H. T.; Levere, M. E.; Fournier, D.; Montembault, V.; Pascual, S.; Fontaine, L. *Australian Journal of Chemistry* **2012**, *65*, 970.
- (35) Basuki, J. S.; Duong, H. T. T.; Macmillan, A.; Whan, R.; Boyer, C.; Davis, T. P. *Macromolecules* **2013**, *46*, 7043.
- (36) Willcock, H.; O'Reilly, R. K. *Polymer Chemistry* **2010**, *1*, 149.
- (37) Polizzi, M. A.; Stasko, N. A.; Schoenfisch, M. H. *Langmuir* **2007**, *23*, 4938.
- (38) Parzuchowski, P. G.; Frost, M. C.; Meyerhoff, M. E. *Journal of the American Chemical Society* **2002**, *124*, 12182.
- (39) Singh, R. J.; Hogg, N.; Joseph, J.; Kalyanaraman, B. *The Journal of Biological Chemistry* **1996**, *271*, 18596.
- (40) Sun, J.; Zhang, X.; Broderick, M.; Fein, H. *Sensors* **2003**, *3*.
- (41) Smith, D. J.; Chakravarthy, D.; Pulfer, S.; Simmons, M. L.; Hrabie, J. A.; Citro, M. L.; Saavedra, J. E.; Davies, K. M.; Hutsell, T. C.; Mooradian, D.

L.; Hanson, S. R.; Keefer, L. K. *Journal of Medicinal Chemistry* **1996**, *39*, 1148.

(42) Carpenter, A. W.; Slomberg, D. L.; Rao, K. S.; Schoenfisch, M. H. *ACS Nano* **2011**, *5*, 7235.

Chapter 6. Conclusion and Future Directions

6.1 Conclusions

The overall objective of this thesis is to design a new NO nanocarriers for different application, using different type of NO donors, via RAFT polymerization. Core Crosslinked Star (CCS) polymer had been choose as the polymeric nanocarriers for NO delivery, based on some advantages that have been explored through previous studies.

In chapter 5, we prepared NO nanoparticles using VBC star as the vehicles and nitrate NO donors. The star nanoparticle was successfully prepared using RAFT polymerization via arm-first method. The well-defined CCS polymers with VBC functional core were subsequently cross-linked in the core by chain extension with N,N'-methylene bisacrylamide cross-linker. The VBC star nanoparticles then been modified with silver nitrate (AgNO₃) in order to substitute the chloro group in corona with nitrate. The success of the cross-linking and modification had been confirmed using series of analytical method, including GPC, ¹H NMR, UV-vis, and FTIR. We also did the Griess Assay analysis to determine NO concentration. The result showed that VBC nitrate has a great potent to be used as NO nanocarriers since it can release NO with high concentration and long of half-life.

In chapter 6, the star polymer with VDM functionality in the core had been prepared using the same method and cross-linker. The VDM star then used to

prepare NONOate nanoparticles for antibiotic application. After the optimum characteristic star polymer had been obtained, it then reacted with spermine and NO gas to form the NONOate nanoparticles. The same analytical methods also had been done to confirm the successfully of cross-linked reaction and NO nanoparticles formation. Antibiofilm and toxicity testing then used to confirm the potent of VDM star-spermine-NONOate as new antibiotic drug. The result showed that the VDM star-spermine-NONOate really promising to be used as antibiotic drug, since it can inhibit the formation of biofilm as the cause of antibiotic resistance and less toxicity.

6.2 Further study

Through this study, we have found that VBC star nitrate has a great potent to be used as the anticancer drug. The slow NO release mechanism and its dependency on numbers of factor, such thiols, light, and enzymatic still become the limitations of this NO nanoparticles. Further studies to improve the release mechanism become more necessary to overcome these limitations.